UNIVERSITY *of the*
WESTERN CAPE

Mini Thesis: The effects of carbon-based nanoparticle surface functionalization on immune responses.

By

Imaad Salie

Submitted in partial fulfillment of the requirements for the degree

Master of Science

Nanoscience

In the

Department of Medical Bioscience

Faculty of Science

University of the Western Cape

Supervisor

Dr. F. Rahiman

Co-Supervisors:

Prof. E.J. Pool and Dr. K.L. Lategan

April 2022

Declaration

I declare that:

The effects of carbon-based nanoparticle surface functionalization on immune responses is my own work, that it has not been submitted for any degree or examination at any other university, and that all the sources I have used or quoted have been indicated and acknowledged by complete references.

Imaad Salie

Signature: 

Date: 19 April 2022

Abstract

Nano-based technologies are highly desired for the unique properties achieved through size restrictions. Nanoparticles (NPs) achieve a higher surface-to-volume ratio during synthesis. As a result there is a greater rate of interaction between the nanostructure, its surrounding environment, and the biological system it is present within. Research into nanomaterial effects on biological systems are imperative to control the functioning of these materials. A way of overcoming limitations and to meet end point goals within biological systems is the altering of nanomaterial surfaces for greater tolerance by cells.

The addition of functional groups to NP surfaces may serve to alter the charge of the NP or provide the foundation upon which a secondary molecule is attached. Surface functionalization and charge are important parameters for the practical implementation of NP-based medical solutions. Amine and carboxyl functional groups are chemical groups typically manipulated for NP surface alteration. These functional groups are often paired where one may functionalize NP surfaces and the other may reside on the desired molecule. The extent to which NPs induce alterations within the immune system, particularly those induced by amine and carboxyl surface functionalization, must be clearly understood for any implementation to occur.

The murine macrophage cell line, RAW 264.7, was used as a model representative to determine the effect of surface functionalization on the immune response. Cells were subject to either stimulation for an immune response using lipopolysaccharide (LPS) or were left unstimulated. The effects of amine functionalized polystyrene NPs (APNPs) and carboxyl functionalized polystyrene NPs (CPNPs) had on the cells of the immune system were compared to unmodified NPs (PPNPs) of the same type. This was done by determining the cytotoxicity of these NPs and their effects on interleukin-6 (IL-6) production, which was followed by a proteome profile analysis.

Positively charged APNPs were the only group of the tested NPs seen to induce reductions in RAW cell viability, regardless of whether cells were stimulated by LPS for an immune response or not. Functionalized APNPs and CPNPs upregulated nitric oxide (NO) production in unstimulated cells at the highest concentration, 500 µg/mL, while unmodified PPNPs did so at concentrations ≥ 125 µg/mL. This indicates that both forms of functionalization decreased the modulatory activity of PNPs on NO production in unstimulated cells. APNPs downregulated NO production when stimulated cells were exposed to all concentrations, where the effect by PPNPs and CPNPs remained unremarkable. The secretion of IL-6 by stimulated

RAW cells was downregulated during exposure to all PNPs, apart from upregulation at the lowest APNP concentration. APNPs therefore possessed the greatest immunomodulatory activity due to the extent and consistency at which the alteration of the inflammatory biomarkers, NO and IL-6, occurred.

Proteome profile analysis revealed APNPs cause the greatest alteration in cytokine and chemokine production under LPS stimulated and unstimulated conditions. Under unstimulated conditions, APNPs downregulate MIP-1β and upregulate IL-16 and MIP-2. Under stimulated conditions, APNPs downregulate IL-1ra, sICAM-1 and MCP-1 and upregulate IL-16. Therefore, of the tested NPs, APNPs were seen to have the greatest immunomodulatory activity on RAW cell secretory molecules.

Acknowledgements:

I would like to express my gratitude to my supervisors; Dr. F. Rahiman, for her support, patience, and guidance during the completion of my thesis; Prof. E.J. Pool, for his encouragement to pursue my Masters in Nanoscience, his guidance during the completion of my experiments, and to his belief in my abilities; and Dr. K.L. Lategan, for her guidance and training during my experiments, assistance in my writing, and words of encouragement when needed. It is truly thanks to the combined efforts of these three individuals that this project was completed.

I thank my fellow postgraduate students in the Medical Bioscience department for the encouragement. Particularly, I thank the students of the Skin Research Lab for their support as fellow postgraduates and as my friends.

I express my appreciation to my grandmother and siblings for the love and support during completion of my studies. To my partner, Rizwaana Suleman, thank you for your support and encouragement.

I am grateful to the National Nanoscience Postgraduate Teaching and Training Platform for the opportunity to pursue my Masters and their financial support throughout.

Lastly and most importantly, I would like to thank Allah (SWT), for it is only through the blessings of Allah that I had reached this point.

List of acronyms and abbreviations

µm	micrometre
Ag	Silver
Ag-NPs	Silver-NPs
ANOVA	analysis of variance
APNPs	amine functionalized polystyrene nanoparticles
Au	gold
Au-NPs	gold-nanoparticles
C	complement component
C1	complement component 1
C1q	complement component 1q
C1r	complement component 1r
C1s	complement component 1s
C2	complement component 2
C2a	complement component 2a
C2b	complement component 2b
C3	complement component 3
C3a	complement component 3a
C3b	complement component 3b
C4	complement component 4
C4a	complement component 4a
C4b	complement component 4b
C5	complement component 5
C5a	complement component 5a

C5b	complement component 5b
C6	complement component 6
C7	complement component 7
C8	complement component 8
C9	complement component 9
CCL5	chemokine ligand 5
Cd	cadmium
CD	cluster of differentiation
CLRs	C-type lectin receptors
CPNPs	carboxylate functionalized polystyrene nanoparticles
CQDs	carbon quantum dots
d.nm	diameter in nanometres
DAMPs	damage associated molecular patterns
DAS-ELISA	Double Antibody Sandwich-Enzyme Linked Immunosorbent Assay
DLS	dynamic light scattering
DMEM	Dulbecco's Modified Eagle's Medium
DPBS	Dulbecco's phosphate buffered saline
FBS	fetal bovine serum
G-CSF	granulocyte colony-stimulating factor
HAP	hydroxyapatite
HRP	horse radish peroxidase
IC_{50}	half maximal inhibitory concentration
ICAM-1	intercellular adhesion molecule-1

Ig	immunoglobulin
IgD	immunoglobulin D
IgM	immunoglobulin M
IL	interleukin
IL-1β	interleukin-1 beta
IL-1ra	interleukin-1 receptor agonist
IL-10	interleukin-10
IL-12	interleukin-12
IL-13	interleukin-13
IL-15	interleukin-15
IL-16	interleukin-16
IL-2	interleukin-2
IL-4	interleukin-4
IL-5	interleukin-5
IL-6	interleukin-6
IL-8	interleukin-8
IL-27	interleukin-27
INF-γ	interferon-gamma
iNOS	inducible nitric oxide synthase
IP-10	interferon gamma-induced protein-10
LFA-1	lymphocyte function-associated antigen-1
LPS	lipopolysaccharide
MAC	membrane attack complex
MASPs	mannose binding lectin-associated serine proteases

MBL	mannose binding lectin
MCP-1	monocyte chemoattractant protein-1
MIP-1α	macrophage inflammatory protein-1 alpha
MIP-1β	macrophage inflammatory protein-1 beta
MIP-2	macrophage inflammatory protein-2
mm	millimetre
mRNA	messenger ribonucleic acid
NK	natural killer
NLRs	Nod-like receptors
nm	nanometre
NO	nitric oxide
NPs	Nanoparticles
PAMPs	pathogen-associated molecular patterns
Pdi	polydispersity index
PEG	poly(ethylene glycol)
pH	potential hydrogen
PNPs	polystyrene nanoparticles
PPNPs	pristine polystyrene nanoparticles
PRRs	pattern recognition receptors
QD	quantum dot
RLRs	RIG-I-like receptors
ROS	reactive oxygen species
SEM	standard error of the mean
sICAM-1	soluble intercellular adhesion molecule-1

Th	T helper
Th1	T helper-1
Th17	T helper-17
Th2	T helper-2
TLRs	Toll-like receptors
TMB	3,3',5,5'-Tetramethylbenzidine
TNF-α	tumour necrosis factor-alpha
WST-1	4-[3-(4-iodophenyl)-2-(4-nitrophenyl)-2H-5-tetrazolio]-1,3-benzene disulfonate

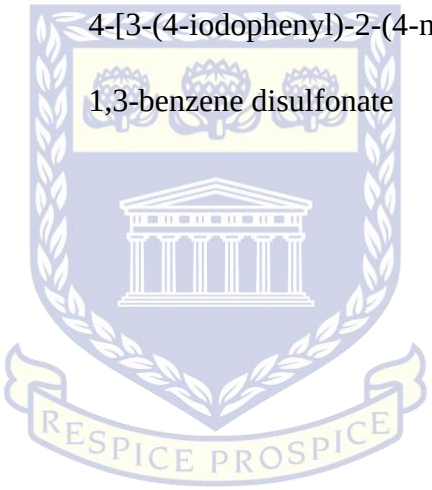

Table of Contents

List of Figures

List of Tables

Chapter 1

Introduction, Objectives, Aims and Hypothesis

1.1. Introduction to Nanoparticles

All matter is composed of atoms that can react with each other under specific conditions to form molecules. These molecules interact with each other to form large complex macrostructures, such as living organisms. The ability of biological organisms to control the arrangement of atoms has resulted in the development of various evolutionary adaptations, such as the ability to climb up walls and the production of fibres stronger than steel (Kumar and Kumbhat, 2016). Throughout the course of ancient technological advancement, humans have also made use of the manipulation of materials at a small scale. Examples of such instances include the Ancient Mayan paint, which has stood the test of time for centuries, and the infamous Lycurgus cup, capable of changing colours (Sanchez *et al.*, 2005; Freestone *et al.*, 2007). It was due to a 1959 presentation by Richard Feynman that a rapid development begun towards the manipulation of atoms and molecules for use in new technologies (Feynman, 1959). This presentation would result in the formation of a new field of study concerned with the assembly of atoms and molecules at the nanometre scale, termed "Nanoscience".

Materials with physical dimensions limited to the nanometre scale have become referred to as "nanomaterials" or "nanoparticles" (NPs). These materials can be further classified based on which of their three dimensions are limited to less than 100 nm in length after synthesis. The four classes formed based on dimensionality are; 0-dimensional (spheres or clusters), 1-dimensional (thin films or surface coatings), 2-dimensional (nanorods or nanotubes) and 3-dimensional nanomaterials (nanocrystallites) (Kumar and Kumbhat, 2016).

Due to the size reduction, the total number of atoms on the materials surface increases which in turn increases the total surface energy. Materials which contain a high surface energy tend to be unstable. For these materials to become stable, the atoms must take up configurations that are not typically seen in bulk counterparts. As a result of these new configurations and higher total surface energy, the atoms interact differently within the material (Gogotsi, 2006). These interactions allow the resulting nanomaterial to adopt new and useful physiochemical properties, which are uncharacteristic of the material used for synthesis. An example of how these size reductions alter material properties can be seen in carbon-based nanomaterials. By limiting the overall size of carbon quantum dots (CQDs) the electrons become restricted to the

smaller dimensions. This results in an increase of the exciton transition energy, altering the absorption-emission spectra of the CQD. These alterations result in CQDs, which consist entirely of carbon atoms, having tuneable luminescent properties dependant on parameters of synthesis (Yoffe, 2002; Bera *et al.*, 2010).

1.2. Polystyrene particles as a carbon-based nanoparticle model

Carbon is an element frequently used as the base material in the synthesis of nanomaterials. A subcategory of engineered nanomaterials has thus been recognized in which the members are characterized as being nanoscaled carbon allotropes (Kumar and Kumbhat, 2016). By extension, this subcategory may also incorporate certain polymeric NPs in which carbon is the predominant element. It should be noted that polymeric NPs form a category of their own, whereby their mesh like arrangement is exploited. In this instance, it is the morphology by which these NPs are classified (Zielińska *et al.*, 2020). Classification of polymeric NPs based on their elemental composition would thus place them within different categories. Polystyrene is one such polymeric NP in which there is an abundance of carbon. The work of Rendón-Patiño *et al.* (2019) shows that polystyrene may even be used as a carbon source for the formation of graphene. Classification of polystyrene NPs (PNPs) based on their elemental composition would therefore allow it to be considered a nanoscaled carbon allotrope.

The aromatic hydrocarbon polymer, polystyrene, is produced through the polymerization of styrene monomers. This plastic is widely used in the production of toys, pens, cups, packing materials and medical supplies (Scheirs and Priddy, 2003). Polystyrene is known to be biocompatible and is routinely used for the production of laboratory equipment, particularly those used in cell-based experiments (Van Midwoud *et al.*, 2012). The nanoscaled PNPs have also been shown to have a broad range of uses within photonics, biosensors, and cellular imaging (Liu *et al.*, 2008; Huang *et al.*, 2018; Kamimura *et al.*, 2019). The commercial availability of PNPs and their easy synthesis over a broad size range, provides a readily available model for studies wishing to assess the effects surface alterations have on biological systems (Chen *et al.*, 2011a; Loos *et al.*, 2014a).

1.3. Safety and environmental release of NPs

The proliferation of nanotechnology in medical advancements and industry would lead to an increased presence within the environment. Once in the environment, the properties of these particles could be further altered when encountering other natural substances. The concerns related to silver-NP (Ag-NP) usage illustrates the potential for environmental release. Ag is considered relatively harmless to humans and hosts antibacterial properties (Silver *et al.*, 2006). This has led to the development of new health supplements, antibacterial soaps, detergents, lotions, cosmetics, water purifying agents, and odour-resistant articles of clothing such as socks (Fabrega *et al.*, 2011; Yu *et al.*, 2013). However, the release of Ag-NPs into the environment can occur through actions as simple as washing of the item containing the NPs, where the Ag ions then enter the environment (Benn and Westerhoff, 2008). Additionally, the release of Ag could occur during the production and manufacturing stages of the Ag-NP containing products. Modelling data suggests that the increased release of Ag-NPs from production to usage may lead to increased prevalence in soil, landfills, surface and ground water, and the atmosphere (Gottschalk *et al.*, 2009). Nanostructures thus represent a potential new class of toxic particles if they were to enter the environment.

While the PNP model is useful for determining effects of NP surface alteration, it must be noted that the plastic from which these NPs are derived persist in the environment. It was reported that in 2015 more plastics, such as polystyrene, were being produced than in the previous decade. The global annual estimation at that time had shown there was approximately 320 million tonnes of plastic being produced (Plasticseurope, 2016). The environmental impact of this had become increasingly evident when investigations begun to show that increased production was met with an exponential increase in plastic pollution (Lebreton *et al.*, 2018). Since then, great effort has been made by some nations to reduce the environmental burden of plastic waste, through the implementation of recycling practices. Despite these efforts, the global annual estimate of 2019 had shown that plastic production had reached 368 million tonnes. Thus, after a four-year period there had been a 48 million tonne increase in the volume of plastics produced. Many nations have yet to implement measures to reduce the growth rate of plastic production, with much of their produced plastic being released into the environment (i.e., landfills) (Plasticseurope, 2020). It should be noted that the growth rate of plastic production during the 2020 period had been considerably reduced due to the Covid-19 pandemic.

The environmental burden of plastic can be attributed to the mismanagement of plastic waste as global plastic production escalates. Plastic may enter the environment in several ways. Examples include littering, illegal dumping, landfills, accidental release, ineffective plastic treatment, and human coastal activity. Most of the plastic released from land-based sources due to mismanagement is thought to enter the oceans (Jambeck *et al.*, 2015). Plastic may also be directly released into the environment through its intended application. Such areas of application include hand cleansers and air-blasting technology (Cole *et al.*, 2011). The released plastic is then susceptible to various biological, chemical, and physical factors. Certain degradation mechanisms occur upon exposure to these factors, in which the plastic is fragmented into dispersed smaller constituents. These smaller constituents may be characterized by the extent of this fragmentation. However, it has been reported that the nomenclature used for this characterization are at times inconsistent. Table 1.1 provides a brief description of the nomenclature used to describe the degraded plastics (Singh and Sharma, 2008; O'brine and Thompson, 2010; Andrady, 2011; Cole *et al.*, 2011; Alimba and Faggio, 2019). These reductions in size allow plastics to be ingested or taken in by organisms which would not otherwise do so. The accumulation of degraded plastics then induce serious health implications within these organisms and, to a greater extent, negatively affect the ecosystems these organisms contribute to (Alimba and Faggio, 2019).

Studies have demonstrated that objects made from polystyrene, subjected to environmental conditions, undergo degradation to form micro- and nanoplastics of various shapes (Lambert and Wagner, 2016; Efimova *et al.*, 2018). These findings show that PNPs are among those NPs considered as a hazardous material already present in the environment. While the intended use for the PNP model is aimed at the assessment of surface alterations and its accompanied effects, literature suggests this model may also be used for the preliminary assessment of polystyrene nanoplastic ecotoxicity.

Table 1.1: A brief description of the nomenclature used to categorize degraded plastics as mentioned in the works of Singh and Sharma (2008), O'brine and Thompson (2010), Andrady (2011), Cole *et al.* (2011), and Alimba and Faggio (2019).

Nomenclature	Description	Diameter
Macroplastic	Plastic directly released into the environment	>25 mm (Easily identified by the naked eye)
Mesoplastic		5 – 25 mm (Barely identifiable by the naked eye)
Primary Microplastic	Produced for use in industry and released upon use	20 µm – 5 mm (Visible through microscopy)
Secondary Microplastic	Produced through degradation of plastic into smaller constituents	
Primary Nanoplastic	Produced for use in industry and released upon use	1 nm – 20 µm (Visible through microscopy)
Secondary Nanoplastic	Produced through degradation of plastic into smaller constituents	

1.4. Surface functionalization and its usage

Nano-based technologies are highly desired for the unique properties achieved through size restrictions. Nanostructures achieve a higher surface-to-volume ratio during synthesis, resulting in a greater rate of interaction between the nanostructure and cellular components (Shang *et al.*, 2014; Singh *et al.*, 2018). This would pose some issue if the NPs used are also involved in reactions with biomolecules other than the target to induce unwanted effects. Therefore, the same desirable commodity is the factor limiting their implementation within a biological environment. A repercussion of this greater interaction is the occurrence of

undesired secondary effects. For new nano-based therapeutic and diagnostic technologies to be successfully implemented, a means of limiting these undesired interactions must be present. This requirement is met through surface functionalization. This process involves the tailoring of nanostructure surfaces to meet endpoint goals (Mout *et al.*, 2012; Sanità *et al.*, 2020). One way in which this tailoring can be done is through the addition of functional groups. Examples of functional groups used to achieve functionalization are amine and carboxylate groups. The PNP model makes use of these functional groups for the study of cationic and anionic surfaces, respectively. These functional groups may also be used in tandem for the bioconjugation of molecules to the surface of NPs (Biju, 2014).

The addition of functional groups to NP surfaces may serve to alter the charge of the NP or provide the foundation upon which a secondary molecule is attached (Verma and Stellacci, 2010; Pavlidis *et al.*, 2012). The altered charge provided by these functional groups have been seen to act as the determining factor of a nanostructure's ability to enter cells. This was demonstrated in the work of Villanueva *et al.* (2009) that showed charge provided by functionalization influenced internalization. Here, positively charged NPs were internalized by HeLa cells over long periods. Those NPs of a more neutral to negative charge were either not internalized under all conditions or had been cytotoxic (Villanueva *et al.*, 2009). This was later shown to also be true for PNP uptake by THP-1 cells, where a positive correlation between the amount of internalization and zeta-potential was found. While positive charges are desirable for when NP-cell interactions require enhancement, negatively charged NPs would be desired in cases where these interactions are to be avoided (Goodman *et al.*, 2004). These results illustrate the contribution of charge for optimal NP functioning. Thus, surface functionalization and charge are important parameters for the practical implementation of NP-based medical solutions.

1.5. Surface functionalization related toxicity

While surface functionalization is intended to be beneficial, these alterations can also contribute to the toxicity of a NP (Oberdörster *et al.*, 2005). Jevprasesphant *et al.* (2003) had shown that in Caco-2 cells, positively functionalized poly(amidoamine) dendrimers induce greater levels of cytotoxicity in comparison to dendrimers which have had the positive functional groups masked (Jevprasesphant *et al.*, 2003). This cytotoxicity is thought to be the result of increased internalization of the NP in question by specific cell types, which is driven

by a positively charged surface (Sanità *et al.*, 2020). A surface charge promoting internalization may, in some cases, be required to ensure the NP functions properly. Such an instance can be seen in the case of MC3T3-E1 osteoblast cells being exposed to positively charged hydroxyapatite-NPs (HAP-NPs). HAP is a primary inorganic component of bone. Positively charged HAP-NPs have improved internalization and, due to the material used for synthesis, increased cell viability of osteoblast cells (Chen *et al.*, 2011b). These results briefly illustrate that; 1) the means of surface functionalization and the charge obtained from functionalization are not preferential but subjective, and 2) the extent to which these same alterations contribute to a NPs toxic potential must be assessed.

1.6. Nanoparticle modulation of immune response and related immunotoxicity

The cells of the immune system are responsible for the removal of foreign material within living organisms. NPs are examples of foreign materials susceptible for removal by cells of the immune system (Parkin and Cohen, 2001; Fadeel, 2019). While NP formulations can be beneficial, they are often first picked up by macrophages of the immune system and cause undesirable interactions, such as immunostimulation and immunosuppression. These modulatory effects may also be beneficial in areas such as vaccine development and treatments of inflammatory disorders (Ryan *et al.*, 2007; Zhao *et al.*, 2014). However, uncontrolled immunostimulation and immunosuppression by NPs could lead to the development of allergic reactions and reduction in the body's ability to mount an effective immune response (Brayner, 2008; Nygaard *et al.*, 2009). The recognition of these foreign NPs by the immune cells with a subsequent response of the immune system could lead to toxicity within the host or a reduced effect caused by the NP (Zolnik *et al.*, 2010).

Immunotoxicity during NP exposure is a phrase used to collectively refer to damaging effects brought about by the NP-immune cell interactions, disturbing the balance of the immune system. These damaging effects include the suppression of immune responses, lymphocyte activation, upregulated cytokine production, and/or interferon response (Brayner, 2008; Dwivedi *et al.*, 2009; Rezaei *et al.*, 2019). The properties of NPs are important considerations for practical applications. These properties also dictate the way NPs interact with biomolecules when applied to a biological system. Therefore, to determine whether a NP can alter immune response/signalling, it is important to understand the way these properties alter immune cell function. Properties which should be assessed include, size, morphology, composition, surface

area and surface chemistry, etc (Brayner, 2008; Gaumet *et al.*, 2008; Chen *et al.*, 2011a; Wang *et al.*, 2021). Modifications in the surface chemistry are of particular importance in mitigating the toxic effect of NPs on immune cells. A report on titania NPs functionalized with poly(ethylene glycol) (PEG) induced little cytotoxicity in L929 fibroblasts and J774.2 macrophages. Here, the addition of PEG was noted to provide anionic surface charges (Kotsokechagia *et al.*, 2012). Another report on the use of nanoprobes coated with anionic silica, had shown the shift to a more negative charge reduced cytotoxicity in L929 fibroblasts. The addition of silica prevents oxidative stress by blocking metal ion interaction with living cells, where the interaction with silica instead had little reductions in cell viability (Atabaev *et al.*, 2016). These studies demonstrate the importance of surface modification of NPs for application in the immune system. It is thus important to understand the effect NP formulations have on cells of the immune system, as to better predict potential side effects which may arise or highlight potential benefits within the immune system.

This study aimed to monitor the effects of differently functionalized PNPs on immune responses using *in vitro* exposures to murine RAW 264.7 cells. This was done by assessment of cytotoxicity, inflammatory biomarkers, and molecular biomarkers of the immune system.

1.7. Project Objectives

There are numerous nanomaterial formulation present within literature, each providing unique benefits associated with their usage. The widespread application of these materials within biological systems still poses many limitations. Research into nanomaterial effects on biological systems are thus imperative to finely controlling the functioning of these materials. A means of overcoming limitations to meet end point goals within biological systems is the altering of nanomaterial surfaces for greater tolerance by cells. One such system important to the fate of nanomaterials in living organisms is the immune system. In order to understand if these surface alterations truly mitigate the adverse effects caused by nanomaterials in cells, research into the effects these surface alterations have on immune response must be undertaken.

1.8. Research Aims

- The aim of this research was to use the murine macrophage cell line, RAW 264.7, to assess the effect amine and carboxylate surface functionalization has on immune response in comparison to unmodified NPs by way of *in vitro* cultures.
- Characterization of nanoparticle size and charge in differing suspension media.
- Determine the effect surface alteration has on cell viability.
- To determine the effect of surface alteration on the production of immune biomarkers (Nitric Oxide and Interleukin-6).
- Qualitatively assess the biochemical signals altered by differing nanoparticle surfaces.

1.9. Hypothesis

H_0: Nanoparticle surface functionalization has no effect on pathways regulating immune response.

H_1: Nanoparticle surface functionalization has an effect on pathways regulating immune response.

Chapter 2:

Literature Review

2.1. The Immune System

The immune system is a system comprised of cells, tissues, organs and molecules which act against the invasion of infectious organisms. The main function of the immune system is to collectively prevent/eradicate infections by eliciting an effective immune response. The immune system achieves this function by discriminating between host elements and those of the infectious agent. This discrimination has also shown to be involved with various other physiological processes, the implementation of which can be seen in the ability to prevent cancerous tissue growth, the removal of dead cells and initiating the repair of tissues (Eming *et al.*, 2009; Nagata *et al.*, 2010; Giraldo *et al.*, 2015). The immune system defence mechanism can be separated into two divisions based on the period in which the defences develop. These divisions are the innate immune system and the adaptive immune system (Chaplin, 2006; Abbas *et al.*, 2016). While these systems are distinctly different, each comprising separate mechanisms, they function together to produce coordinated responses against invading organisms.

2.1.1. Divisions of the immune system

2.1.1.1. Innate Immune System

The innate immune system is the first form of immunity present in the host. This form of immunity is present in healthy individuals from birth. This division of immunity is passed down through germline cells resulting in the mechanisms of this division being coded within host genes. These genes are responsible for the production of effector cells, anti-microbial peptides, soluble compounds, cellular barriers and cell receptors which respond to invading microbe antigens. This division is not capable of responding to microbial components of an individual organism. Instead, this division focuses on responding to those antigens conserved across groups of microbes (Chaplin, 2006; Anaya *et al.*, 2013; Abbas *et al.*, 2016).

The innate immune system includes the cellular barriers which provide both physical and chemical protection. The physical barriers separate the host's internal environment from the external environment. These barriers are formed from epithelial and mucociliary cell lined

surfaces which serve to halt the microbe invasion. The skin is one such barrier, providing both physical and chemical protection. The physical aspects of this barrier can be attributed to the presence of keratinocytes which are firmly held together by desmosomes. Keratinocytes also contribute to the chemical barrier of the skin (Szolnoky *et al.*, 2001). These cells contain receptors which, when stimulated by injury and/or infection, initiates the production of anti-microbial peptides and cytokines. Together, these molecules induce an inflammatory response for the destruction of invading microbes. Sebaceous glands within the skin acts to lower the pH of the skin through the production of fatty acids. As a result, microbes struggle to thrive in this hostile environment (Afshar and Gallo, 2013).

Cells associated with the innate immune system have the ability to detect microbial components, known as pathogen-associated molecular patterns (PAMPs). PAMPs are components within microbes which are shared and are relatively conserved across various microbial species. The recognition of PAMPs is made possible by the presence of specialized proteins, known as pattern recognition receptors (PRRs) (Takeuchi and Akira, 2010). The genetic information encoding PRRs are passed down through the germline cells. In this way, the host is thus capable of initiating an immune response against commonly encountered microbial components. However, this mechanism is not capable of identifying various components of a single microbe. This recognition is not solely limited to invading microbial components but host components as well. These components, or damage associated molecular patterns (DAMPs), are produced due to tissue injury and/or the presence of microbial components (Andersson *et al.*, 2000). The PRRs used by the innate immune system include Nod-like receptors (NLRs), Toll-like receptors (TLRs), RIG-I-like receptors (RLRs) and C-type lectin receptors (CLRs). NLRs function to detect bacterial components located within the host cell cytoplasm and TLRs are located on host cell membranes and detect microbe specific components. These components vary from microbial lipoproteins to nucleic acids. Endogenous host components produced during infection may also serve as a TLR stimulus (Funderburg *et al.*, 2007). RLRs function to detect viral RNA produced during viral replication within host cells. CLRs detect similarly constructed sugar molecules within bacteria and fungi (Hoffmann *et al.*, 2013).

Effector cells of the innate immune system are those capable of immediately responding to infection through stimulation of PRRs. These cells include epithelial and endothelial cells, innate lymphoid cells, natural killer (NK) cells, platelets and phagocytes. Phagocytes are cells which are recruited to the site of infection during an injury. Once recruited, phagocytes ingest

the foreign material for intracellular degradation (Tonetti *et al.*, 1994). Phagocytes consist of dendritic cells, granulocytes and monocytes/macrophages. Dendritic cells function as antigen presenting cells. These cells ingest microbial antigens produced during the initial immune response. The dendritic cells then transport the antigens from the peripheral lymph nodes to the primary lymph nodes. It is in the primary lymph nodes that the antigens are presented to cells of the acquired immune system, thus serving as a linkage point between the division. These cells also serve to produce a co-stimulatory signal required for T-cell activation (Banchereau and Steinman, 1998). Granulocytes are the cells which are active during the early stages of the innate immune response. These cells identify and ingest invading pathogens. The mechanism by which this ingestion occurs depends on the cell type observed. These cells further assist in the immune responses through the production of inflammatory mediators, antimicrobial peptides and proteases (Reeves *et al.*, 2002; Varadaradjalou *et al.*, 2003; Verreck *et al.*, 2006).

The innate immune system also employs an assortment of circulating and membrane-bound proteins in the defence against invading pathogens, known collectively as the complement system (Abbas *et al.*, 2016). The activation of the complement proteins is followed by an enzymatic cascade, or complement pathways, for the production of anaphylatoxins which illicit various physiological responses. Given the nature and multitude of responses, these pathways are subject to a great degree of regulation at various points (Sarma and Ward, 2011). The three complement pathways responsible for this complement activation is the alternative, classical and lectin pathways. Figure 2.1 illustrates the different complement pathways. These pathways differ in their requirements for activation but all function around the central plasma protein, complement component 3 (C3) (Abbas *et al.*, 2016). The alternative complement pathway is initiated by pathogen derived surface proteins, lipids and carbohydrates. C3 is constantly hydrolysed and stabilized when bound to pathogen, where this C3(H_2O) will be used to form the initial C3 convertase of the alternative pathway. The membrane bound C3(H_2O) then binds to Factor B, that is susceptible for cleavage by Factor D. This results in the formation of the of the initial C3 convertase C3(H_2O)Bb, which cleaves C3 into C3a and C3b. The produced C3b replaces the initial C3(H_2O) when bound to pathogen surface components and through amplification gives rise to the membrane bound C3 convertase, C3bBb. These convertases require the presence of properdin to prevent their cleavage by Factors H and I (Qu *et al.*, 2009; Abbas *et al.*, 2016). The lectin pathway is activated through the binding of mannose binding lectin (MBL) with the carbohydrate complexes on pathogen surfaces (Wallis, 2007). This MBL circulates as complexes with MBL-associated serine proteases (MASPs), where upon the

binding to pathogens initiates MASPs for the cleavage of C4 to for C4a and C4b. The produced C4b bind to the pathogen surface to associate with C2, which is then cleaved by MASP to form C2a and C2b. The bound C4b associates with the newly formed C2a to form the lectin pathway C3 convertase, C4bC2a (Wallis, 2007; Qu *et al.*, 2009). Unlike the previous pathways, the classical pathway makes use of antibodies and is thus considered a component of the adaptive immune system (Abbas *et al.*, 2016). The classical pathway is initiated by the binding of IgM or IgG to pathogen antigens and the C1 complex. This C1 complex consists of C1q, the recognition element, bound to the serine proteases C1r and C1s. Binding to the C1q leads to activation in C1s and C1r for the cleavage of complement proteins. These proteins are C4 and C2, giving rise to the formation of the C3 convertase C4bC2a (Nauta *et al.*, 2004). The C3 convertases C3bBb and C4bC2a produce C3a and C3b, where the released C3b will function as an opsonin to amplify the complement activation. The released C3b will also form complexes with the C3 convertases to produce the C5 convertases, C3bBbC3b and C4bC2aC3b. The C5 convertases will cleave C5 to form C5a and C5b. The produced anaphylatoxins C3a, C4a and C5a serve as proinflammatory mediators during an immune response. The produced C5b binds to the pathogen membrane to associate with the C6, C7, C8 and several C9 molecules to form the membrane attack complex (MAC). The MAC creates pores in the membranes causing cell lysis for the elimination of the pathogen (Nauta *et al.*, 2004; Wallis, 2007; Qu *et al.*, 2009). While these pathways each make use of an individual recognition mechanism, the alternative pathway may serve as an amplification loop for the classical and lectin pathways (Harboe and Mollnes, 2008).

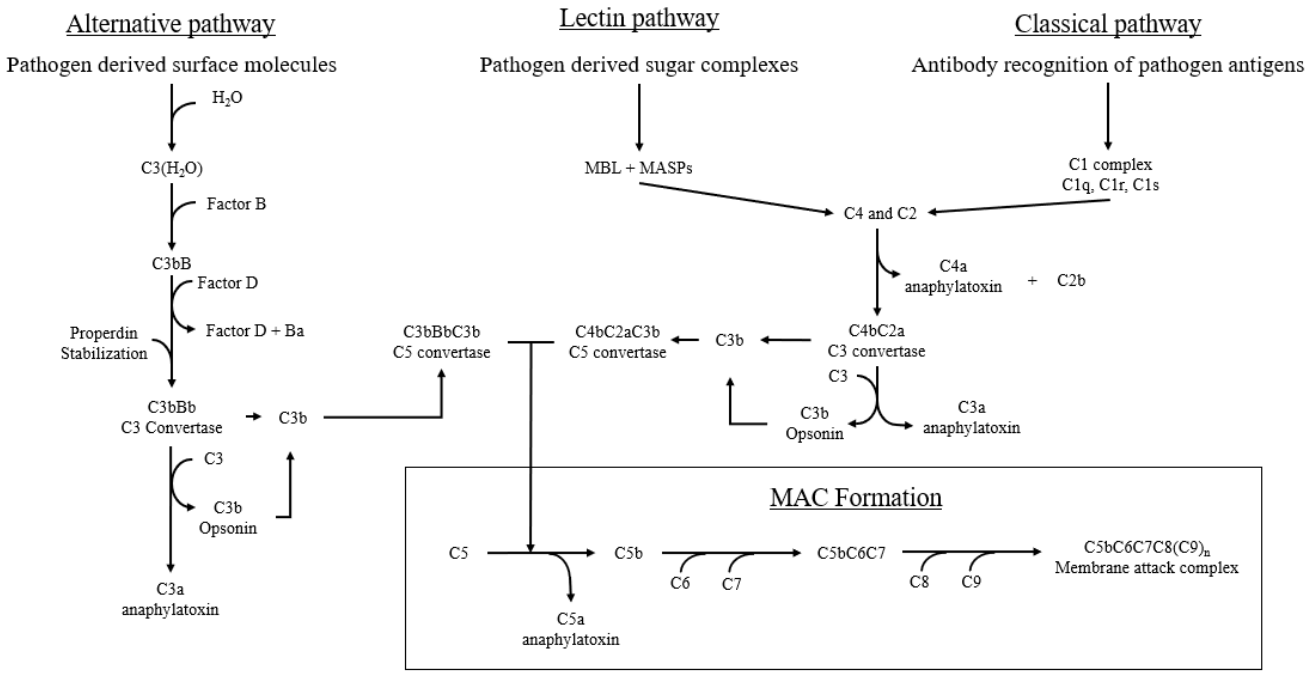

Figure 2.1: A figure depicting the three pathways for complement activation. Adapted from the work of Nauta *et al.* (2004), Wallis (2007), Qu *et al.* (2009) and Sarma and Ward (2011).

2.1.1.2. Adaptive Immune System

Throughout the life of a multicellular organism, there is constant exposure to various microbial species. These organisms have developed simple defence mechanisms against pathogens, which form the first line of defence. However, vertebrates possess more elaborate defence mechanisms capable of tailoring the immune response toward various components of a single invading microbe. These mechanisms will also ensure that the immune system has memory of exposure to an organism and that the immune response to recurrent infections will be faster. These defences make up the adaptive immune system (Cooper and Alder, 2006). The adaptive immune system will function to produce efficient removal responses to both invading microbes and their associated toxins. To achieve this specific removal of foreign material or invaders, the innate immune responses recruit the most appropriate aspect of the adaptive immune response. The adaptive immune system can be subdivided into the humoral and cell-mediated immune responses (Banchereau and Steinman, 1998; Abbas *et al.*, 2016). Each subdivision of the adaptive immune system makes use of a different type of lymphocyte. The lymphocytes which participate in the adaptive immune response include T-cells and B-cells (Abbas *et al.*,

2016). Growth of these cells will begin in the bone marrow and end in the thymus and peripheral lymph nodes, respectively.

T-cells house receptors which specifically detect special complexes formed from microbial peptide antigens and host proteins. These receptors are assembled from three gene elements. These gene elements are randomly altered within each T-cell, where a single T-cell will contain a single type of T-cell receptor. Selection of a functional T-cell receptor gene sequence is then carried out within the thymus (Gellert, 2002; Miller, 2002). T-cells which undergo this selection will house two co-receptors. These co-receptors bind specifically to one of two host molecules which form a complex with invader antigens. T-cell selection will first include a positive selection, ensuring that the receptor reacts with a specific complex of foreign peptides and host peptides. This is followed by a subsequent negative selection, where the receptor is differed from strong reactivity with complex host peptides. T-cells which fail each selection process are terminated, where only those with moderate reactivity with host peptides remain (Miller, 2002; Abbas *et al.*, 2016). The T-cells produced will be cluster of differentiation (CD) 8+ and CD4+ T-cells.

The recognition of foreign peptides only serves as a single stimulus for a given CD4+ T-cell. In order for these cells to produce an immune response, co-stimulatory signals produced by the innate immune response to microbes must also be present. CD4+ T-cell proliferation and differentiation genes are activated once this requirement has been met. CD4+ T-cells differentiate into effector T-cells which migrate toward the origin of the foreign antigen. The direction of this differentiation is determined by the nature of the activating signal (Mosmann and Coffman, 1989; Amsen *et al.*, 2009). Regardless of which direction differentiation occurs, the alternate direction is inhibited by that direction's biochemical signals. Biochemical signals produced by macrophages and natural killer cells result in the differentiation of T helper (Th) 1 cells. Th1 cells will function to enhance the activity of these cells to destroy ingested extracellular invaders. When the biochemical signals are produced by natural killer T-cells and mast cells, Th2 differentiation occurs. Th2 cells produce signals which cause alternative macrophage activation which results in anti-inflammatory effects and wound repair. Th2 cells will also assist antibody production. CD8+ T-cells, or cytotoxic T-cells, may be stimulated by any cell infected with an intracellular invader. During the infection, the cells degrade peptides of the invaders and present them on the cell surface. Cytotoxic T-cells will function to eliminate these infected cells through the release of cytotoxic proteins (Barry and Bleackley, 2002).

B-cells are characterized by the development of specialized recognition proteins known as antibodies or immunoglobulins (Ig's). These Ig molecules are separated into classes based on protein chain structure. These cells are derived from the cells within bone marrow and use a similar mechanism to those used for T-cell receptor production. However, unlike the T-cell receptors, the antibodies produced have the ability to recognize complex structures. Antibodies that are produced through naïve B-cell development are membrane-bound and are of the IgM and IgD classes. It is only after binding to antigen and stimulation by T-cells will the specific B-cells produce progeny which secrete the IgM molecules, while others produce Ig molecules of different classes. This process is known as isotype switching and may be assisted by the biochemical signals of the responding CD4+ T-cells, where the class of the new Ig molecule is based on the specific signal. This process may also occur without the T-cell if the B-cell is stimulated by multiple units of the same antigen. It is also during this isotype switching that mutations are produced in the antigen-binding segments of the encoding genes. These mutations influence the binding affinity of the new Ig molecule for the same antigen where those of higher affinity are selected (Honjo *et al.*, 2002; Cerutti, 2008; Peled *et al.*, 2008). The adaptive immune response produced is dependent on the class of Ig molecule produced. These responses include pathogen destruction pathways, promote inflammation, enhance phagocyte activity and enhance immune cell response to pathogen (Chaplin, 2003; Abbas *et al.*, 2016).

2.1.2. Macrophages

2.1.2.1. Origin

Macrophages are produced through the differentiation of blood born monocytes. These monocytes are derived from bone marrow. It is when these monocytes migrate into the inflamed tissues that they become macrophages (Van Furth and Cohn, 1968; Abbas *et al.*, 2016). These phagocytic cells then ingest invading microbes via the process of phagocytosis. Macrophages may be initiated to undergo this process via various mechanisms. The exact mechanism will depend on the immune response occurring. This may be either that of the innate or adaptive immune system. Upon stimulation, phagocytosis will begin with the extension of the macrophage plasma membrane to internalize the invading microbe in an intracellular vesicle known as a phagosome. This phagosome will fuse with a digestive enzyme containing vesicle, known as the lysosome, to form the phagolysosome (Abbas *et al.*, 2016). At the same time, the macrophage will receive signals via receptors as the immune response takes place. This additional stimulation will serve to activate phagolysosome enzymes such as phagocyte

oxidase, lysosomal proteases and inducible nitric oxide synthase (iNOS) (Schnyder *et al.*, 1980; Shiloh *et al.*, 1999). Phagocyte oxidase functions to increase production of microbicidal reactive oxygen species (ROS). The lysosomal enzymes will act to degrade microbial proteins within the phagolysosome. iNOS will catalyse the conversion of arginine to nitric oxide (NO). NO is one of the most immunologically active molecules as its functions range from the killing of invading microbes to regulating immune responses (Bogdan, 2001).

2.1.2.2. Role in the adaptive and innate immune system

Macrophages, like dendritic cells, are cells which play roles in both the innate and adaptive immune system. In the innate immune system, macrophages are responsible for the immediate defence against invaders and recruitment of other immune cells. In the adaptive immune system, macrophages coordinate the immune response based on the present biochemical signals (Abbas *et al.*, 2016). Macrophages may be classically activated via the co-stimulation by interferon-gamma (INF-γ) and microbial products/antigens (Adams, 1989). As part of the innate immune system, macrophages may be solely activated through PAMP stimulation of PRR (Mukhopadhyay *et al.*, 2004). Macrophage recognition of invaders may be enhanced via coating with specialized proteins, or opsonization. These opsonin molecules are produced by the catalytic pathway used for the killing of microbes, known as the complement system. Opsonin molecules are detected by macrophage surface receptors and facilitate ingestion by macrophages. Macrophages subsequently produce proinflammatory mediators and cytokines, including tumour necrosis factor-alpha (TNF-α), NO, interleukin-12 (IL-12), etc. The produced IL-12 may stimulate NK cell receptors to increase NK cell production of INF-γ. NK cells then produce INF-γ which activates macrophages for the killing of ingested microbes (Kobayashi *et al.*, 1989; Abbas *et al.*, 2016). This innate response will direct events of the adaptive immune system. The combined cytokine response which accompanies macrophage activation directs Th1 differentiation and inhibits Th2 differentiation. The cytokines produced by Th1 cells include TNF, IL-2 and INF-γ. The produced Th1 cell membranes house the CD40 ligand. The increased presence and binding of the CD40 ligand to macrophage receptors initiate transcription factors within macrophages. The produced proteins increases the mechanism used to destroy ingested microbes (Mosmann and Coffman, 1989; Abbas *et al.*, 2016). This classical activation is accompanied by macrophage secretion of proinflammatory cytokines IL-1β, IL-15, TNF-α, IL-6 and IL-12 (Cavaillon, 1994). Th2 cells may serve to induce alternative activation of macrophages. Th2 cell differentiation requires the presence of IL-4 produced by

mast cells and other tissues at the sight of a parasitic infection. The activated Th2 cells then produce IL-4, IL-10, IL-5 and IL-13. The produced IL-4/IL-13 act to upregulate macrophage surface receptors while reducing the microbicidal activity. Macrophages then act to assist in wound repair by stimulating fibroblast proliferation and collagen production. These events occur through the macrophage secretion of polyamines and proline, respectively (Gordon, 2003; Abbas *et al.*, 2016).

2.2. Alterations in the immune system

As briefly discussed, the immune system is a complex system functioning together to maintain the health of the host. The functioning of the immune system may be impaired by various toxic compounds which may leave the host susceptible to disease. These compounds altering the normal functionality of the immune system are referred to as immunotoxic compounds. These compounds may do this by supressing, elevating, or increasing the sensitivity of the immune response. Immunosuppression is the event in which a compound will prevent the completion or inhibit the activation of the immune response. As a result, the affected host will have an increased susceptibility to a potentially severe infection. This will occur in the event the compound decreases the number of immune cells, hinders the activity of signalling molecules and/or cause damage to organs of the immune system (Luster and Rosenthal, 1993; Dewitt *et al.*, 2012). Immunostimulation is the event in which a compound enhances the immune system response, manifesting as an enhanced or reduced ability to respond to external stimuli (De Jong and Van Loveren, 2007). Autoimmunity is an altered state of the immune system where host molecules are targeted for attack. This state may be the result of an enhanced immune response, stimulated immune activity or targeting of host molecules that have been altered during contact with toxic compounds (De Jong and Van Loveren, 2007). This state has been shown to be associated with pharmaceutical drugs or therapies. Reactions may occur within specific organs/tissues or may vary in the type of reaction observed. The affected organ/tissues may be affected by functional impairments, inflammation, or permanent damage (Luster and Rosenthal, 1993; Barrons, 1997; Vial and Descotes, 2000). The immune system may become altered to produce an amplified response directed toward foreign toxic molecules, where these responses are accompanied by tissue damage. This state is known as a hypersensitivity reaction that manifests as an allergic response to a foreign molecule. Hypersensitivities are the most common immunotoxic effect produced by pharmaceutical drugs, making these reactions

important areas of research when investigating the toxic potential of foreign materials (Luster and Rosenthal, 1993; Descotes, 2004; De Jong and Van Loveren, 2007).

2.3. Nanoparticle Toxicity

Nanotechnology is a field associated with the development of new technologies through the limitation of material dimensions to a nanometre scale. The dimensions of these produced materials, or nanomaterials, typically limited to less than 100 nm are the: length, breadth and/or width. Nanomaterials may form naturally, unintentionally through combustion reactions or be intentionally engineered. (Kumar and Kumbhat, 2016). The reduced size and altered dimensionality of engineered materials have been shown to give rise to unique physiochemical properties not typically associated with the base material (Yoffe, 2002). There are various methods employed to intentionally engineer nanomaterials, including laser ablation, biosynthesis, spinning, etc. Despite the exact method used for synthesis, it remains an extension of either two central approaches to nanomaterial synthesis: the top-down and bottom-up methods (Ealia and Saravanakumar, 2017). Figure 1.1 illustrates the differences between these approaches. Top-down methods are methods which rely on the reduction of bulk materials to particles within the nanometre scale. This is best exemplified by the process of mechanical milling, in which nanometre sized grain is produced through an energy transfer from a high energy mill to the material undergoing reduction (Yadav *et al.*, 2012). Bottom-up methods were inspired by the ability of biological structures to self-assemble from a set of preprogramed instructions. As a result, approaches to synthesis shifted from using bulk materials as the starting point to allowing atoms to self-assemble into clusters and later NPs. This is easily demonstrated by the process of chemical vapor deposition. In its most simple form, a gas is allowed to flow into a chamber housing a heated object and the chemical reaction at the surface of the object results in the formation of a nanometre sized film (Carlsson and Martin, 2010).

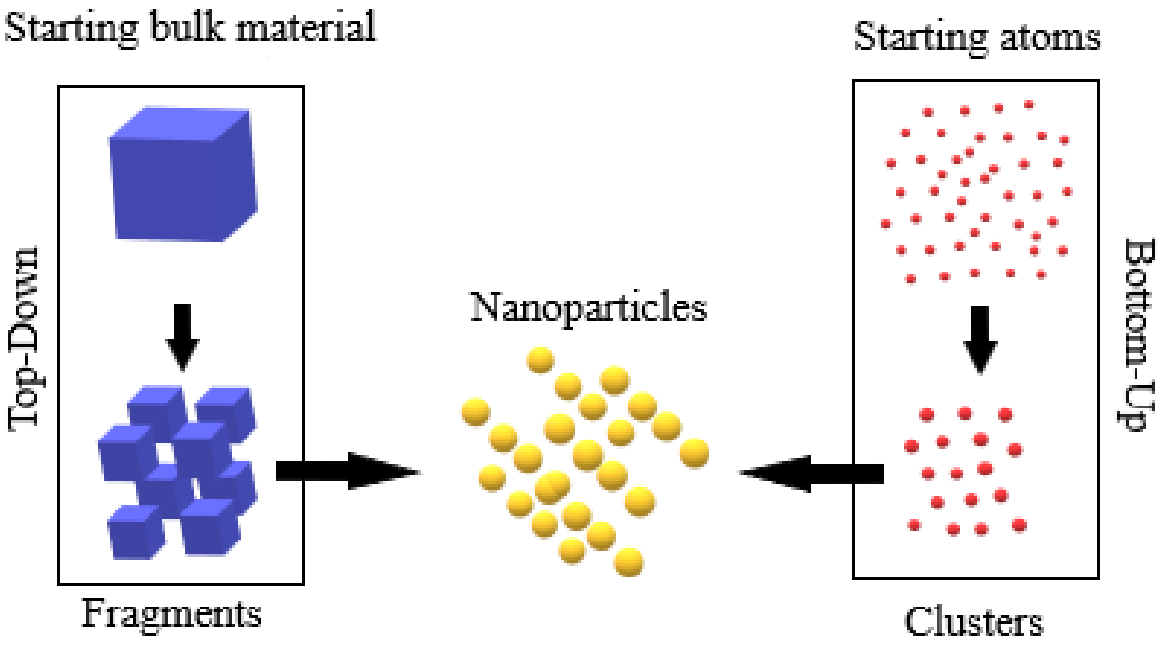

Figure 2.2. A figure depicting the top-down and bottom-up approaches to the synthesis of nanomaterials, adapted from the work of Ealia and Saravanakumar (2017).

These unique materials are coveted as they can be used in the improvement of existing products or development of new products. However, it is the same alterations of these materials which alter their interactions with biological tissues (Nel *et al.*, 2006). The repercussions of such interactions are often severe and would otherwise not be possible without the alteration. In light of the harm which may accompany these materials, nanotoxicology strives to guide and improve the usage of nanomaterials (Oberdörster *et al.*, 2007). The resulting toxicity of nanomaterials when in contact with living cells may be caused by four attributes; 1) chemical toxicity of the material which has been used to synthesize the nanomaterial; 2) the small size of nanomaterials which enhances the uptake nanomaterials, the nanomaterials may then interfere with cellular functions of cells; 3) nanomaterials of a certain shape may overcome cell membranes more efficiently than others; and 4) surface charge of the nanomaterial (Kirchner *et al.*, 2005; Fröhlich, 2012). The exact toxicological profile a given NP produces occurs through these attributes occurring simultaneously.

2.3.1. Influence of material type

There are various approaches to the synthesis of nanomaterials. All these approaches make use of a starting material, of which the entire nanomaterial is composed. The material used to synthesize a given nanomaterial may be the underlying cause of the toxic effects seen. A key example of such an occurrence has been seen in cadmium-containing quantum dot (QD) toxicity. Cadmium (Cd) is a highly toxic element capable of exhibiting toxicity at concentrations lower than commonly found minerals. This element may impair the functioning of various biological systems either directly or indirectly (Rani *et al.*, 2014). These toxic effects have been attributed to the release of Cd^{2+} ions from QDs which in turn disrupts the ROS balance of cells (Kirchner *et al.*, 2005; Rani *et al.*, 2014). In contrast, gold (Au) has historically been considered "biocompatible and inert". As a result, research has shown the vast medical applications of Au-NPs with the associated toxicity having been attributed to the properties manifesting at the nanoscale rather than due to the composition. (Murphy *et al.*, 2008; Naahidi *et al.*, 2013; Daraee *et al.*, 2016).

2.3.2. Influence of size

Small size is the most characteristic trait of all nanomaterials and majorly contributes to the toxicity associated with NPs. The size of NPs often resembles those of signalling molecule recognized by cells (Iversen *et al.*, 2011). Size of the NP in question may serve as the determining factor as to whether cells will internalize NPs. Prior to contact with cells, NPs first encounter many biomolecules. These biomolecules comprise the various sugars, lipids and proteins associated with biological tissues. The NPs are coated by these molecules in what is known as a "protein corona", which dictates how the NP in question interacts with a given cell (Lynch *et al.*, 2009). The unique combination of biomolecules making up a given protein corona depends on the environment the NP must traverse, and which biomolecules are currently present in that environment. The internalization is then driven by cell membrane receptor recognition of the biomolecules on the corona. Size dependant toxicity has been shown to occur in various cell lines with Au-NPs, PNPs, silica NPs and iron oxide NPs (Lu *et al.*, 2009; Huang *et al.*, 2010; Malugin and Ghandehari, 2010; Varela *et al.*, 2012). It should be noted that the NPs reported had varying surface chemistry and where exposed to different cell lines. However, the NP sizes taken up by cells remained between 30-50 nm. NPs of decreasing size, below this range, have a higher surface area relative to the total mass of the NP. The higher surface area provides a higher rate of reactivity of the protein corona coated NP with the surrounding

biological tissues. Thus, the biomolecules of the smaller NPs have a greater chance to interact with the cellular components for the initiation of adverse reactions (Shang *et al.*, 2014).

2.3.3. Influence of charge

Biological environments consist of various molecules, each with distinct weak charges. At the nanometre scale, these weak charges dictate the interactions of the NP. This is particularly important for Au-NPs. Reports on charge related Au-NP toxicity are at times contradictory. This can be attributed to the various synthesis methods employed, resulting in the reported NPs having variable surface chemistry. This is highlighted by the work of Goodman *et al.* (2004) , where Au-NPs of 2 nm with positive surface charges are shown to produce moderate levels of toxicity. When considering size as the sole contributor to toxicity, AuNPs of 13 nm size and above are considered non-toxic within the micromolar concentration range (Jahnen-Dechent and Simon, 2008). However, the work of Connor *et al.* (2005) shows no toxicity in human leukemia cell lines (K562) when exposed to differently capped batches of 4 nm, 12 nm and 18 nm Au-NPs. Shukla *et al.* (2005) reported that lysine and poly-L-lysine capped Au-NPs of 35 nm are weakly cytotoxic to RAW 264.7 macrophage cells over a period of 3 days. These discrepancies may be the result of varying cell lines, differences in the protein corona, and/or the variability of NP surface chemistry. It is commonly accepted that NPs of negative surface charges have greater biocompatibility. The is due to the cell bilayer possessing a negative charge, where positively charged molecules exhibit strong electrostatic attraction to this bilayer (Goodman *et al.*, 2004). This charge related toxicity has been shown to occur in Ag-NPs, zinc oxide NPs and dendrimers (Baek *et al.*, 2011; El Badawy *et al.*, 2011; Greish *et al.*, 2012).

2.4. Surface Functionalization

The application of NPs and nanomaterial structures as part of biomedical solutions has proven to be a complex undertaking. One of the major limiting factors of these solutions is the challenge of lessening interactions with secondary biomolecules while enhancing binding affinity for the primary target (Chou *et al.*, 2011). As mentioned previously, the intrinsic properties of NPs may dictate its fate within biological systems. To mitigate the effect of such occurrences, the surface of nanomaterials may be altered by means of surface functionalization. This process strives to alter nanomaterial surfaces to that of a surface of well-defined chemistry with the greatest specific surface area (Myhra and Rivière, 2012). Once the surface chemistry has been well defined, the nanomaterial can then be conjugated to secondary molecules by means of controlled reactions. These secondary molecules make it possible for the NP in question to have improved solubility, limited aggregation, used in disease diagnostics, biomolecule detection, the detection and differentiation of cells, and drug delivery (Paciotti *et al.*, 2006; Bajaj *et al.*, 2009; El-Boubbou *et al.*, 2010; Jiang *et al.*, 2010; Sperling and Parak, 2010).

The functional group used to modify the surface of nanomaterials depends on the desired molecule/ligand which will be used and the intended use of the NP. Bioconjugation of Au-NPs to antibodies illustrates the various forms of interaction between the surface functional group and the desired molecule which may be exploited (Jazayeri *et al.*, 2016). These interactions can be simply divided into those of absorption on the NP surface, electrostatic, covalent, and non-covalent interactions (Sperling and Parak, 2010; Sanità *et al.*, 2020). For nanomaterial systems intended to be used in biological systems, covalent interactions are usually desired. Covalent interactions ensure that the bound molecule will not be removed from the NP surface in biological fluids while also controlling the orientation of the bound molecule (Kumar *et al.*, 2008; Sanità *et al.*, 2020).

Amine and carboxyl functional groups are groups typically manipulated during NP bioconjugation (Lee *et al.*, 2008; Jazayeri *et al.*, 2016). These functional groups are often used in conjunction where either may be used to functionalize NP surfaces while the other may reside on the desired molecule. These functional groups react by means of a condensation reaction, whereby a peptide bond is formed. Alternatively, the presence of both functional groups on the surface of a single NP my serve to provide a system in which a drug is linked by way of the amine group and targeting antibody linked by way of a carboxyl group (Kralj *et al.*, 2011; Biju, 2014; Zhan *et al.*, 2014; Jazayeri *et al.*, 2016). Amine functional groups alone on

the surface of NPs shift charge to a more positive one. This positive charge then permits bioconjugation by electrostatic attraction (Lee *et al.*, 2008; Bajaj *et al.*, 2009). However, the positive charge contributes to this functional group having been noted to induce considerable toxicity. These reports included comparisons of negatively charged carboxyl functional groups, showing them to be more favourable in NP systems where secondary conjugation is not desired (Greish *et al.*, 2012; Ruenraroengsak *et al.*, 2012). This is an important point of consideration as the number of nano-based biomedical solutions increases within literature. The extent to which NPs induce alterations within the immune system, particularly those induced by amine and carboxyl surface functionalization, must be clearly understood for any implementation to occur (Muhammad *et al.*, 2020).

2.5. Carbon-based Nanoparticle Toxicity

Carbon-based nanomaterials are a broad family of materials which primarily consist of carbon atoms. The reason for this great diversity is as the result of its electron configuration allowing it to adopt a great number of crystalline and disordered structures. These include carbon black, fullerenes, carbon nanotubes, nano-graphite, carbon nano-diamonds, and carbon quantum dots. This diversity has also contributed to a variety of unique properties which may be used in high-performance appliances (Kumar and Kumbhat, 2016). During the synthesis of these materials, the purity of the carbon in the final product differs with the method of synthesis utilized (Jia *et al.*, 2005). The same can be said for other nanomaterials, where trace amounts of different elements can be found in the final structure (Rostek *et al.*, 2011). Polystyrene is an aromatic hydrocarbon polymer, where the predominant element is carbon (Lock *et al.*, 2010). Polystyrene based NPs can thus be, due to its elemental composition, classified as a carbon-based nanomaterial.

PNPs are frequently used as a model to assess NP toxicity (Nemmar *et al.*, 2003; Xia *et al.*, 2006; Loos *et al.*, 2014a). The PNP model provides a means to study the effect of size and surface characteristics in differing biological environments. Cationic and anionic surfaces are provided by way of amine and carboxylate functionalization, respectively. Studies have shown that amine functionalized PNPs (APNPs) are potent inducers of cytotoxicity in a number of cell lines, namely RAW 264.7 (~90 nm and ~415 nm), TT1 (~50 nm), HeLa (~50 nm) and BEAS-2B (~90 nm and ~415 nm) (Xia *et al.*, 2006; Xia *et al.*, 2008; Ruenraroengsak *et al.*, 2012; Sharma *et al.*, 2019). Carboxylate functionalized PNPs (CPNPs) in comparison, shows a

considerable reduction in cytotoxicity. However, cytotoxicity may still be seen in comparison to control cells (Xia *et al.*, 2006; Xia *et al.*, 2008). It has been noted that the differences in charge does not completely account for all instances of uptake and subsequent cytotoxicity, while there is evidence to suggest that phagocytic cell uptake of PNPs does occur in a charge specific manner. These results indicate that APNPs are more efficiently taken up by monocytes and CPNPs by differentiated macrophages (Lunov *et al.*, 2011a; Fröhlich, 2012).

Information related to the immunotoxicity of the PNP model is fairly limited within literature (Muhammad *et al.*, 2020). Unmodified PNPs, CPNPs and APNPs (50 nm, 100 nm) have been shown to increase IL-6 and IL-8 release in TT1 cells after a 24 hour exposure period (Ruenraroengsak *et al.*, 2012). The works of Fuchs *et al.* (2016) shows that the PNPs have complex functioning within the immune system, in which classically activated human macrophage cytokine expression is not impaired by the presence of differently functionalized PNPs. However, both the CPNPs and APNPs are shown to hinder the expression of alternatively activated human macrophage surface receptors and IL-10 release. APNPs reduce the phagocytic ability in both macrophage subsets while protein expression and cellular energy levels of alternatively activated macrophages experience greater alterations by CPNPs. These findings suggest that PNPs may be used as a means of controlling diseases originating from a compromised immune response (Fuchs *et al.*, 2016). Lunov *et al.* (2011b) has also shown that APNPs induce proton accumulation within the lysosome, IL-1β release, cathepsin B release and mitochondrial membrane damage (Lunov *et al.*, 2011b). It is important to consider the extent of PNP alterations on the immune system is the result of protein corona formation (Fadeel, 2019). Both size and charge may significantly impact the type, number and conformation of proteins bound to PNP surfaces (Feiner-Gracia *et al.*, 2017). This may alter the immune response and produce discrepancies in the resulting data (Lundqvist *et al.*, 2008). In order to fully understand the manner in which differently functionalized NPs can alter the signalling of the immune system, comprehensive profiles of immune cell-NP interactions must be established. These profiles should include cytokine profiles of immunologically active cell types, the assessment of functional group activity under different states of immune cell function with the corresponding cellular toxicity, and the quantification of immune cell biomarkers under NP stimulation.

Chapter 3:

Materials and Methods

3.1. Characterization of Polystyrene Nanoparticles

Polystyrene latex NPs (PNPs) were purchased from Sigma-Aldrich (Schnelldorf, Germany). These nanoparticles included the unmodified – pristine polystyrene NPs (PPNPs, 55 nm, Product no. L1148), amine-functionalized polystyrene NPs (APNPs, 50 nm, Product no. L0780) and carboxyl-functionalized polystyrene NPs (CPNPs, 30 nm, Product no. L5155). The surface of unmodified PPNPs were stipulated by the manufacturer to have hydroxyl functional groups present. The surface charge of the interface point between the NP and the surrounding environment was determined by zeta potential. NP size distribution, determined as hydrodynamic diameter, was obtained by dynamic light scattering (DLS). Both properties were assessed for NPs suspended in culture media containing 5 % serum, and NPs suspended in aqueous solution (distilled water) via ZetaSizer (ZetaSizer Nano ZS, Malvern Instruments Ltd.). For measurements of NPs characteristics, stock solution NPs were resuspended in sterile distilled water or serum containing media to a desired concentration of 10 µg/mL. Measurements of NPs within serum containing culture media were taken using washed NPs resuspended in serum containing media, where the final serum concentration was 5 % (v/v).

The concentration of the PNPs to be measured within the respective dispersants was set at 10 µg/mL. Hydrodynamic diameter measurements were taken in disposable sizing cuvettes (Model no. DTS0012) using 4 mL NP suspension. Zeta potential measurements were taken in folded capillary cells (Model no. DTS1060) using 1 mL NP suspension. Measurements were taken at room temperature in triplicate, following the standard operating procedures.

3.2. Preparation of Polystyrene Nanoparticles

A 2 mg/mL stock solution of NP suspended in serum-free media was prepared for all NPs. The commercially obtained polystyrene NPs were resuspended in sodium azide during production. To limit the potential cytotoxicity by sodium azide, NPs were washed prior to exposure to cells (Jones *et al.*, 1980). Washing was performed by centrifugation using ultrafiltration units with a 100 000 molecular weight cut off (Vivaspin®). A volume of 70 µL PPNP stock solution and 280 µL functionalized NP stock solution was placed into individual units. The NPs were

washed 3 times using 1X Dulbecco's Phosphate Buffered Saline (DPBS, Lonza) at 40 000 rpm for 10 minutes. After the final wash, NP solutions were brought to 3.5 mL using serum-free media.

Solutions were then sonicated by a probe sonicator (QSonica, LLC. Misonix Sonicators, XL-200 Series, Newtown, CT, USA) in short bursts on ice for 5 minutes. Solutions were then sterilized by pasteurization at 60 ºC for one hour. Aliquots were stored at room temperature until use.

3.3. RAW 264.7 Cells and Treatment

The cell line used for the experiments were the murine macrophage cell line, RAW 264.7 (American Type Culture collection, Manassas, VA, USA). Cells were cultured in Dulbecco's Modified Eagle's Medium (DMEM, Lonza, Cape Town, South Africa) supplemented with 10 % fetal bovine serum (FBS, Hyclone), 1 % glutamax (Sigma-Aldrich), 1 % antibiotic-antimycotic (Sigma-Aldrich), 0.5 % gentamycin (Sigma-Aldrich). Cells were incubated at 37 ºC with a humidified atmosphere of 5 % CO_2 throughout the experiments. Cells were sub-cultured every 3-4 days when cells were between 70-80 % confluent.

For the experimental procedures, cells were exposed to nanoparticles in 96-well and 24-well plates. The 24-well plates were used to obtain greater volumes of supernatant required for the proteome profile assessment. Cell exposure to PNPs for all other experimental procedures were carried out in 96-well plates. An initial doubling dilution of PNPs was done in the wells, where the resulting concentrations were double the required working concentrations, to a final volume of 100 µL in the 96-well plates and 150 µL in the 24-well plates respectively. The NPs were diluted in serum free media containing 1 % glutamax, 1 % antibiotic-antimycotic, and 0.5 % gentamycin. Each well of the 96-well plates received 100 µL of RAW 264.7 cells ($1x10^5$ cells/mL) in complete culture media containing 10 % FBS, where the resulting FBS concentration was 5 %. For the 24-well plates, each well received 150 µL of RAW 264.7 cells ($1x10^7$ cells/mL) in complete culture media containing 10 % FBS, with a resulting FBS concentration of 5 %. Thereafter, the plates were incubated at 37 ºC with a humidified atmosphere of 5 % CO_2 for 24 hours. This incubation was done to allow cells to reach 80-90 % confluency. Cells were divided into stimulated and unstimulated groups. In the 96-well plates, stimulated cells received 50 µL of serum free media containing 0.2 µg/mL of lipopolysaccharide (LPS, Sigma-Aldrich) with each well having a final LPS concentration of

0.07 µg/mL. Stimulated cells will hereafter be referred to as LPS positive (LPS+). Unstimulated cells (hereafter referred to as LPS negative samples (LPS-)) received 50 µL plain serum free media. For the 24-well plates, wells received 100 µL of the same conditioned media as used in the LPS+ and LPS- 96-well plates. Each group included control cells which were not exposed to nanoparticles. Control cells stimulated with LPS served to imitate an immune response through macrophage activation, whereas unstimulated control cells served to imitate cells in which no immune response was initiated. Plates were incubated for approximately 20 hours. Thereafter, supernatants were removed for analysis of NO, cytokines and proteome profiles.

3.3.1. Cytotoxicity Assay

Cytotoxicity was measured by means of a 4-[3-(4-iodophenyl)-2-(4-nitrophenyl)-2H-5-tetrazolio]-1,3-benzene disulfonate (WST-1) assay (Roche). Briefly, this assay relies of the cleavage of the WST-1 salt into a soluble formazan dye by the metabolic reactions of viable cells. The amount of formazan produced is therefore proportional to the number of metabolically viable cells present.

The assay reagent was prepared by performing a 1 in 10 dilution of stock reagent in complete culture media. Cell culture supernatants were collected after treatment and incubation steps, and cells were washed with 1X DPBS to ensure PNP residue was removed. Washed cells received 50 µL diluted assay reagent. Formazan production by cellular mitochondrial dehydrogenase within the wells was measured at 450 nm (FLUOstar, Omega, BMG Labtech). Absorbance readings were taken immediately after the assay reagent was added. The plate was then incubated at 37 ºC. Thereafter, readings were taken at 30 min and 1-hour incubation intervals. The data was then transferred to Microsoft Excel, where it was used to calculate viability as a percentage of the control.

3.3.2. Nitric Oxide Assay

Cells released measurable amounts of nitrite during overnight exposure to PNPs, serving as an indicator of NO production. Quantification of NO was carried out according to the Griess reaction (Granger *et al.*, 1996). A linear nitrite standard curve, created from the doubling dilutions of a 100 µM nitrite standard (Sigma-Aldrich), was used to quantify the amount of NO produced by cells exposed to PNPs. Griess reagent was made using a 1:1 mixture of 1 % sulfanilamide and 0.1 % naphtylethlemidimine-dihydrochloride in 2.5 % phosphoric acid

(Sigma-Aldrich). Each well had either received 50 µL of the respective cell culture supernatant or nitrite standard, as well as 50 µL of the Griess reagent. After mixing the spent culture supernatant and Griess reagent the absorbance was read immediately using a microplate reader at 540 nm (FLUOstar, Omega, BMG Labtech). The linear standard curve was created in Microsoft Excel by plotting the concentrations of the diluted nitrite standard against the corresponding absorbance readings. The amount of NO produced by the cells was quantified from the resulting linear equation.

3.3.3. Interleukin-6 Double Antibody Sandwich (DAS) Enzyme Linked Immunosorbent Assay (ELISA)

The secretion of the pro-inflammatory cytokine interleukin-6 (IL-6) in the cell culture supernatants was measured by DAS-ELISA (e-Bioscience). All ELISA procedures were carried out in 96-well Maxisorb plates (Nunc, Germany). Dilutions of the cell culture supernatants with the ELISA diluent were performed to ensure produced IL-6 was within detectable levels. A 1:100 (v/v) dilution of LPS+ cell culture supernatant and a 1:5 (v/v) dilution of LPS- cell culture supernatant was performed. All reagents were provided by the kit and the assay was carried out as per the manufacturer's instructions.

3.3.4. Proteome Profile Analysis

Cell to cell communication within a network is regulated through the production of and response to various signalling molecules. The pattern of proteins expressed under specific conditions is known as the proteome profile. Proteome profile kits are commercially available for various cellular pathways such as cytokine pathway, apoptosis, and cell stress. Cytokine proteome profiles of the RAW 264.7 cells under PNP exposure were obtained by using the commercially available mouse cytokine array kit (Proteome Profiler, Mouse Cytokine Array Panel A, R&D Systems). The kit provides a means of assessing the relative expression levels of 40 mouse cytokines in duplicate on a single pre-treated nitrocellulose membrane.

The nitrocellulose membranes were incubated with 500 µL of cell culture supernatant, which was obtained from the 24-well plates. Profiles were obtained from cells incubated under various conditions; without PNPs in the absence of LPS stimulation, 15 µg/mL PNPs in the absence of LPS stimulation, without PNPs in the presence of LPS stimulation, and with 15 µg/mL PNPs in the presence of LPS stimulation. All reagents used, with the exception of the chromogenic

TMB insoluble Western blotting substrate (3,3',5,5'-Tetramethylbenzidine, Thermo Scientific), were provided within the kit and the assay was performed as per manufacturer's instructions. Qualitative analysis was done by adding substrate to sample-antibody complexes labelled with streptavidin-horse radish peroxidase (HRP), where the membrane is stained with the TMB insoluble substrate.

3.4. Statistical analysis

The experiments were performed in triplicate where the resulting data was managed in Microsoft Excel prior to statistical analysis using SigmaPlot (Ver. 12.0). The data is represented as the average ± the standard error of the mean (SEM). Samples were compared by using a one-way analysis of variance (ANOVA) test with results being considered statistically significant at the $P<0.01$ level. After more detailed analysis of the statistical reports, it was seen that the sample comparisons had P-values of weaker ($P<0.05$) and greater ($P<0.001$) statistical significance.

Chapter 4

Results

4.1. Characterization of PNPs in water and biological media

4.1.1. NP characterization within distilled water

ZetaSizer measurements revealed the hydrodynamic diameter and zeta potential of PNPs within distilled water (Table 4.1). Particle size measurements closely resembled those provided by the manufacturer (see Chapter 3). The polydispersity index (Pdi) values provide an indication of particle size uniformity within the given suspension. APNPs size was seen to have the most uniform distribution (0.152 ± 0.018) in water among the tested NPs (Table 4.1). Zeta potential measurements within water indicate that the PPNPs have the most negatively charged interface layer (-28.6 ± 5.7 mV), while APNPs possess the most positively charged layer (19.1 ± 6.4 mV).

Table 4.1: Hydrodynamic diameter and zeta potential of PNPs within distilled water. The data is represented as the average ± SEM where n = 3.

Particle	Manufacturer Mean Diameter (nm)	Z-Average (d.nm) ± SEM	Pdi ± SEM	Zeta Potential (mV) ± SEM
APNP	50*	60.06 ± 0.50	0.152 ± 0.018	19.1 ± 6.4
PPNP	55*	47.08 ± 0.32	0.189 ± 0.008	-28.6 ± 5.7
CPNP	30*	32.46 ± 1.56	0.256 ± 0.027	-14.1 ± 21.8

Measurement parameters: PNP concentration = 10 µg/mL; Viscosity = 0.8872 cP; Dispersant refractive index = 1.330; Dispersant dielectric constant = 78.5; pH = 7.2; Material refractive index = 1.59; Measurement duration = 30 seconds. * - Measurements taken within sodium azide solution. The manufacturers specification sheet did not provide zeta potential measurements.

4.1.2. NP characterization within 5 % serum containing culture media

ZetaSizer measurements revealed the hydrodynamic diameter and zeta potential of PNPs within serum containing culture media (Table 4.2). The diameters of all tested NPs were seen to exceed

50 nm, the greatest increase in diameter being seen in the PPNPs (341.2 ± 21.35 d.nm). The Pdi values for size distribution were seen to be > 0.5 for all the tested NPs. PPNPs were shown to be the most polydispersed within serum containing culture media, with a Pdi of 0.911 ± 0.059 (Table 4.2). Zeta potential measurements within serum containing culture media indicate that the all the PNPs adopted a negatively charged interface layer of similar voltage.

Table 4.2: Hydrodynamic diameter and zeta potential of PNPs within 5 % serum containing culture media. The data is represented as the average ± SEM where n = 3.

Particle	Manufacturer Mean Diameter (nm)	Z-Average (d.nm) ± SEM	Pdi ± SEM	Zeta Potential (mV) ± SEM
APNP	50*	148.9 ± 4.80	0.55 ± 0.049	-29.5 ± 2.0
PPNP	55*	341.2 ± 21.35	0.911 ± 0.059	-29.3 ± 0.8
CPNP	30*	59.5 ± 9.37	0.523 ± 0.060	-28.9 ± 1.7

Measurement parameters: PNP concentration = 10 µg/mL; Viscosity = 3.0 cP; Dispersant refractive index = 1.345; Dispersant dielectric constant = 80; pH = 7.8; Material refractive index = 1.59; Measurement duration = 30 seconds. * - Measurements taken within sodium azide solution. The manufacturers specification sheet did not provide zeta potential measurements.

4.2. The effects of PNPs on LPS- RAW 264.7 cell immune response

4.2.1. Cytotoxicity induced by PNPs in LPS- RAW 264.7 cells

In the absence of LPS stimulation, APNP concentrations ≥ 7.8125 µg/mL were seen to cause highly significant reductions (P<0.001) in cell viability when compared to the 0 µg/mL control (Figure 4.1). At the lowest concentration of APNPs (7.8125 µg/mL), cell viability had decreased by ~55 %. At APNP concentrations of 15.625 µg/mL and 31.25 µg/mL, cell viability had decreased by ~70 % and ~90 %, respectively. For APNP concentrations ≥ 62.5 µg/mL, cell viability remained significantly reduced by ~98 %. Using the data generated, an IC_{50} of ± 8.24 µg/mL APNP for cell viability under no LPS stimulation was calculated (Figure 4.2).

Between 15.625 µg/mL and 250 µg/mL PPNP, significant increases (P<0.01) in cell viability were observed when compared to the 0 µg/mL LPS- control (Figure 4.1). Cell viability at 15.625 µg/mL PPNP had increased by ~70 %. Cell viability increased by ~80 % at both 31.25 µg/mL and 62.5 µg/mL PPNP respectively. At 125 µg/mL PPNP, an increase of ~85 % in viability was seen. The subsequent concentration of 250 µg/mL PPNP, cell viability had increased by ~75 %. No significant changes in cell viability were observed at 500 µg/mL PPNP. For all concentrations of CPNP, no observable cytotoxic effects were seen (Figure 4.1).

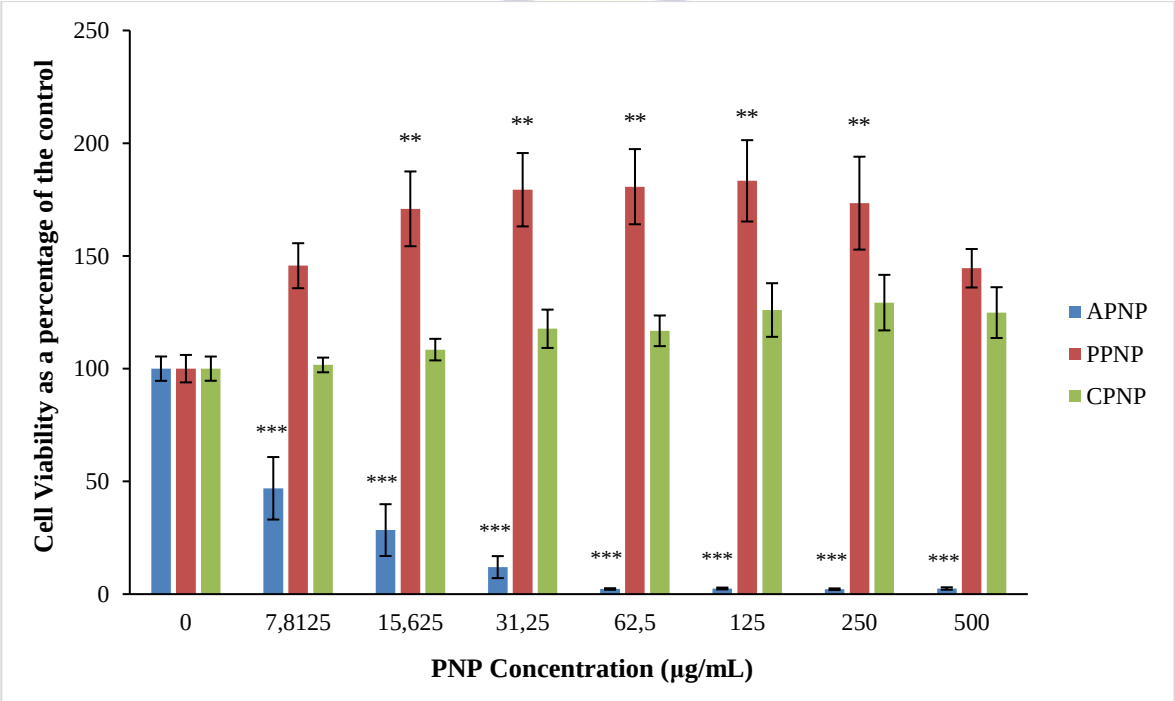

Figure 4.1: Cell viability of RAW 264.7 monocyte cells after exposure to PNPs, in the absence of LPS stimulation. The data is represented as the average percentage ± SEM where n = 9.

Concentrations which are significantly different (P<0.01) to the control are noted by the presence of stars. ** - values are significantly different (P<0.01) from the 0 µg/mL control; *** - values are significantly different (P<0.001) from the 0 µg/mL control.

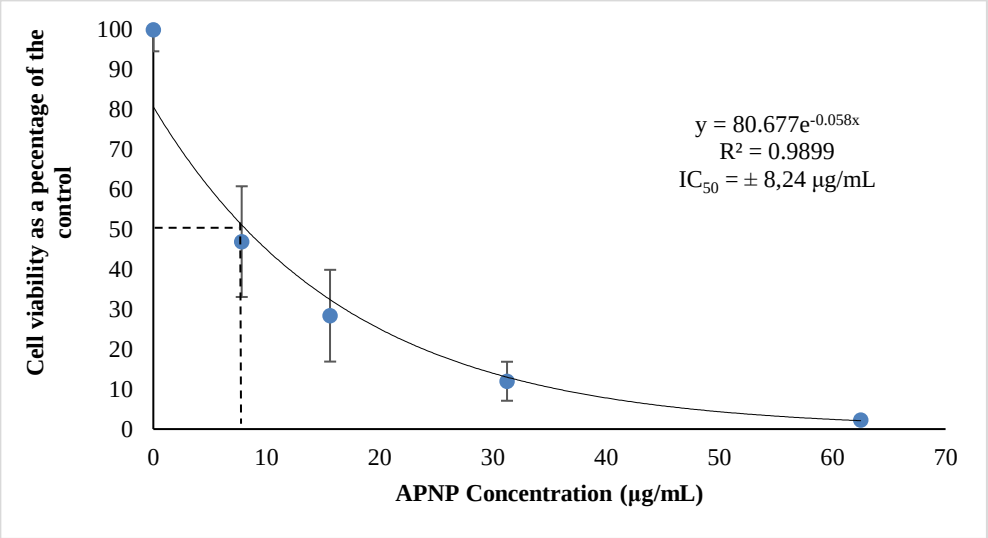

Figure 4.2: Calculation of the APNP IC_{50} value for cell viability in the absence of LPS, represented as a percentage of the control (0 µg/mL APNP).

4.2.2. The effects of PNPs on the NO biomarker production in LPS- RAW 264.7 cells

4.2.2.1. APNP effect on NO production in LPS- RAW 264.7 cells

In the absence of LPS stimulation, no significant changes in the production of NO by RAW 264.7 cells were seen in APNP concentrations ≤ 250 µg/mL, compared to the 0 µg/mL control (Figure 4.3). However, at 500 µg/mL APNP a highly significant increase (P<0.001) in the production of NO was observed. NO levels had increased by ~800 % when compared to the 0 µg/mL control (Figure 4.3).

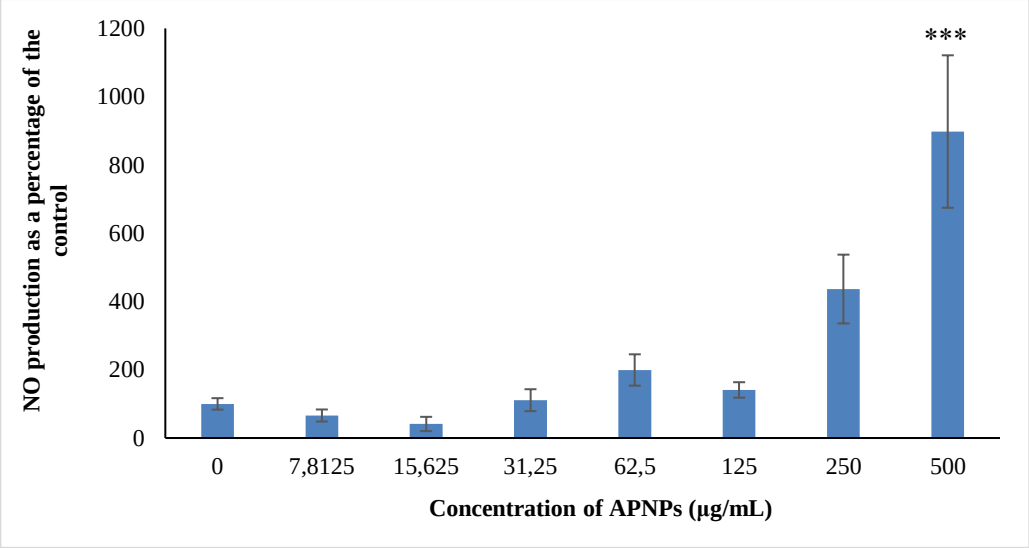

Figure 4.3: NO production by RAW 264.7 monocyte cells after exposure to APNPs, in the absence of LPS stimulation. The data is represented as the average percentage ± SEM where n = 9. Concentrations which are significantly different ($P<0.01$) to the control are noted by the presence of stars. ∗∗∗ - values are significantly different ($P<0.001$) from the 0 µg/mL control.

4.2.2.2. PPNP effect on NO production in LPS- RAW 264.7 cells

Exposure to PPNP concentrations ≤ 62.5 µg/mL revealed, no significant changes in the production of NO by RAW 264.7 cells were seen when compared to the 0 µg/mL control. Significant increases in NO production were seen at PPNP concentrations 125 µg/mL ($P<0.01$), 250 µg/mL ($P<0.001$) and 500 µg/mL ($P<0.001$). NO levels had increased approximately by 700 %, 1000 % and 1100 %, respectively (Figure 4.4).

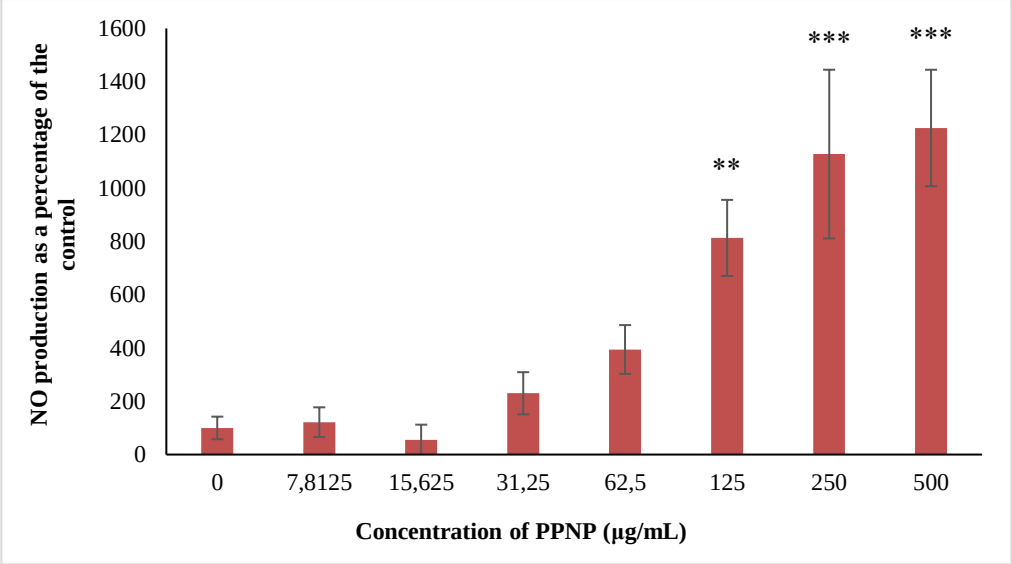

Figure 4.4: NO production by RAW 264.7 monocyte cells after exposure to PPNPs, in the absence of LPS stimulation. The data is represented as the average percentage ± SEM where n = 9. Concentrations which are significantly different ($P<0.01$) to the control are noted by the presence of stars. ** - values are significantly different ($P<0.01$) from the 0 µg/mL control; *** - values are significantly different ($P<0.001$) from the 0 µg/mL control.

4.2.2.3. CPNP effect on NO production in LPS- RAW 264.7 cells

No significant changes in the production of NO were seen in CPNP concentrations ≤ 250 µg/mL, when compared to the 0 µg/mL control under no LPS stimulation. Exposure of RAW 264.7 cells to 500 µg/mL CPNP indicated NO levels had significantly increased ($P<0.001$) by ~845 % (Figure 4.5).

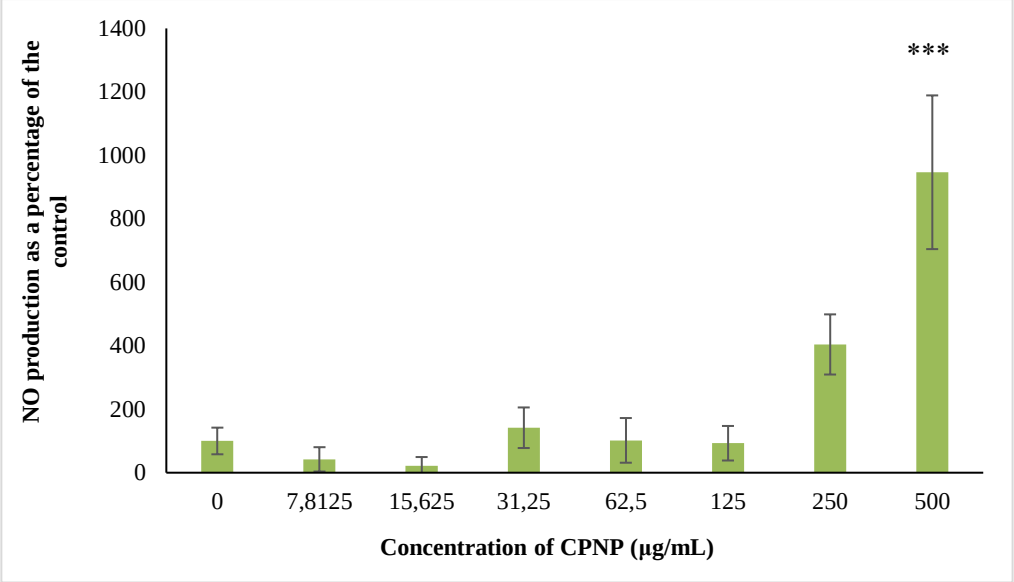

Figure 4.5: NO production by RAW 264.7 monocyte cells after exposure to CPNPs, in the absence of LPS stimulation. The data is represented as the average percentage ± SEM where n = 9. Concentrations which are significantly different ($P<0.01$) to the control are noted by the presence of stars. ∗∗∗ - values are significantly different ($P<0.001$) from the 0 µg/mL control.

4.3. The effects of PNPs on LPS+ RAW 264.7 cell immune response

4.3.1. Cytotoxicity induced by PNPs in LPS+ RAW 264.7 cells

Significant reductions ($P<0.001$) in cell viability were observed in RAW 264.7 cells exposed to APNP concentrations ≥ 15.625 µg/mL, when compared to the 0 µg/mL control in the presence of LPS stimulation (Figure 4.6). Under exposure to 15.625, 31.25, 62.5, 125, 250 and 500 µg/mL APNP, cell viability had been reduced by approximately 50 %, 70 %, 95 %, 95 %, 96 % and 95 % respectively. Based on the reductions in cell viability, the IC_{50} of APNP under LPS stimulation was calculated to be ± 19.41 µg/mL (Figure 4.7). No indications of cytotoxicity, when compared to the 0 µg/mL control under LPS stimulation, were observed in RAW 264.7 cells exposed to PPNPs and CPNPs (Figure 4.6).

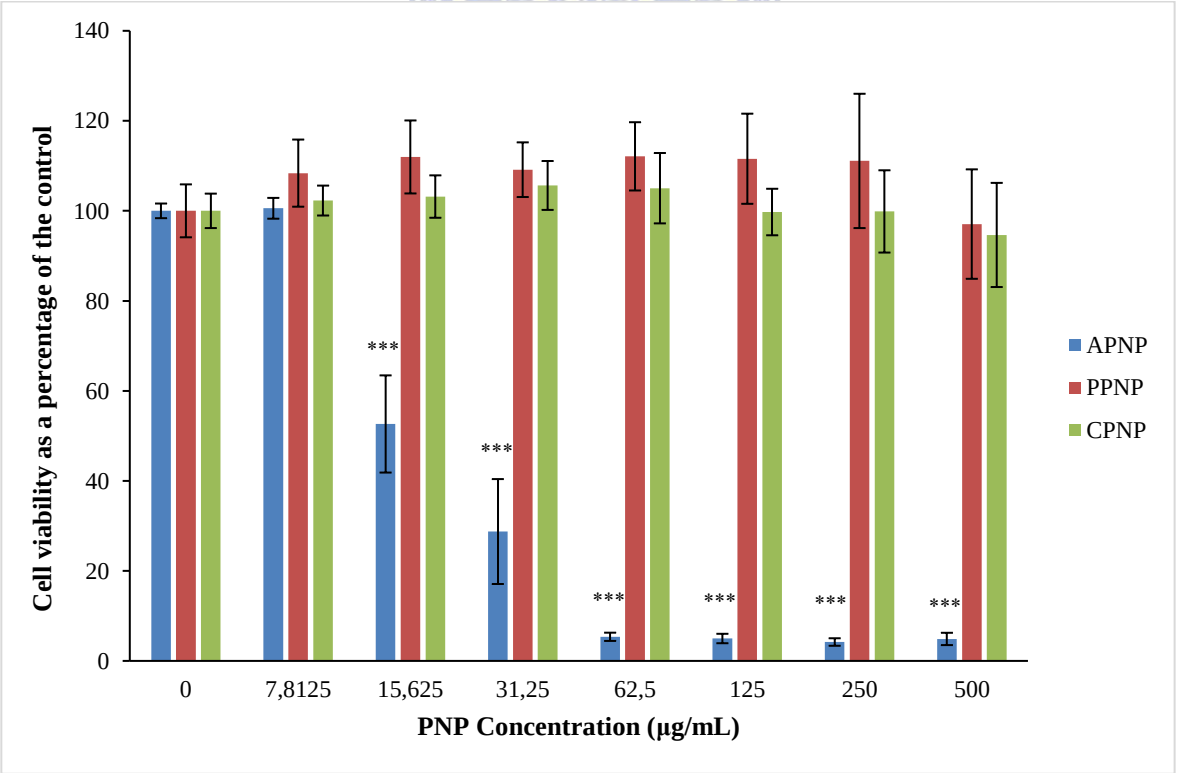

Figure 4.6: Cell viability of RAW 264.7 monocyte cells after exposure to PNPs, in the presence of LPS stimulation. The data is represented as the average percentage ± SEM where n = 9. Concentrations which are significantly different ($P<0.01$) to the control are noted by the presence of stars. *** - values are significantly different ($P<0.001$) from the 0 µg/mL control.

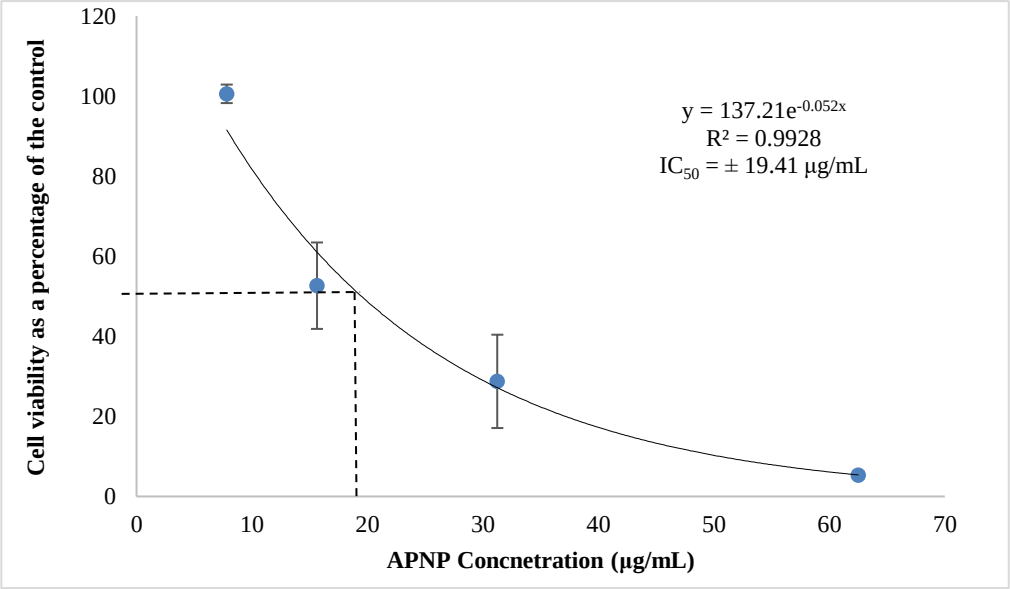

Figure 4.7: Calculation of the APNP IC_{50} value for cell viability in the presence of LPS, represented as a percentage of the control (0 µg/mL APNP).

4.3.2. The effects of PNPs on the NO biomarker production in LPS+ RAW 264.7 cells

The amount of NO produced by RAW 264.7 cells was reduced after exposure to all concentrations of APNP, when compared to the control in the presence of LPS stimulation (Figure 4.8). Exposure to 7.8125 µg/mL APNP, significantly reduced ($P<0.01$) NO levels by ~30 %. As APNP concentration increased i.e., 15.625, 31.25, 62.5 and 125 µg/mL, NO production was significantly reduced ($P<0.001$) by approximately 60 %, 80 %, 92 % and 92 % respectively. Thereafter, NO production had significantly reduced ($P<0.001$) by ~85 % at 250 µg/mL APNP and by ~75 % at 500 µg/mL APNP (Figure 4.8). Based on the reductions in the amount of NO produced, the IC_{50} of APNP for NO production under LPS stimulation was calculated to be ± 14.23 µg/mL (Figure 4.9). The amount of NO produced under exposure to 500 µg/mL CPNP had significantly increased ($P<0.05$) by ~15 %. No other statistically significant changes in the amount of NO produced, compared to the 0 µg/mL control under LPS stimulation, were seen in RAW 264.7 cells under PPNPs and CPNPs exposure (Figure 4.10).

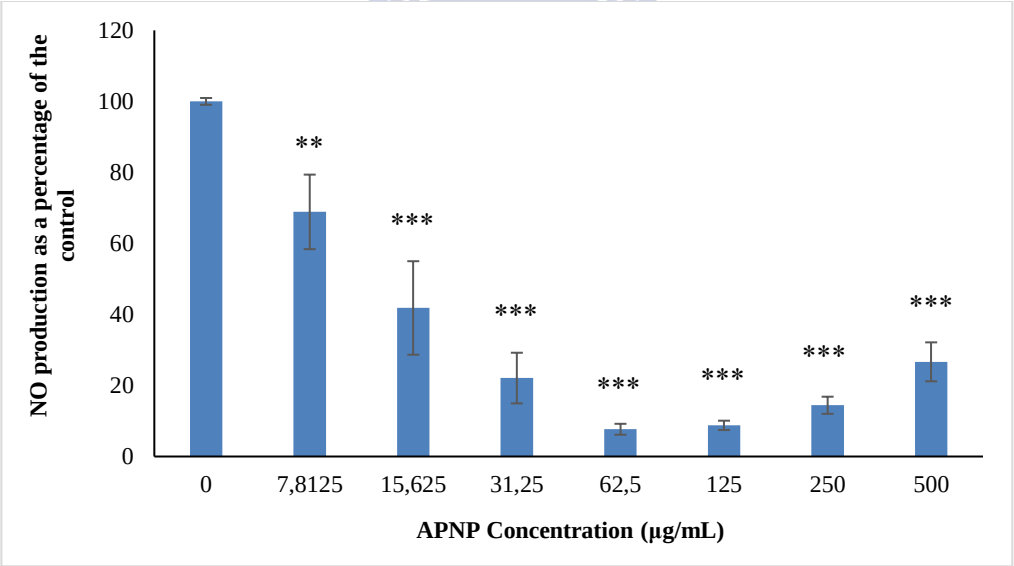

Figure 4.8: NO production by RAW 264.7 monocyte cells after exposure to APNPs, in the absence of LPS stimulation. The data is represented as the average percentage ± SEM where n = 9. Concentrations which are significantly different ($P<0.01$) to the control are noted by the presence of stars. ** - values are significantly different ($P<0.01$) from the 0 µg/mL control; *** - values are significantly different ($P<0.001$) from the 0 µg/mL control.

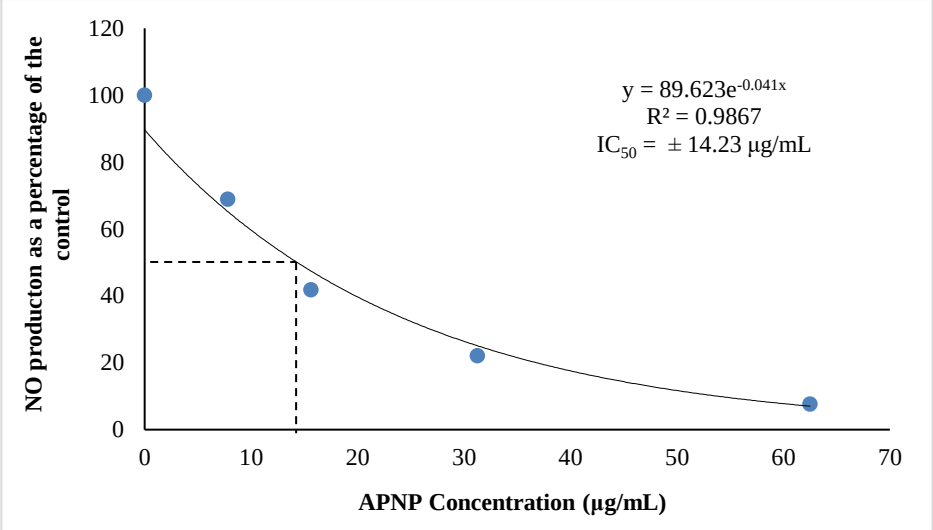

Figure 4.9: Calculation of the APNP IC_{50} value for NO production in the presence of LPS, represented as a percentage of the control (0 µg/mL APNP).

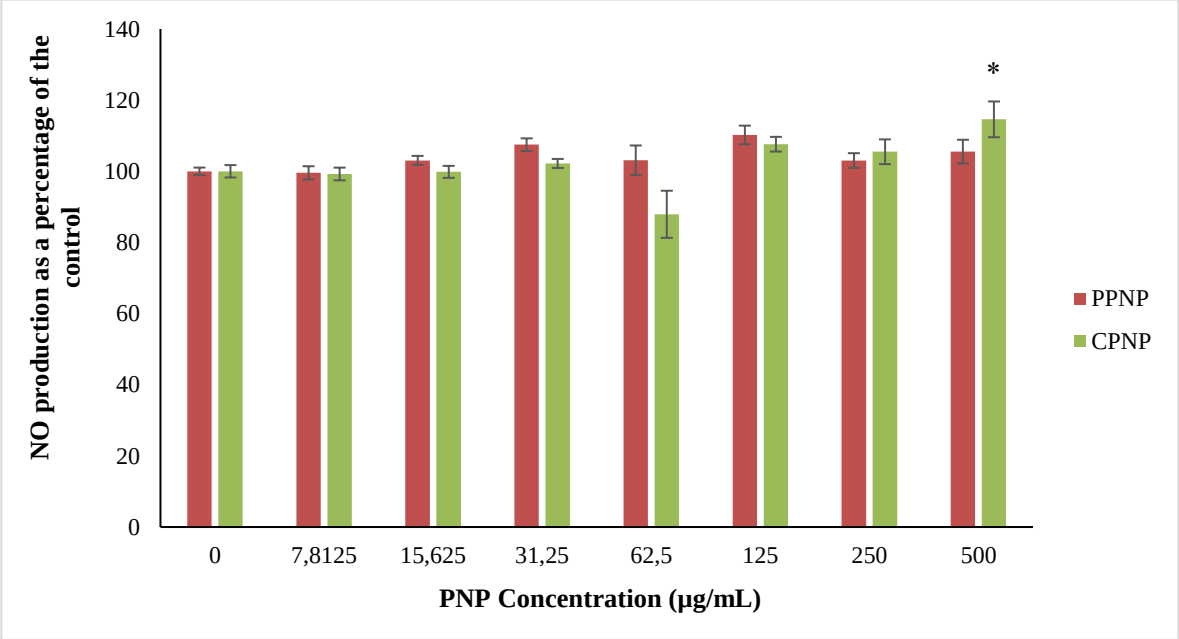

Figure 4.10: NO production by RAW 264.7 monocyte cells after exposure to PPNPs and CPNPs, in the presence of LPS stimulation. The data is represented as the average percentage ± SEM where n = 9. Concentrations which are significantly different ($P<0.01$) to the control are noted by the presence of stars. ∗ - values are significantly different ($P<0.05$) from the 0 µg/mL control.

4.4. The effects of PNPs on the IL-6 biomarker production in RAW 264.7 cells

4.4.1. APNP effect on IL-6 production in LPS+ RAW 264.7 cells

RAW 264.7 cells exposed to PNPs in the absence of LPS stimulation did not produce IL-6 (data not shown). However, cells exposed to 7.8125 µg/mL APNP had caused a weakly significant increase ($P<0.05$) in the amount of IL-6 produced, when compared to the 0 µg/mL control under LPS stimulation. Here, the amount of IL-6 produced was ~40% greater than the control (Figure 4.11). For APNP concentrations ≥ 31.25 µg/mL, significant reductions in the amount of IL-6 produced were seen. Exposure of RAW 264.7 cells to 31.25 µg/mL APNP, significantly reduced ($P<0.05$) IL-6 levels by ~45 %. At 62.5 µg/mL APNP, the IL-6 levels were significantly reduced($P<0.001$) by ~94 %. Thereafter, for all APNP concentrations ≥ 125 µg/mL, the amount of IL-6 produced had significantly reduced ($P<0.001$) by ~100 % compared to the 0 µg/mL control (Figure 4.11). Based on the reductions in the amount of IL-6 produced, the IC_{50} of APNP for IL-6 production under LPS stimulation was calculated to be ± 35.06 µg/mL (Figure 4.12).

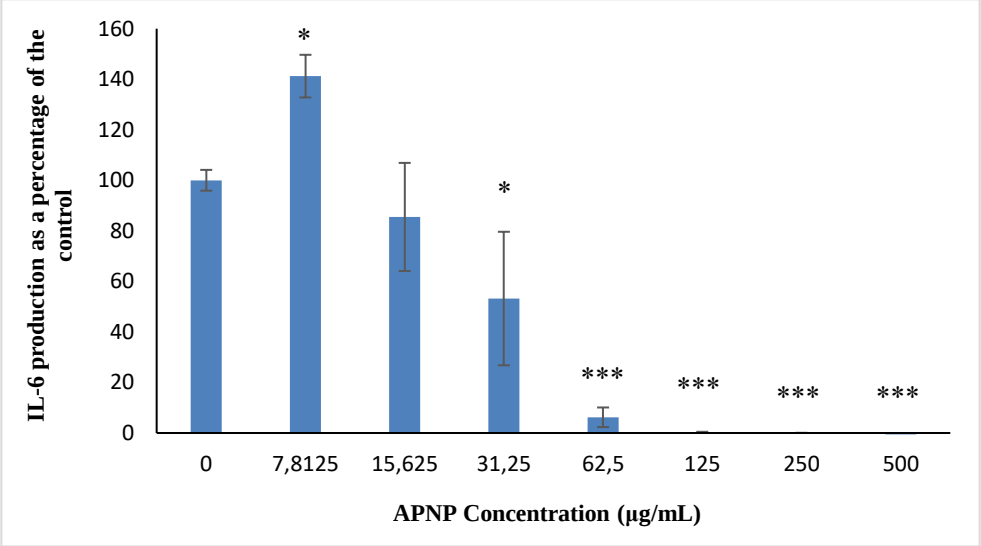

Figure 4.11: IL-6 production by RAW 264.7 monocyte cells after exposure to APNPs, in the presence of LPS stimulation. The data is represented as the average percentage ± SEM where n = 9. Concentrations which are significantly different ($P<0.05$) to the control are noted by the presence of stars. ∗ - values are significantly different ($P<0.05$) from the 0 µg/mL control; ∗∗∗ - values are significantly different ($P<0.001$) from the 0 µg/mL control.

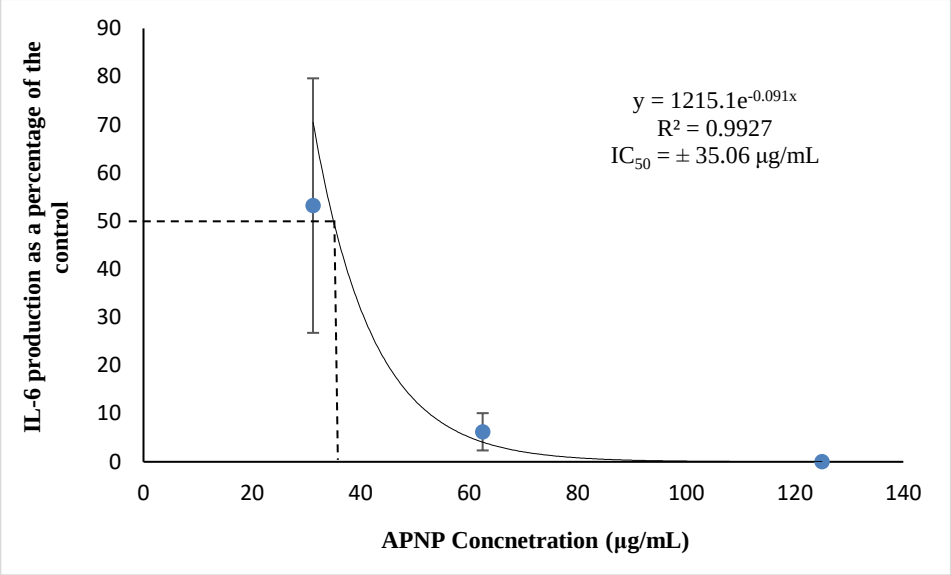

Figure 4.12: Calculation of the APNP IC_{50} value for IL-6 production in the presence of LPS, represented as a percentage of the control (0 µg/mL APNP).

4.4.2. PPNP effect on IL-6 production in LPS+ RAW 264.7 cells

A dose-dependent reduction in the amount of IL-6 produced by RAW 264.7 cells under LPS stimulation occurred after exposure to PPNPs, when compared to the 0 µg/mL control (Figure 4.13). After exposure to 7.1825 µg/mL PPNP, the amount of IL-6 produced by RAW 264.7 cells had been significantly reduced ($P<0.01$) by ~25 %. At 15.625, 31.25, 62.5 and 125 µg/mL PPNP, IL-6 production had significantly reduced ($P<0.001$) by approximately 35 %, 50 %, 60 % and 85 %, respectively (Figure 4.13). The production of IL-6 by RAW 264.7 cells exposed to 250 µg/mL and 500 µg/mL PPNP were both significantly reduced ($P<0.001$) by ~91 % (Figure 4.13). Based on the data generated, an IC_{50} of ± 44.8 µg/mL PPNP for IL-6 production was calculated (Figure 4.14).

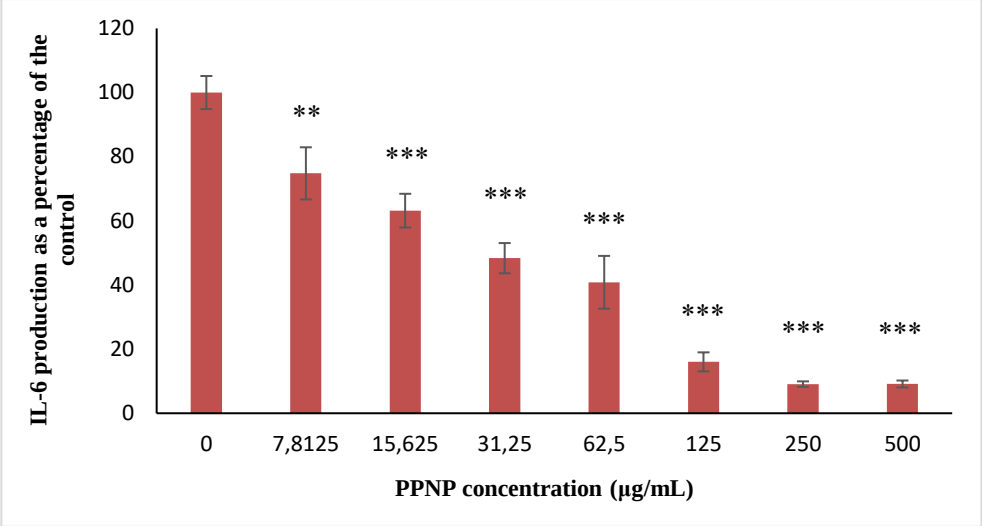

Figure 4.13: IL-6 production by RAW 264.7 monocyte cells after exposure to PPNPs, in the presence of LPS stimulation. The data is represented as the average percentage ± SEM where n = 9. Concentrations which are significantly different (P<0.01) to the control are noted by the presence of stars. ** - values are significantly different (P<0.01) from the 0 µg/mL control; *** - values are significantly different (P<0.001) from the 0 µg/mL control.

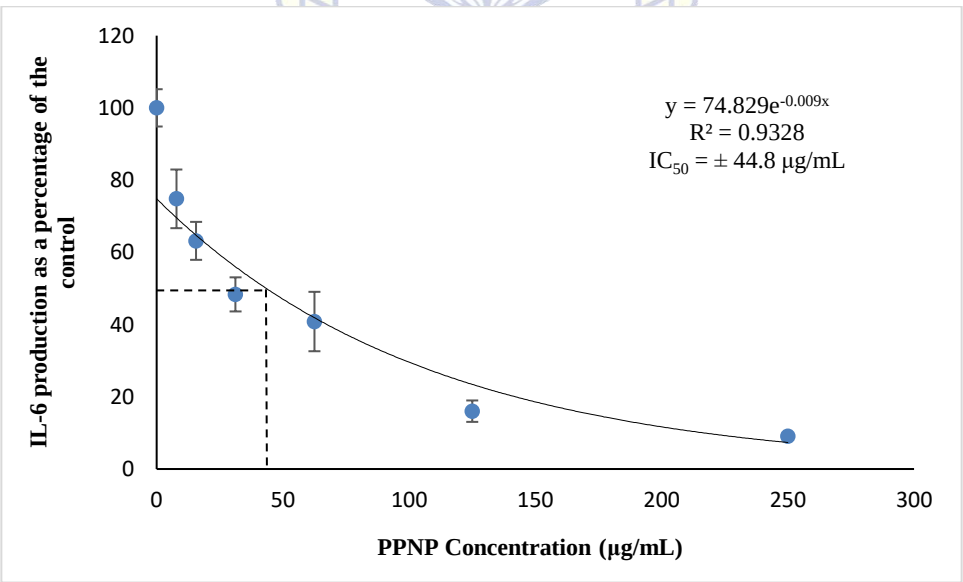

Figure 4.14: Calculation of the PPNP IC_{50} value for IL-6 production in the presence of LPS, represented as a percentage of the control (0 µg/mL PPNP).

4.4.3. CPNP effect on IL-6 production in LPS+ RAW 264.7 cells

Significant reductions (P<0.01) in the IL-6 production were seen in cells exposed to CPNP concentrations ≥ 31.25 µg/mL, when compared to the 0 µg/mL control under LPS stimulation (Figure 4.15). After exposure to 31.25 µg/mL CPNP, IL-6 production was significantly reduced (P<0.01) by ~20 %. Thereafter, IL-6 production by cells exposed to 62.5, 125, 250 and 500 µg/mL CPNP were significantly reduced (P<0.001) by approximately 25 %, 45 %, 60 % and 70 % respectively (Figure 4.15). Based on the data generated, an IC_{50} of ± 232.21 µg/mL CPNP for IL-6 production was calculated (Figure 4.16).

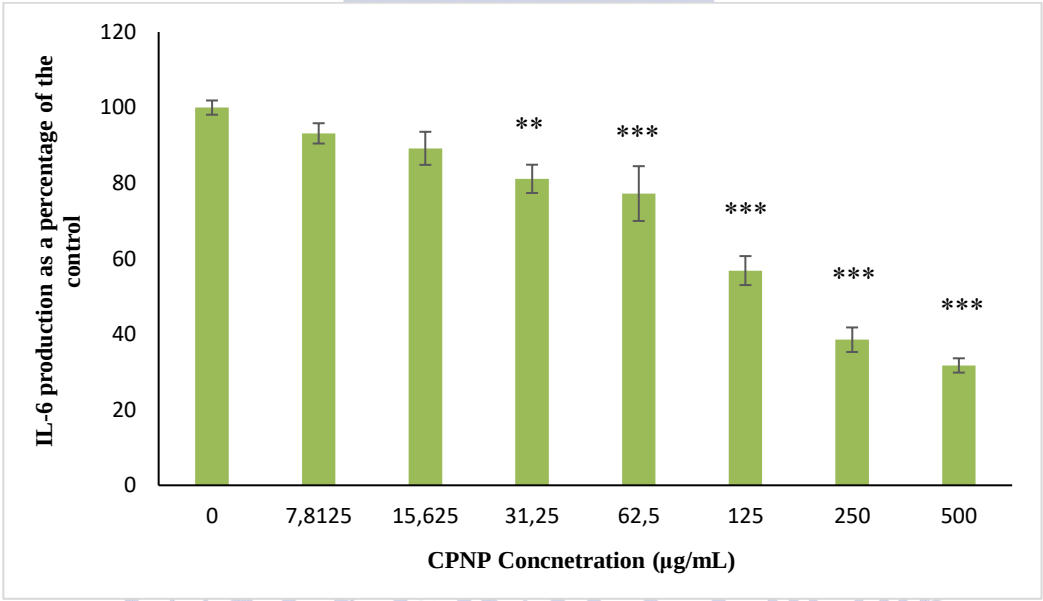

Figure 4.15: IL-6 production by RAW 264.7 monocyte cells after exposure to CPNPs, in the presence of LPS stimulation. The data is represented as the average percentage ± SEM where n = 9. Concentrations which are significantly different (P<0.01) to the control are noted by the presence of stars. ** - values are significantly different (P<0.01) from the 0 µg/mL control; *** - values are significantly different (P<0.001) from the 0 µg/mL control.

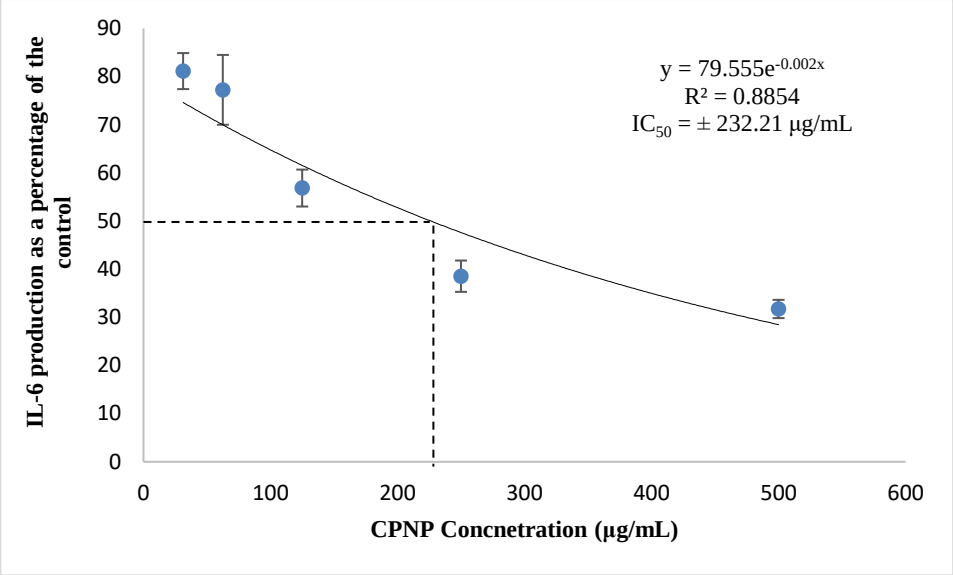

Figure 4.16: Calculation of the CPNP IC_{50} value for IL-6 production in the presence of LPS, represented as a percentage of the control (0 µg/mL CPNP).

4.5. Proteome Profiles of RAW 264.7 cells exposed to PNPs

4.5.1. Proteome Profiles of LPS- RAW 264.7 cells exposed to PNPs

Proteome profiles were obtained to assess the effects PNPs had on the production of signalling molecules by RAW 264.7 cells. The profiles obtained allow for the identification of potential biomarkers and indicate the extent to which each PNP may alter cell signalling patterns. Profiles discussed within this section were obtained after PNP exposure in the absence of LPS stimulation (Figure 4.17).

Supernatant obtained from cells incubated solely with culture media (control) revealed the production of TNF-α, soluble intercellular adhesion molecule-1 (sICAM-1/CD54), macrophage inflammatory protein (MIP)-1α and MIP-1β (Figure 4.17 i). After incubation with 15 µg/mL APNP, signalling molecules produced resembled the control with the additional production/upregulation of IL-16 and MIP-2 (Figure 4.17 ii). Here, a visible decrease in the intensity of MIP-1β was observed and serves to highlight possible downregulation (Figure 4.17 ii). After incubation with 15 µg/mL PPNP, signalling molecules produced resembled the control with the additional production/upregulation of monocyte chemoattractant protein-1 (MCP-1/CCL2) (Figure 4.17 iii). The pattern of expression seen after PPNP exposure was also present after incubation with 15 µg/mL CPNP (Figure 4.17 iv).

i)

ii)

iii)

iv)

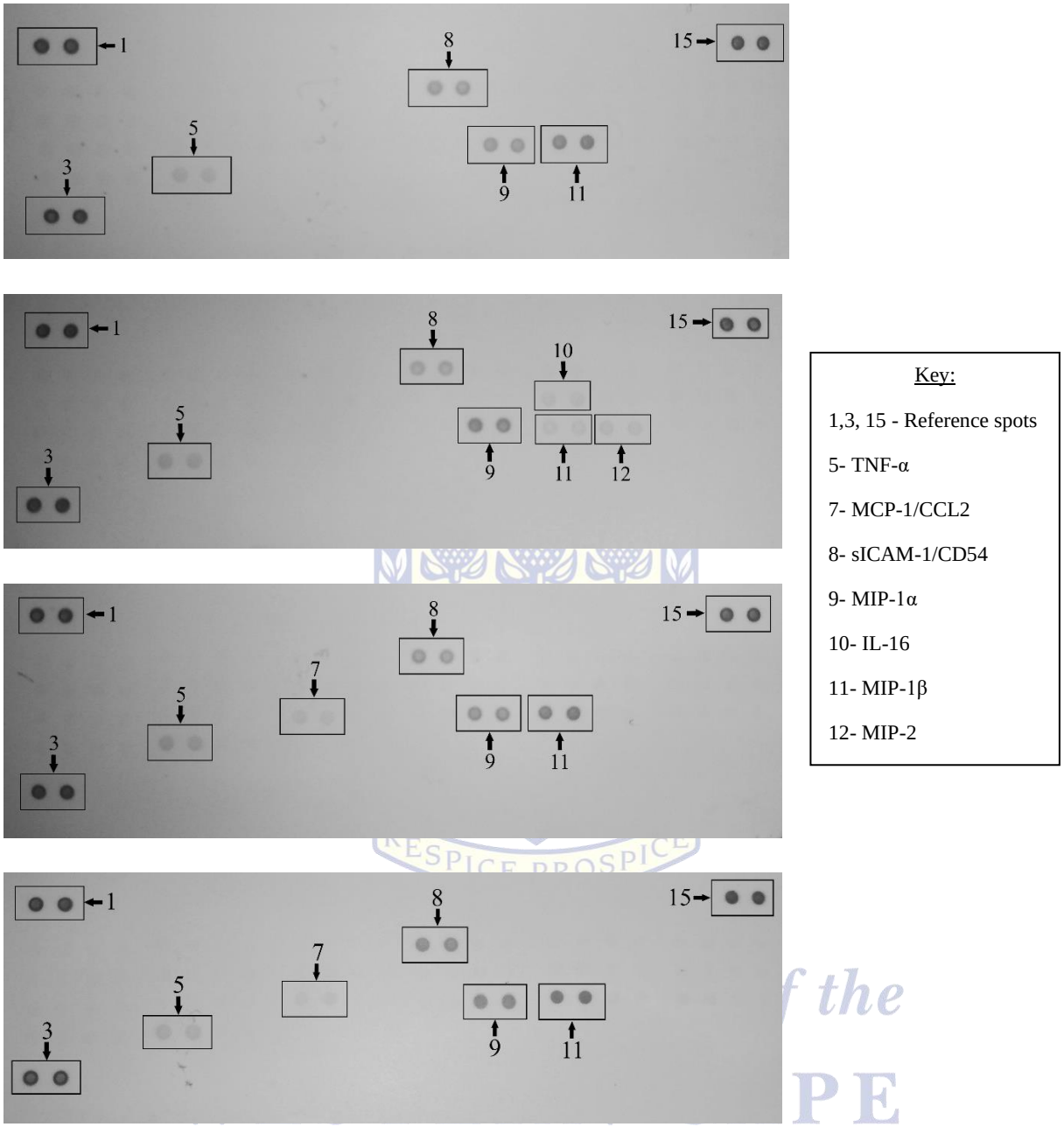

Key:

1,3, 15 - Reference spots

5- TNF-α

7- MCP-1/CCL2

8- sICAM-1/CD54

9- MIP-1α

10- IL-16

11- MIP-1β

12- MIP-2

Figure 4.17: The effect of PNPs exposure on RAW 264.7 cells in the absence of LPS stimulation. Exposure occurred wherein cells were i) treated solely with media, ii) treated with 15 µg/mL APNP, iii) treated with 15 µg/mL PPNP, and iv) treated with 15 µg/mL CPNP. Profiles were obtained using the procedures described in the methodology section. Numbering system: 1,3 and 15 are reference spots used to assist identification of substances; 5- TNF-α; 7- MCP-1/CCL2; 8- sICAM-1/CD54; 9- MIP-1α; 10- IL-16; 11- MIP-1β; and 12- MIP-2.

4.5.2. Proteome Profiles of LPS+ RAW 264.7 cells exposed to PNPs

Profiles discussed within this section were obtained after PNP exposure in the presence of LPS stimulation (Figure 4.18).

Control cell culture supernatant revealed the production of interferon gamma-induced protein-10 (IP-10/CXCL10), granulocyte colony-stimulating factor (G-CSF), TNF-α, IL-6, MCP-1, sICAM-1/CD54, MIP-1α, MIP-1β, MIP-2, IL-1 receptor agonist (IL-1ra), chemokine ligand 5 (CCL5/RANTES), and IL-27 (Figure 4.18 i). After incubation with 15 μg/mL APNP, signalling molecules produced resembled the control with the additional production/upregulation of IL-16. IL-1ra production was not detectable, indicating downregulation by APNPs. A visible reduction in the intensity of sICAM-1 and MCP-1 was observed, indicating downregulation had occurred (Figure 4.18 ii). After incubation with 15 μg/mL PPNP and CPNP, signalling molecules produced resembled the control with no visible change in the levels of expression (Figure 4.18 iii and iv).

i)

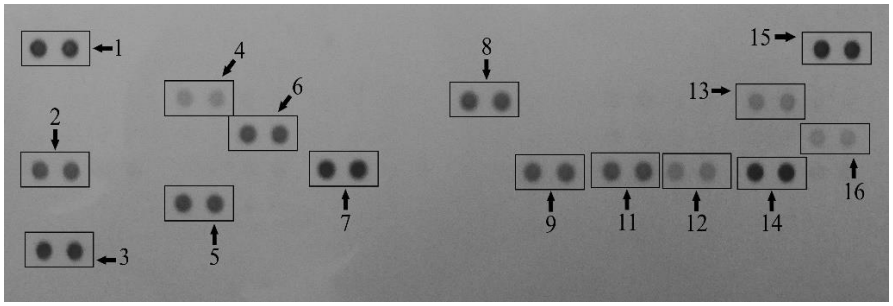

ii)

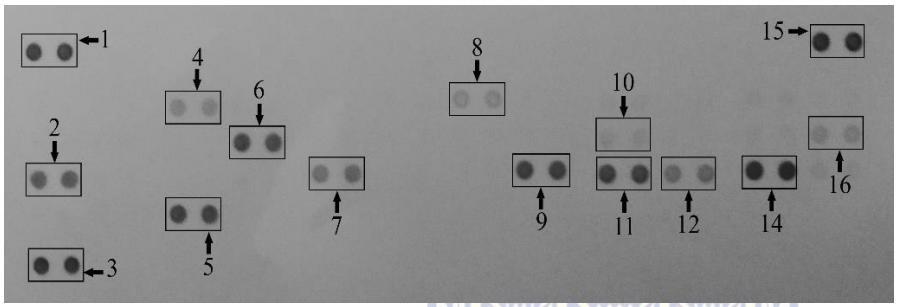

iii)

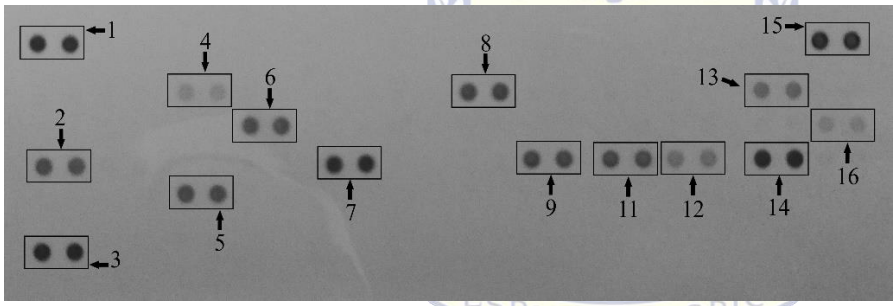

iv)

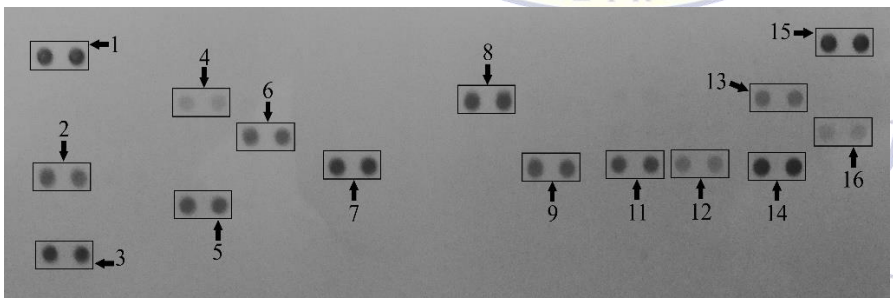

Key:

1,3, 15 - Reference spots

2 - IP-10

4 - G-CSF

5 - TNF-α

6 - IL-6

7 - MCP-1/CCL2

8 - sICAM-1/CD54

9 - MIP-1α

10 - IL-16

11 - MIP-1β

12 - MIP-2

13 - IL-1ra

14 - CCL5/RANTES

16 - IL-27

Figure 4.18: The effect of PNPs exposure on RAW 264.7 cells in the presence of LPS stimulation. Exposure occurred wherein cells were i) treated solely with media, ii) treated with 15 µg/mL APNP, iii) treated with 15 µg/mL PPNP, and iv) treated with 15 µg/mL CPNP. Profiles were obtained using the procedures described in the methodology section. Numbering system: 1,3 and 15 are reference spots used to assist identification of substances; 2- IP-10; 4- G-CSF; 5- TNF-α; 6- IL-6; 7- MCP-1/CCL2; 8- sICAM-1/CD54; 9- MIP-1α; 10- IL-16; 11- MIP-1β; 12- MIP-2; 13- IL-1ra, 14- CCL5/RANTES; and 16- IL-27.

Chapter 5

Discussion and Conclusion

5.1. Characterization of PNPs

Binding and uptake of NPs by cells are prerequisites prior to observing their effects on cellular functioning and signalling. NP surface functionalization and size are pivotal in this uptake, as these properties may determine the mechanisms of uptake utilized by cells. To understand the contribution of PNP surface functionalization in immune response, PNPs were characterized based on their size distribution and zeta potential. Characterization of commercially available PNPs within sterile distilled water had revealed average diameters closely resembling those given by the manufacturer (Table 4.1). The corresponding Pdi values fell between 0.1 – 0.4, revealing all NPs to be moderately dispersed within sterile distilled water. The presence of different functional groups on the PNP surfaces were evident in the zeta potential measurements (Table 4.1). APNP and CPNP charges within sterile distilled water had shown to have characteristic cationic and anionic surfaces, respectively. However, unmodified PPNPs were seen to possess anionic surfaces greater to that of CPNPs.

PNP properties within the 5 % serum containing culture media were notably different when measured in sterile distilled water (Table 4.2). All tested NPs had undergone size alterations, in which the resultant PNPs having diameters greater than 50 nm. The greatest increase in size was seen in the PPNPs with an average diameter of 341.2 ± 36.98 nm. A possible explanation for this altered size may be obtained through correlation of the altered size distribution and the Pdi values. The corresponding Pdi values for all tested NPs were > 0.4, indicating the PNPs to have become polydispersed when placed in culture media. These values indicate the formation of agglomerates when placed in media but not when placed in sterile distilled water. Thus, the formation of larger particles may be the result of PNP agglomeration with media constituents. This interpretation is supported by the work of Abdelkhaliq *et al.* (2018), in which culture media proteins absorbed by CPNP surfaces were seen to alter size over time. This agglomerated state has been shown to enhance cellular uptake of NPs, thereby impeding biological functions through a cytotoxic effect (Müller *et al.*, 2014; Halamoda-Kenzaoui *et al.*, 2017). However, Jeon *et al.* (2018) had attempted to show the relationship between PNP agglomerate size and cellular uptake efficacy in THP-1 cells. The authors observed that there was no direct

correlation between these parameters, indicating a greater dependence on the initial size of PNPs.

Zeta potential measurement for surface charge had shown that within culture media, all tested NPs had relatively similar anionic charges (Table 4.2). Reports suggest that cationic amine functional groups of the APNPs are most likely to exhibit strong electrostatic attraction to the negatively charged lipid bilayer and thus exhibit greater reactivity (Goodman *et al.*, 2004). Based on the cytotoxicity assessment, cationic APNPs were seen to have the greatest reactivity with cells. This indicates that APNPs had produced the expected level of cytotoxicity as indicated by Goodman *et al.* (2004) despite the presence of an anionic interface layer of agglomerates in culture media. There are reports that both cationic and anionic NPs experience neutralization of the particle surface charge, which is only possible through the binding of oppositely charged particles (Monopoli *et al.*, 2011; Hühn *et al.*, 2013). Jeon *et al.* (2018) had shown the degree of PNP uptake is determined by the charge provided through functionalization. The authors also determined that the cellular uptake of positively charged PNPs were greater in phagocytic cells (Jeon *et al.*, 2018). A greater emphasis is then placed on the individual particles and their respective charges, as differently charged PNPs are known to utilize different methods of uptake. Cationic PNPs have shown charge specificity for clathrin mediated uptake. Whereas, anionic PNPs has shown specificity for caveolin mediated uptake. The utilization of different uptake mechanisms would also imply that the amount of PNPs trafficked into cells is different (Bhattacharjee *et al.*, 2013). Another factor which should be considered when examining cellular uptake is the nature of the protein corona coating the surfaces of differently functionalized NPs as contact with the cells occurred. The number and type of proteins of the corona may differ due to the surface properties of the PNP, surface area of the PNP, and pH of the surrounding environment (Abdelkhaliq *et al.*, 2018). Thus, as APNPs were the only NPs to possess cationic charges, there exists a possibility that the unique corona formed may be responsible as it would differ greatly to that of the PPNPs and CPNPs. This is supported by the work of Pustulka *et al.* (2020) and Lundqvist *et al.* (2008), with further analysis being required to confirm this assumption within the present experiment. It has also been suggested that the toxic potential of PNPs is due to the simultaneous influence of surface charge and protein binding affinity of the PNP in question (Hwang *et al.*, 2016).

5.2. Cytotoxicity of differently functionalized PNPs

Alteration in immune response may occur as the result of the NPs ability to reduce cell number populations. Improper signalling and responses may be facilitated through the lost regulatory ability these cells would provide (Hotchkiss and Karl, 2003). To assess this effect, cytotoxicity of PNP exposure was determined by the number of viable cells present. Cell populations were divided into two groups based on their stimulation with LPS. Populations which had remained unstimulated with LPS had served to simulate the PNP exposure under physiological conditions. Populations stimulated with LPS had served to simulate PNP exposure during an immune response associated with the classical activation of macrophage cells. During APNP exposure to RAW 264.7 cells under unstimulated conditions, cytotoxicity was seen to first occur at the lowest concentration of 7.8125 μg/mL APNP (Figure 4.1). This pattern of cytotoxicity was seen to only occur from double the prior concentration (15.625 μg/mL APNP) in classically activated RAW 264.7 cells (Figure 4.6). The work of Xia *et al.* (2006) had shown that 10 μg/mL APNP of similar size could induce oxidative stress by way of ROS production and thiol depletion. Mitochondrial damage and cellular toxicity were also noted to have occurred in RAW 264.7 cells. Amine functionalized polystyrene spheres have been shown to be taken up during phagocytosis, in which certain lysosomal proteases were degraded with no replacement of the enzyme (Oh and Swanson, 1996). Xia *et al.* (2008) had suggested that within lysosomal compartment, amine functional groups initiate proton pump activity to cause rupturing of the lysosome. The increased cytosolic presence of the APNPs will then be accompanied by apoptosis induced through increased intracellular calcium and leakage of lysosomal enzymes (Xia *et al.*, 2008). It should be noted that both the current investigation and that conducted by Xia *et al.* (2008) had produced identical IC_{50} values for APNPs with an initial diameter 60 nm (Figure 4.2). Although the presence of cytosolic APNPs were not assessed in this investigation, the toxicity observed could be attributed to the amine-functional groups ability to cause lysosomal rupture and subsequent APNP leakage into the cytosol. This would be applicable for both stimulated and unstimulated cell populations.

In the group of tested PNPs, unmodified PPNPs were the only group to produce significant increases ($P<0.01$) in cell viability when administered to unstimulated RAW 264.7 cells (Figure 4.1). These increases had only occurred between 15.625 – 250 μg/mL PPNP, with the highest concentration (500 μg/mL) showing no significant alteration from the control. Various studies have reported that unmodified PNPs are either non-toxic to RAW 264.7 cells or may induce apoptosis (Lunov *et al.*, 2011b; Mckenzie *et al.*, 2015; Yuan *et al.*, 2020; Hu *et al.*, 2021).

During exposure to human macrophages and RAW 264.7 cells, PPNPs undergo cellular uptake with lysosome co-localization. The RAW 264.7 cells have demonstrated a limit to their ability to engulf PPNP, with uptake slowing down as cells are saturated with particles. However, no lysosomal leakage occurs in human macrophages nor are they known to induce spontaneous ROS production (Xia *et al.*, 2006; Lunov *et al.*, 2011b; Yuan *et al.*, 2020). As no alteration was present at 500 μg/mL PPNP, the effect seen at lower concentrations may be the result of enhanced mitochondrial enzyme activity due to an optimal saturation of PPNPs. This enhanced activity would promote enhanced cleavage of the tetrazolium salts. Thereby, producing a greater signal at the aforementioned concentrations. It should be noted that these particles are not thought to impede the mitochondrial functioning of RAW 264.7 cells (Xia *et al.*, 2006). To our knowledge, this investigation presents the first instance of enhanced RAW 264.7 cellular viability at various concentrations of PPNP exposure. Repeated experimentation and further investigation are required to elucidate the cause of this phenomenon.

Cell viability remained unaffected during exposure to CPNPs, regardless of immune response stimulation (Figure 4.1). This may be explained by CPNPs cytotoxic ability being greatly dependant on size. CPNPs with diameters of 20 nm have been shown to induce little-to-no reduction in the cell viability of phagocytic cell types, at concentrations ≤ 200 μg/mL. The viability of these same cell types had undergone greater reductions when particles of diameters 100, 500 and 1000 nm were used at concentrations ≤ 500 μg/mL (Prietl *et al.*, 2014). The results obtained from this investigation coincide with previous reports in which CPNPs between 20 – 120 nm are not cytotoxic to RAW 264.7 cells, THP-1 cells (both differentiated and undifferentiated), U937 cells, DMBM-2 cells, and human blood derived macrophages (Xia *et al.*, 2008; Lunov *et al.*, 2011a; Loos *et al.*, 2014b; Prietl *et al.*, 2014). Thus, smaller CPNPs at low concentrations show no indication of altering the immune response through the reduction of phagocytic cell populations.

5.3. RAW 264.7 NO production under PNP exposure

NO is a compound intimately involved in the immune system. NO production is responsible for inhibiting the activation of various immunological pathways, regulation of various signalling molecules which modulate the immune response, and activation of cells which combat intracellular infections (Bogdan, 2001). This molecule is also involved in physiological processes, and deviations in its normally regulated levels has been shown to be associated with

various disease states (Knott and Bossy-Wetzel, 2009). Unmodified PPNPs were seen to have the greatest impact on the NO release by unstimulated cell populations (Figure 4.4). Uniquely to the PPNPs, significant upregulation was seen at 125 μg/mL ($P<0.01$) and 250 μg/mL ($P<0.001$). All tested PNPs were seen to significantly upregulate ($P<0.001$) NO release after exposure to 500 μg/mL (Figure 4.4). This indicates that; i) the functionalization of PNP surfaces with either cationic or anionic functional groups prevent the significant upregulation of NO in unstimulated (LPS-) RAW 264.7 cells at concentrations ≤ 250 μg/mL, and ii) high doses of all particle types can provoke unstimulated (LPS-) RAW 264.7 cells into initiating an inflammatory response. The former of these two indications related to CPNP exposure is of particular interest. These results are consistent with the work of Prietl *et al.* (2014), in which smaller CPNPs at ≤ 200 μg/mL where shown to not induce significant alterations in the NO release by DMBM-2 macrophage cells.

An important distinction is that under unstimulated (LPS-) conditions APNPs initiate a proinflammatory NO response, while simultaneously diminishing cell populations (Figures 4.1 and 4.3). CPNP did not affect unstimulated cell populations but caused an increase in NO production by cells (Figures 4.1 and 4.4). In order for the former response to occur at high APNP concentrations, the elevated production and release of NO by unstimulated cells must have preceded the observed cytotoxicity. This observation can also be made for cells stimulated by LPS to initiate an immune response at high APNP exposure. The extent of NO downregulation by these cells at 125 μg/mL is greater compared to cells being exposed to 500 μg/mL APNP, with both groups having similar viability readings (Figures 4.6 and 4.8). This indicates cells exposed to 500 μg/mL APNP had upregulated NO production prior to cell stimulation with LPS.

When assessing the effects of surface functionalization on the production of NO by stimulated cells (LPS+), PPNPs do not appear to not interfere with the NO levels which had accompanied an immune response. This is also true for CPNPs, with exception to exposure at 500 μg/mL (Figure 4.10). Here, NO levels were significantly increased ($P<0.05$) with the extent of this increase being lower than in unstimulated cell populations (Figure 4.5), with stimulated cell populations also remaining unaffected (Figure 4.6). While these results display upregulation of NO occurring under CPNP exposure, the extent of the response is minor, where the dose at which this occurs is not likely to be used within physiological systems (Prietl *et al.*, 2014). This limited deviation of immune response signalling highlights the potential practical implementation of CPNP and similarly altered particles.

The APNPs were seen to infer the greatest downregulation of NO production in stimulated cells (Figure 4.8). This indicates that amine surface functionalization is primarily responsible for altering immune response mechanisms mediated by NO. Fuchs *et al.* (2016) had shown that within the classically activated human macrophage cells, the presence of 100 μg/mL APNP and CPNP had not altered iNOS expression. Viability readings of these cell populations had also shown to not deviate from the control after a 24-hour exposure to APNP concentrations ≤ 100 μg/mL. The data generated within the present study is comparable to the observed effect in human cell lines, despite the difference in origin. It should be mentioned that detection for the presence of iNOS does not indicate the level of activity (Thomas and Mattila, 2014). As such, the producing enzyme may remain present within human cells under APNP exposure with its level of activity being altered. This may be demonstrated under 7.8125 μg/mL APNP exposure to stimulated RAW 264.7 cells (Figure 4.6) as cell populations, and potentially their cellular contents, were not affected while NO levels were (Figure 4.8). The detection of iNOS versus the detection of produced NO under APNP exposure thus constitutes a required area of expansion. The IC_{50} for stimulated RAW 264.7 cell viability under APNP exposure was determined to be ± 19.41 μg/mL (Figure 4.7) with human cells being tolerant to concentrations ≤ 100 μg/mL (Fuchs *et al.*, 2016). Therefore, the data suggests the ability of APNPs to reduce NO production seen herein is primarily the result of greater cytotoxic susceptibility, where NO levels are consistent with diminishing cell numbers.

5.4. RAW 264.7 IL-6 production under PNP exposure

IL-6 is a cytokine known to not solely be produced by macrophages and may originate from a variety of cell types. These include, and are not limited to, macrophages, fibroblasts, endothelial cells, keratinocytes, and mast cells (Weissenbach *et al.*, 1980; Baumann *et al.*, 1984; Corbel and Melchers, 1984; Aarden *et al.*, 1987; Plaut *et al.*, 1989). A systemic response is initiated during infection or trauma to tissues. This response consists of a series of humoral and cellular reactions. These reactions are collectively known as the acute inflammatory response. IL-6 serves as the primary stimulator for majority of the proteins secreted during this acute inflammation (Gauldie *et al.*, 1987). Macrophages are important sources of this cytokine at the site of inflammation. The production of IL-6 during acute inflammation will cause the suppression of proinflammatory cytokines with no alteration to the levels of anti-inflammatory cytokines. In this way IL-6 serves to regulate the extent of the acute inflammatory responses, both locally and systemically (Xing *et al.*, 1998; Kaplanski *et al.*, 2003).

IL-6 secretion by unstimulated cell populations was not observed within controls nor by cells subject solely to PNP exposure (data not shown). The lack of secretion by control cells was expected as IL-6 secretion is one of the proinflammatory markers signifying classical macrophage activation (Cavaillon, 1994). More importantly, within the present study, none of the observed PNPs exhibit the ability to modulate IL-6 secretion in unstimulated RAW 264.7 cells. This finding stands in contrast with those of Hu *et al.* (2021) and Ruenraroengsak and Tetley (2015). Primary human alveolar macrophages have been shown to secrete IL-6 in response to PPNPs, APNPs and CPNPs (diameters: 50 and 100 nm; 1-50 μg/mL). This signifies the ability of PNPs to induce macrophage activation with the subsequent release of IL-6 (Ruenraroengsak and Tetley, 2015). A similar activation was demonstrated by Hu *et al.* (2021) in which PPNP exposure at 5 and 10 μg/mL significantly upregulated IL-6 secretion in RAW 264.7 cells. The absence of this activation within the present study may be explained by the differing duration of PNP exposure. Unstimulated cell populations were exposed to PNPs for a period almost double to that of Hu *et al.* (2021). The secretion of IL-6 by RAW 264.7 cells under PNP exposure may thus be time specific as to explain these differing observations. Further expansion on this time dependency over a smaller concentration range is required.

IL-6 secretion by stimulated cell populations was an expected consequence of RAW 264.7 exposure to LPS. All PNPs, apart from two irregularities during APNP exposure, had shown the potential to downregulate the secretion of IL-6 by cells stimulated for an immune response. Unmodified PPNP exposure to these cell populations were shown to downregulate the secretion of IL-6, beginning at the lowest level of exposure (7.8125 μg/mL; Figure 4.13). The extent of this downregulation, when compared to the control, was noted to become greater with increasing PPNP concentration. These findings differ to those of Semete *et al.* (2010), in which plasma IL-6 levels after PPNP exposure had not differed to the negative control indicating that the downregulation brought about by PPNPs may be mitigated *in vivo*. In comparison to these PPNPs, CPNPs may also cause a downregulation in the secretion of IL-6 (Figure 4.15). The carboxyl-group surface modification, however, causes this downregulation to occur at a much higher concentration than in the case of PPNPs. The magnitude of the downregulation under CPNP exposure was also lower than that caused by PPNPs, where concentration was the same. This is further emphasized by the IL-6 IC_{50} values for PPNPs and CPNPs being found to be ± 44.8 μg/mL (Figure 4.14) and ± 232.21 μg/mL (Figure 4.16), respectively. CPNPs have been previously shown to induce significant upregulation of IL-6 by differentiated THP-1 macrophage cells (Prietl *et al.*, 2014). This upregulation was noted to not occur with CPNPs of

diameters 200 nm at a 20 μg/mL exposure. Based on these findings and those presented within this manuscript, results suggest smaller CPNPs may not greatly impair IL-6 secretion accompanying macrophage activation during an immune response.

The IL-6 secretion by stimulated RAW 264.7 cells under APNP exposure was seen to exhibit greater irregularities in comparison to the other PNPs (Figure 4.11). Exposure to APNP concentrations ≥ 62.5 μg/mL resulted in little to no secretion of IL-6 from the cells. These findings were most likely a consequence of the reduced cell viability at the same concentrations, as there are fewer cells available for IL-6 production at these concentrations. A signal instance of significant ($P<0.05$) IL-6 upregulation compared to the control had occurred during exposure to APNPs, occurring at the lowest level of APNP exposure (7.8125 μg/mL, Figure 4.11). Interestingly, the cell viability data at this exposure concentration indicates no statistically significant deviation from the control. This was most likely a result of the mitogenic effects of the LPS improving clearance of the APNPs. The subsequent concentration, 15.625 μg/mL APNP, had induced significant ($P<0.001$) reductions in cell viability (Figure 4.6) while no significant reduction in the secretion of IL-6 was evident (Figure 4.11). Stimulated cell viability was seen to have an APNP IC_{50} value greater than unstimulated cell viability due to the presence of LPS, which served to alter the cellular metabolism (Figures 4.2 and 4.7). As such, the results indicate stimulated cell populations may not be affected greatly at lower concentrations with the increase in IL-6 being the result of APNP presence. Less cells would therefore be required to produce the same amount of IL-6 as the control and would account for the events at 15.625 μg/mL APNP. This observation agrees with that of previous reports on PNP related IL-6 secretion (Ruenraroengsak and Tetley, 2015; Hu *et al.*, 2021). Thus, at low concentrations in which no alteration in cell viability will occur, APNPs may upregulate the secretion of IL-6 by stimulated cell populations.

5.5. Proteome profiles of RAW 264.7 under PNP exposure

Proteome profiles were obtained from RAW 264.7 cultures exposed to PNPs under both stimulated and unstimulated conditions and compared to the respective profiles of control cultures. The stimulated control culture media contained LPS while, unstimulated control culture media did not contain LPS. Under these conditions, the profiles highlight the possible way in which PNPs may alter cellular signalling either during an immune response or under basal conditions.

Under unstimulated conditions, control cells had only produced four secretory molecules, namely TNF-α, sICAM-1, MIP-1α and MIP-1β (Figure 4.17 i). These molecules remained present within supernatants of all unstimulated cultures exposed to 15 μg/mL PNPs. The data presented within this manuscript is consistent with findings that unmodified PPNPs upregulate MIP-1α, MIP-1β and MCP-1 in mouse plasma and skin lesions (Semete *et al.*, 2010; Yanagisawa *et al.*, 2010). This would signify that the alterations in cytokine production during APNP and CPNP exposure can be attributed to the associated modifications of the particles. APNPs had shown to uniquely downregulate the secretion MIP-1β due to a lack of visual intensity (Figure 4.17 ii). Due to a similar, but opposite, increase in intensity, APNPs were seen to uniquely upregulate MIP-2 (Figure 4.17 ii). The MIP chemokines serve as important chemoattractant molecules of various immune cell populations essential to immune response and mediate cellular events such as degranulation of target cells, synthesis of mediator molecules, and phagocytosis (Taub *et al.*, 1993; Uguccioni *et al.*, 1995; Loetscher *et al.*, 1996; Maurer and Von Stebut, 2004). This potential loss of MIP-1β may result in an ineffective regulation of immune cells. Thus, carboxyl modification of PNPs produces similar patterns of secretions to that of unmodified PNPs. While the amine surface modification of APNPs cause the unstimulated RAW 264.7 cells to take on a unique pattern of secretion, due to its differing surface chemistry. APNP exposure did not facilitate the secretion of MCP-1, impairing the secretion of MIP-1β, and upregulating the production of IL-16 and MIP-2 (Figure 4.17 ii).

In both the PPNP and CPNP exposure groups, slight traces of MCP-1 upregulation were seen to occur under unstimulated conditions (Figure 4.17 iii and iv). The secretion of MCP-1 has been shown to contribute to the adaptive immune system through directing CD4+ T-cell polarization towards the Th2 subset and chemotaxis of B, T cells, and Th17 cells (Gu *et al.*, 2000; Marshall, 2004; Hodge *et al.*, 2012). An important effect of the innate immune response by MCP-1 during an infection is the promotion of monocyte migration from the bone marrow into circulating blood. The absence of MCP-1 is accompanied by the impaired clearance of the infectious agent (Jia *et al.*, 2008). MCP-1 has also been shown to be pivotal to inflammatory tissue healing dependant on MIP-1α and MIP-2. These chemokines along with TNF-α are cytokines necessary for this process (Hoh *et al.*, 2011). Proteome profile data also indicates these cytokines are not altered under CPNP and PPNP exposure. The upregulation of MCP-1 by PPNPs and CPNPs would therefore result in the enhanced recruitment of inflammatory cells through its chemotactic effects for clearance of the stimulating NPs, accompanied by the associated inflammatory responses particularly for that of tissue repair. Further study is

required to understand the extent of increased MCP-1 production during long term exposure to PNPs, as MCP-1 is also known to mediate various diseases such as cancer, inflammatory bowel disease, and rheumatoid arthritis (Deshmane *et al.*, 2009).

The addition of LPS in stimulated control cells saw an appropriate increase in the number of secretory molecules produced by RAW 264.7 cells. Control cells had produced twelve secretory molecules solely under LPS exposure, namely IP-10, G-CSF, TNF-α, IL-6, MCP-1, sICAM-1, MIP-1α, MIP-1β, MIP-2, IL-1ra, CCL5 and IL-27 (Figure 4.18 i). These molecules had remained present during exposure to PNPs under stimulated conditions, apart from IL-1ra downregulation during APNP exposure (Figure 4.18 ii). Of these PNPs, there was no visual indication that the secretion under PPNP and CPNP exposure had differed to the stimulated control (Figure 4.18 i, iii and iv).

APNP exposure during stimulated conditions was seen to be capable of downregulating MCP-1, sICAM-1 and IL-1ra (Figure 4.18 i). This was determined by a loss of visual intensity or by the signal of the detected molecule being indistinguishable from the background staining. The dual downregulation of MCP-1 and sICAM-1 implies APNPs may greatly impede the function of the adaptive immune system. MCP-1 influences CD4+ T cell polarization toward the Th2 subset by promoting the production of IL-4. sICAM-1, the soluble form of membrane-bound ICAM-1, competes for binding with the ICAM-1 β_2-integrins required for leukocyte tracking (Gu *et al.*, 2000; Müller, 2019). sICAM-1 also serves as an important marker and regulatory molecule during immunological conditions where the Th1 cell response is the primary mechanism of action (Müller *et al.*, 1999). These molecules thus contribute to the function of cellular (Th1) and humoral (Th2) immune responses. There is a clear consequence accompanying APNP presence during Th2 cell response, as IL-4 is necessary for polarization (Gu *et al.*, 2000). The selection of the cellular or humoral response is based on the initiating antigen presenting cell present, such as dendritic cells (Kidd, 2003). Dendritic cells may initiate an antigen independent T-cell response, the ability for which relies partially on ICAM-1 interaction with lymphocyte function-associated antigen-1 (LFA-1) for T-cell motility and adhesion (Real *et al.*, 2004; Sethu *et al.*, 2012). While these reductions do constitute some concern as a potential disturbance to the normal pattern of immunological function, the cytotoxicity of APNPs is the most probable cause of sICAM-1 downregulation seen within this manuscript. The amount of sICAM-1 secreted is considered to reflect the degree of expression of ICAM-1 on cell surfaces, where the release of the soluble form occurs through proteolytic cleavage of membrane bound ICAM-1 (Champagne *et al.*, 1998; Witkowska and Borawska,

2004). The isolation of sICAM-1 messenger ribonucleic acid (mRNA) transcripts has also been performed, indicating sICAM-1 generation to be in part through genetic expression (Whiteman *et al.*, 2003). Reductions in cell populations would explain the decreased presence of sICAM-1 in either of these instances.

Similar to the response observed with unstimulated cells, APNPs had also upregulated IL-16 production in stimulated cells (Figures 4.17 ii and 4.18 ii). This indicates increased IL-16 production to be a potential and consistent consequence of APNP exposure, regardless of whether cells are stimulated by LPS or not. This upregulation of IL-16 is consistent with a study by Ballesteros *et al.* (2021), in which whole blood cultures were exposed to various graphene based NPs. No extensive investigation into surface properties was performed, however, greater amounts of IL-16 were produced by the more positive NPs compared to the more negative NPs. IL-16 serves as a chemoattractant for cells bearing the CD4 co-receptor, particularly for the CD4+ Th1 cells and monocytes (O'shea *et al.*, 2019). Alternatively, IL-16 also inhibits antigen-driven Th2 cell-mediated immune responses. While IL-16 directly attracts CD4+ T cells, it is simultaneously capable of indirectly inhibiting chemoattraction. This inhibition occurs through cross-desensitization of receptors preventing ligands from properly initiating their effects, particularly CCL5, MIP-1α and MIP-1β (Wilson *et al.*, 2004). This would indicate that while APNP exposure does not directly impair the production of the aforementioned chemokines in stimulated cells, as their function is indirectly inhibited by IL-16 upregulation. Therefore, during exposure of APNPs to stimulated cells, Th1 cell polarization is promoted due to IL-16 upregulation and MCP-1 downregulation, as MCP-1 is required for Th2 cell polarization. With regards to macrophage activity, IL-16 modulates macrophage polarization towards the classically activated subset and enhances the phagocytotic activity of these cells (Huang *et al.*, 2019). Thus, stimulated cells under APNP exposure would promote the presence of Th1 cells and classically activated macrophages.

The production of IL-1ra by the control cells is to be expected with LPS stimulation (Figure 4.18 i), as LPS is one of the best inducers of IL-1ra production by mononuclear phagocytes *in vitro* (Mak and Saunders, 2006). Of the observed PNPs, the addition of APNPs to stimulated RAW 264.7 cells were the only condition in which a complete inhibition of the IL-1ra cytokine occurred (Figure 4.18 ii). IL-1ra is a natural competitive inhibitor to the highly inflammatory cytokine IL-1, an important cytokine for host defence against intracellular infection. Both IL-1 and IL-1ra bind to the same receptor where IL-1ra does not initiate signal transduction required for IL-1 receptor associated inflammatory responses. This is important for biological

functioning as there needs to be a 100-fold excess of IL-1ra compared to IL-1 to achieve a 50 % inhibition of IL-1-induced responses. As such, IL-1ra is responsible for modulating the activity of IL-1 signalling through its anti-inflammatory ability (Arend *et al.*, 1990; Arend, 2002). A study assessing the effects of polymeric NP protein corona on cellular uptake by monocytes and macrophages, revealed that the NPs of an initially negative charge had not induced any significant alterations in IL-1ra levels (Yan *et al.*, 2013). These findings are consistent with the findings of this investigation, as exposure to the more negatively charged CPNPs and PPNPs had not affected or showed little effect on the secretion of IL-1ra by RAW 264.7 cells. This inhibition can thus be attributed to the amine surface functionalization of the APNPs, as cells of the control and those exposed to the other PNPs had not experienced a similar event (Figure 4.18 i, iii and iv). APNPs would therefore decrease the modulation of IL-1 during instances in which an immune response is already underway, by inhibiting anti-inflammatory IL-1ra secretion. Thus, this may potentially lead to damage associated with IL-1 over secretion. Various inflammatory diseases are associated with an excess of IL-1 and/or deficiency of IL-1ra, such as pulmonary diseases, renal diseases, and diseases of the liver and pancreas, etc (Mulligan and Ward, 1992; Fujioka *et al.*, 1995; Norman *et al.*, 1995; Tesch *et al.*, 1997; Arend, 2002).

5.6. Conclusion

Unmodified PPNPs were the only of the tested NPs to induce an increase in cell viability under unstimulated conditions. CPNPs were not to seen alter cell viability under unstimulated conditions, while positively charged APNPs exhibited the greatest cytotoxic potential in unstimulated RAW 264.7 cells. Under stimulation of LPS for an immune response, PPNPs and CPNPs were not seen to alter RAW cell viability. APNP exposure at concentrations ≥ 15.625 µg/mL reduced stimulated RAW cell viability. APNPs therefore, retained their cytotoxic potential in stimulated cells but doing so at higher APNP concentrations due to the mitogenic effects associated with LPS stimulation.

Functionalized APNPs and CPNPs upregulated NO production in unstimulated cells at the highest concentration, 500 µg/mL, while unmodified PPNPs did so at concentrations ≥ 125 µg/mL. This indicates that both forms of functionalization decreased the modulatory activity of PNPs on NO production in unstimulated RAW 264.7 cells. PPNPs and CPNPs had not altered NO levels in stimulated RAW cells, with the sole exception of slight NO upregulation

at 500 µg/mL CPNP. APNPs downregulated NO production when stimulated cells were exposed to all concentrations. IL-6 secretion by stimulated RAW cells was downregulated during exposure to all PNPs, apart from upregulation at the lowest two APNP concentrations. Therefore, the functionalization of APNPs and CPNPs lessens the productions of NO in unstimulated cell while PPNPs and CPNPs were seen to not alter NO production of stimulated cells. APNPs, however, possess the greatest immunomodulatory activity due to the extent and consistency at which the alteration of the inflammatory biomarkers NO and IL-6 occurs.

The cytokines and chemokines secreted by unstimulated RAW cells under PNP exposure were TNF-α, sICAM-1/CD54, MIP-1α and MIP-1β. APNPs were the only of the functionalized PNPs to downregulate MIP-1β and upregulate IL-16 and MIP-2, where PPNPs and CPNPs only upregulated MCP-1 secretion. This indicates that greater immunomodulatory activity was associated with APNPs in unstimulated cells. Unmodified PNPs and CPNPs showed no indication of immunomodulatory activity, where MCP-1 shows potential as a biomarker of exposure specific to these PNPs.

The cytokines and chemokines secreted by stimulated RAW cells under PNP exposure were IP-10/CXCL10, G-CSF, TNF-α, IL-6, MCP-1, sICAM-1/CD54, MIP-1α, MIP-1β, MIP-2, IL-1ra, CCL5/RANTES, and IL-27. APNPs were seen to provide the greatest alteration in immune response under stimulated conditions by downregulation of IL-1ra, sICAM-1 and MCP-1, while upregulating IL-16. Quantitative differences in secretion were not assessed but are a potential area of investigation for future studies.

Of the tested PNPs, the effects produced by the CPNPs closely resembles that of unmodified PPNPs. These PNPs exhibit little immunomodulatory activity under both stimulated and unstimulated conditions. In contrast, the amine functionalized APNPs have the greatest potential to alter immune response under these conditions. This is achieved through the reduction in cell populations, reduction in the production of inflammatory biomarkers and alteration in the production of secretory molecules.

5.7. Future perspectives and recommendations

- The characterization of nanoparticles revealed initial charge differences in aqueous solution. These differences were no longer present in culture media, where size was also altered. Future research should aim to identify the differences in the composition of the specific protein coronas formed.

- Only a single type of functionalization for each charge was assessed in this study. The effects seen should be reassessed with the addition of other functional groups which provide similar differences in charges. This should be done to definitively say whether the effects seen are a result of the specific charge provided or if it is dependent on the specific functional group used.
- Intracellular studies focusing on cellular uptake and internal localization should be done. This will provide better understanding of the interaction between cells of the immune system and differently functionalized nanoparticles.
- The effect of chronic exposure by differently functionalized nanoparticles should also be assessed in future studies as the duration of exposure may alter cellular secretions.
- The same effects should be assessed in many immune system cell types to develop a holistic view on how nanoparticle surface functionalization may alter immune response.
- Quantitative measurements should be performed for the excreted cytokines and chemokines that were monitored qualitatively in this study.
- Intracellular signals were not monitored in this study and should be done in future research. This will provide understanding of the intracellular signalling pathways affected, internal cell stressors, and if apoptosis is at play during the interaction of immune cells and differently functionalized nanoparticles.

References

Aarden, L. A., De Groot, E. R., Schaap, O. L. & Lansdorp, P. M. 1987. Production of hybridoma growth factor by human monocytes. *European Journal of Immunology,* 17**,** 1411-1416.

Abbas, A. K., Litchmann, A. & Pillai, S. 2016. Basic Immunology: Functions and Disorders of the Immune System. St Louis. 5th ed.: USA: WB Saunders Company.

Abdelkhaliq, A., Van Der Zande, M., Punt, A., Helsdingen, R., Boeren, S., Vervoort, J. J. M., Rietjens, I. M. C. M. & Bouwmeester, H. 2018. Impact of nanoparticle surface functionalization on the protein corona and cellular adhesion, uptake and transport. *Journal of Nanobiotechnology,* 16**,** 70.

Adams, D. O. 1989. Molecular interactions in macrophage activation. *Immunology Today,* 10**,** 33-35.

Afshar, M. & Gallo, R. L. 2013. Innate immune defense system of the skin. *Veterinary Dermatology,* 24**,** 32-e9.

Alimba, C. G. & Faggio, C. 2019. Microplastics in the marine environment: Current trends in environmental pollution and mechanisms of toxicological profile. *Environmental Toxicology and Pharmacology,* 68**,** 61-74.

Amsen, D., Spilianakis, C. G. & Flavell, R. A. 2009. How are TH1 and TH2 effector cells made? *Current Opinion in Immunology,* 21**,** 153-160.

Anaya, J.-M., Shoenfeld, Y., Rojas-Villarraga, A., Levy, R. A. & Cervera, R. 2013. *Autoimmunity: From Bench to Bedside*, El Rosario University Press.

Andersson, U., Wang, H., Palmblad, K., Aveberger, A.-C., Bloom, O., Erlandsson-Harris, H., Janson, A., Kokkola, R., Zhang, M., Yang, H. & Tracey, K. J. 2000. High Mobility Group 1 Protein (Hmg-1) Stimulates Proinflammatory Cytokine Synthesis in Human Monocytes. *Journal of Experimental Medicine,* 192**,** 565-570.

Andrady, A. L. 2011. Microplastics in the marine environment. *Marine Pollution Bulletin,* 62**,** 1596-1605.

Arend, W. P. 2002. The balance between IL-1 and IL-1Ra in disease. *Cytokine & Growth Factor Reviews,* 13**,** 323-340.

Arend, W. P., Welgus, H., Thompson, R. C. & Eisenberg, S. 1990. Biological properties of recombinant human monocyte-derived interleukin 1 receptor antagonist. *The Journal of Clinical Investigation,* 85**,** 1694-1697.

Atabaev, T. S., Lee, J. H., Han, D.-W., Choo, K. S., Jeon, U. B., Hwang, J. Y., Yeom, J. A., Kang, C., Kim, H.-K. & Hwang, Y.-H. 2016. Multicolor nanoprobes based on silica-

coated gadolinium oxide nanoparticles with highly reduced toxicity. *RSC Advances,* 6**,** 19758-19762.

Baek, M., Kim, M., Cho, H., Lee, J., Yu, J., Chung, H. & Choi, S. Factors influencing the cytotoxicity of zinc oxide nanoparticles: particle size and surface charge. Journal of Physics: Conference Series, 2011. IOP Publishing, 012044.

Bajaj, A., Miranda, O. R., Kim, I.-B., Phillips, R. L., Jerry, D. J., Bunz, U. H. & Rotello, V. M. 2009. Detection and differentiation of normal, cancerous, and metastatic cells using nanoparticle-polymer sensor arrays. *Proceedings of the National Academy of Sciences,* 106**,** 10912-10916.

Ballesteros, S., Domenech, J., Velázquez, A., Marcos, R. & Hernández, A. 2021. Ex vivo exposure to different types of graphene-based nanomaterials consistently alters human blood secretome. *Journal of Hazardous Materials,* 414**,** 125471.

Banchereau, J. & Steinman, R. M. 1998. Dendritic cells and the control of immunity. *Nature,* 392**,** 245-252.

Barrons, R. W. 1997. Drug-induced neuromuscular blockade and myasthenia gravis. *Pharmacotherapy: The Journal of Human Pharmacology and Drug Therapy,* 17**,** 1220-1232.

Barry, M. & Bleackley, R. C. 2002. Cytotoxic T lymphocytes: all roads lead to death. *Nature Reviews Immunology,* 2**,** 401-409.

Baumann, H., Jahreis, G., Sauder, D. & Koj, A. 1984. Human keratinocytes and monocytes release factors which regulate the synthesis of major acute phase plasma proteins in hepatic cells from man, rat, and mouse. *Journal of Biological Chemistry,* 259**,** 7331-7342.

Benn, T. M. & Westerhoff, P. 2008. Nanoparticle silver released into water from commercially available sock fabrics. *Environmental Science & Technology,* 42**,** 4133-4139.

Bera, D., Qian, L., Tseng, T.-K. & Holloway, P. H. 2010. Quantum dots and their multimodal applications: a review. *Materials,* 3**,** 2260-2345.

Bhattacharjee, S., Ershov, D., Gucht, J. V. D., Alink, G. M., Rietjens, I. M. M., Zuilhof, H. & Marcelis, A. T. 2013. Surface charge-specific cytotoxicity and cellular uptake of tri-block copolymer nanoparticles. *Nanotoxicology,* 7**,** 71-84.

Biju, V. 2014. Chemical modifications and bioconjugate reactions of nanomaterials for sensing, imaging, drug delivery and therapy. *Chemical Society Reviews,* 43**,** 744-764.

Bogdan, C. 2001. Nitric oxide and the immune response. *Nature Immunology,* 2**,** 907.

Brayner, R. 2008. The toxicological impact of nanoparticles. *Nano Today,* 3**,** 48-55.

Carlsson, J.-O. & Martin, P. M. 2010. Chapter 7 - Chemical Vapor Deposition. *In:* Martin, P. M. (ed.) *Handbook of Deposition Technologies for Films and Coatings (Third Edition).* Boston: William Andrew Publishing.

Cavaillon, J. 1994. Cytokines and macrophages. *Biomedicine & Pharmacotherapy,* 48**,** 445-453.

Cerutti, A. 2008. The regulation of IgA class switching. *Nature Reviews Immunology,* 8**,** 421-434.

Champagne, B., Tremblay, P., Cantin, A. & Pierre, Y. S. 1998. Proteolytic cleavage of ICAM-1 by human neutrophil elastase. *The Journal of Immunology,* 161**,** 6398-6405.

Chaplin, D. D. 2003. Overview of the immune response. *Journal of Allergy and Clinical Immunology,* 111**,** S442-S459.

Chaplin, D. D. 2006. Overview of the human immune response. *Journal of Allergy and Clinical Immunology,* 117**,** S430-S435.

Chen, H. C., Sun, B., Tran, K. K. & Shen, H. 2011a. Effects of particle size on toll-like receptor 9-mediated cytokine profiles. *Biomaterials,* 32**,** 1731-1737.

Chen, L., Mccrate, J. M., Lee, J. C. & Li, H. 2011b. The role of surface charge on the uptake and biocompatibility of hydroxyapatite nanoparticles with osteoblast cells. *Nanotechnology,* 22**,** 105708.

Chou, L. Y., Ming, K. & Chan, W. C. 2011. Strategies for the intracellular delivery of nanoparticles. *Chemical Society Reviews,* 40**,** 233-245.

Cole, M., Lindeque, P., Halsband, C. & Galloway, T. S. 2011. Microplastics as contaminants in the marine environment: A review. *Marine Pollution Bulletin,* 62**,** 2588-2597.

Connor, E., Mwamuka, J., Gole, A., Murphy, C. & Wyatt, M. 2005. Gold nanoparticles are taken up by human cells but do not cause acute cytotoxicity. *Small (Weinheim an der Bergstrasse, Germany),* 1**,** 325-327.

Cooper, M. D. & Alder, M. N. 2006. The Evolution of Adaptive Immune Systems. *Cell,* 124**,** 815-822.

Corbel, C. & Melchers, F. 1984. The Synergism of Aecessory Cells and of Soluble a-Factors Derived from Them in the Activation of B Cells to Proliferation. *Immunological Reviews,* 78**,** 51-74.

Daraee, H., Eatemadi, A., Abbasi, E., Fekri Aval, S., Kouhi, M. & Akbarzadeh, A. 2016. Application of gold nanoparticles in biomedical and drug delivery. *Artificial Cells, Nanomedicine, and Biotechnology,* 44**,** 410-422.

De Jong, W. H. & Van Loveren, H. 2007. Screening of xenobiotics for direct immunotoxicity in an animal study. *Methods,* 41**,** 3-8.

Descotes, J. 2004. Importance of immunotoxicity in safety assessment: a medical toxicologist's perspective. *Toxicology Letters,* 149**,** 103-108.

Deshmane, S. L., Kremlev, S., Amini, S. & Sawaya, B. E. 2009. Monocyte chemoattractant protein-1 (MCP-1): an overview. *Journal of Interferon & Cytokine Research,* 29**,** 313-326.

Dewitt, J. C., Peden-Adams, M. M., Keller, J. M. & Germolec, D. R. 2012. Immunotoxicity of perfluorinated compounds: recent developments. *Toxicologic Pathology,* 40**,** 300-311.

Dwivedi, P. D., Misra, A., Shanker, R. & Das, M. 2009. Are nanomaterials a threat to the immune system? *Nanotoxicology,* 3**,** 19-26.

Ealia, S. a. M. & Saravanakumar, M. A review on the classification, characterisation, synthesis of nanoparticles and their application. IOP Conference Series: Materials Science and Engineering, 2017. IOP Publishing, 032019.

Efimova, I., Bagaeva, M., Bagaev, A., Kileso, A. & Chubarenko, I. P. 2018. Secondary Microplastics Generation in the Sea Swash Zone With Coarse Bottom Sediments: Laboratory Experiments. *Frontiers in Marine Science,* 5.

El-Boubbou, K., Zhu, D. C., Vasileiou, C., Borhan, B., Prosperi, D., Li, W. & Huang, X. 2010. Magnetic glyco-nanoparticles: a tool to detect, differentiate, and unlock the glyco-codes of cancer via magnetic resonance imaging. *Journal of the American Chemical Society,* 132**,** 4490-4499.

El Badawy, A. M., Silva, R. G., Morris, B., Scheckel, K. G., Suidan, M. T. & Tolaymat, T. M. 2011. Surface charge-dependent toxicity of silver nanoparticles. *Environmental Science & Technology,* 45**,** 283-287.

Eming, S. A., Hammerschmidt, M., Krieg, T. & Roers, A. Interrelation of immunity and tissue repair or regeneration. Seminars in cell & developmental biology, 2009. Elsevier, 517-527.

Fabrega, J., Luoma, S. N., Tyler, C. R., Galloway, T. S. & Lead, J. R. 2011. Silver nanoparticles: Behaviour and effects in the aquatic environment. *Environment International,* 37**,** 517-531.

Fadeel, B. 2019. Hide and seek: Nanomaterial interactions with the immune system. *Frontiers in Immunology,* 10**,** 133.

Feiner-Gracia, N., Beck, M., Pujals, S., Tosi, S., Mandal, T., Buske, C., Linden, M. & Albertazzi, L. 2017. Super-resolution microscopy unveils dynamic heterogeneities in nanoparticle protein corona. *Small,* 13**,** 1701631.

Feynman, R. P. There's Plenty of Room at the Bottom. APS annual meeting, 1959.

Freestone, I., Meeks, N., Sax, M. & Higgitt, C. 2007. The Lycurgus cup—a roman nanotechnology. *Gold Bulletin,* 40**,** 270-277.

Fröhlich, E. 2012. The role of surface charge in cellular uptake and cytotoxicity of medical nanoparticles. *International Journal of Nanomedicine,* 7**,** 5577-5591.

Fuchs, A.-K., Syrovets, T., Haas, K. A., Loos, C., Musyanovych, A., Mailänder, V., Landfester, K. & Simmet, T. 2016. Carboxyl- and amino-functionalized polystyrene nanoparticles differentially affect the polarization profile of M1 and M2 macrophage subsets. *Biomaterials,* 85**,** 78-87.

Fujioka, N., Mukaida, N., Harada, A., Akiyama, M., Kasahara, T., Kuno, K., Ooi, A., Mai, M. & Matsushima, K. 1995. Preparation of specific antibodies against murine IL-1ra and the establishment of IL-1ra as an endogenous regulator of bacteria-induced fulminant hepatitis in mice. *Journal of Leukocyte Biology,* 58**,** 90-98.

Funderburg, N., Lederman, M. M., Feng, Z., Drage, M. G., Jadlowsky, J., Harding, C. V., Weinberg, A. & Sieg, S. F. 2007. Human β-defensin-3 activates professional antigen-presenting cells via Toll-like receptors 1 and 2. *Proceedings of the National Academy of Sciences,* 104**,** 18631-18635.

Gauldie, J., Richards, C., Harnish, D., Lansdorp, P. & Baumann, H. 1987. Interferon beta 2/B-cell stimulatory factor type 2 shares identity with monocyte-derived hepatocyte-stimulating factor and regulates the major acute phase protein response in liver cells. *Proceedings of the National Academy of Sciences,* 84**,** 7251-7255.

Gaumet, M., Vargas, A., Gurny, R. & Delie, F. 2008. Nanoparticles for drug delivery: the need for precision in reporting particle size parameters. *European Journal of Pharmaceutics and Biopharmaceutics,* 69**,** 1-9.

Gellert, M. 2002. V (D) J recombination: RAG proteins, repair factors, and regulation. *Annual Review of Biochemistry,* 71**,** 101-132.

Giraldo, N. A., Becht, E., Vano, Y., Sautès-Fridman, C. & Fridman, W. H. 2015. The immune response in cancer: from immunology to pathology to immunotherapy. *Virchows Archiv,* 467**,** 127-135.

Gogotsi, Y. 2006. *Nanomaterials handbook,* CRC press.

Goodman, C. M., Mccusker, C. D., Yilmaz, T. & Rotello, V. M. 2004. Toxicity of gold nanoparticles functionalized with cationic and anionic side chains. *Bioconjugate Chemistry,* 15**,** 897-900.

Gordon, S. 2003. Alternative activation of macrophages. *Nature Reviews Immunology,* 3**,** 23-35.

Gottschalk, F., Sonderer, T., Scholz, R. W. & Nowack, B. 2009. Modeled environmental concentrations of engineered nanomaterials (TiO2, ZnO, Ag, CNT, fullerenes) for different regions. *Environmental Science & Technology,* 43**,** 9216-9222.

Granger, D. L., Taintor, R. R., Boockvar, K. S. & Hibbs Jr, J. B. 1996. Measurement of nitrate and nitrite in biological samples using nitrate reductase and Griess reaction. *Methods in Enzymology.* Elsevier.

Greish, K., Thiagarajan, G., Herd, H., Price, R., Bauer, H., Hubbard, D., Burckle, A., Sadekar, S., Yu, T. & Anwar, A. 2012. Size and surface charge significantly influence the toxicity of silica and dendritic nanoparticles. *Nanotoxicology,* 6**,** 713-723.

Gu, L., Tseng, S., Horner, R. M., Tam, C., Loda, M. & Rollins, B. J. 2000. Control of TH 2 polarization by the chemokine monocyte chemoattractant protein-1. *Nature,* 404**,** 407-411.

Halamoda-Kenzaoui, B., Ceridono, M., Urbán, P., Bogni, A., Ponti, J., Gioria, S. & Kinsner-Ovaskainen, A. 2017. The Agglomeration State of Nanoparticles Can Influence the Mechanism of Their Cellular Internalisation. *Journal of Nanobiotechnology,* 15**,** 48.

Harboe, M. & Mollnes, T. E. 2008. The alternative complement pathway revisited. *Journal of Cellular and Molecular Medicine,* 12**,** 1074-1084.

Hodge, D. L., Reynolds, D., Cerbán, F. M., Correa, S. G., Baez, N. S., Young, H. A. & Rodriguez-Galan, M. C. 2012. MCP-1/CCR2 interactions direct migration of peripheral B and T lymphocytes to the thymus during acute infectious/inflammatory processes. *European Journal of Immunology,* 42**,** 2644-2654.

Hoffmann, J., Akira, S. & Hoffmann, J. 2013. Innate Immunity Editorial Overview. *Current Opinion in Immunology [Internet],* 25**,** 1-3.

Hoh, B. L., Hosaka, K., Downes, D. P., Nowicki, K. W., Fernandez, C. E., Batich, C. D. & Scott, E. W. 2011. Monocyte chemotactic protein-1 promotes inflammatory vascular repair of murine carotid aneurysms via a macrophage inflammatory protein-1α and macrophage inflammatory protein-2-dependent pathway. *Circulation,* 124**,** 2243-2252.

Honjo, T., Kinoshita, K. & Muramatsu, M. 2002. Molecular mechanism of class switch recombination: linkage with somatic hypermutation. *Annual Review of Immunology,* 20**,** 165-196.

Hotchkiss, R. S. & Karl, I. E. 2003. The pathophysiology and treatment of sepsis. *The New England Journal of Medicine,* 348 2**,** 138-150.

Hu, Q., Wang, H., He, C., Jin, Y. & Fu, Z. 2021. Polystyrene nanoparticles trigger the activation of p38 MAPK and apoptosis via inducing oxidative stress in zebrafish and macrophage cells. *Environmental Pollution,* 269**,** 116075.

Huang, D., Zeng, M., Wang, L., Zhang, L. & Cheng, Z. 2018. Biomimetic colloidal photonic crystals by coassembly of polystyrene nanoparticles and graphene quantum dots. *RSC Advances,* 8**,** 34839-34847.

Huang, J., Bu, L., Xie, J., Chen, K., Cheng, Z., Li, X. & Chen, X. 2010. Effects of nanoparticle size on cellular uptake and liver MRI with polyvinylpyrrolidone-coated iron oxide nanoparticles. *ACS Nano,* 4**,** 7151-7160.

Huang, Y., Du, K. L., Guo, P. Y., Zhao, R. M., Wang, B., Zhao, X. L. & Zhang, C. Q. 2019. IL-16 regulates macrophage polarization as a target gene of mir-145-3p. *Molecular Immunology,* 107**,** 1-9.

Hühn, D., Kantner, K., Geidel, C., Brandholt, S., De Cock, I., Soenen, S., Gil, P., Montenegro, J., Braeckmans, K. & Müllen, K. 2013. Polymer-Coated Nanoparticles Interacting with Proteins and Cells: Focusing on the Sign of the Net Charge. *ACS Nano,* 7**,** 3253-3263.

Hwang, S.-H., Thielbeer, F., Jeong, J., Han, Y., Chankeshwara, S. V., Bradley, M. & Cho, W.-S. 2016. Dual contribution of surface charge and protein-binding affinity to the cytotoxicity of polystyrene nanoparticles in nonphagocytic A549 cells and phagocytic THP-1 cells. *Journal of Toxicology and Environmental Health, Part A,* 79**,** 925-937.

Iversen, T.-G., Skotland, T. & Sandvig, K. 2011. Endocytosis and intracellular transport of nanoparticles: Present knowledge and need for future studies. *Nano Today,* 6**,** 176-185.

Jahnen-Dechent, W. & Simon, U. 2008. Function follows form: shape complementarity and nanoparticle toxicity. *Nanomedicine,* 3**,** 601-603.

Jambeck, J. R., Geyer, R., Wilcox, C., Siegler, T. R., Perryman, M., Andrady, A., Narayan, R. & Law, K. L. 2015. Plastic waste inputs from land into the ocean. *Science,* 347**,** 768-771.

Jazayeri, M. H., Amani, H., Pourfatollah, A. A., Pazoki-Toroudi, H. & Sedighimoghaddam, B. 2016. Various methods of gold nanoparticles (GNPs) conjugation to antibodies. *Sensing and Bio-Sensing Research,* 9**,** 17-22.

Jeon, S., Clavadetscher, J., Lee, D.-K., Chankeshwara, S. V., Bradley, M. & Cho, W.-S. 2018. Surface charge-dependent cellular uptake of polystyrene nanoparticles. *Nanomaterials,* 8**,** 1028.

Jevprasesphant, R., Penny, J., Jalal, R., Attwood, D., Mckeown, N. B. & D'emanuele, A. 2003. The influence of surface modification on the cytotoxicity of PAMAM dendrimers. *International Journal of Pharmaceutics,* 252**,** 263-266.

Jia, G., Wang, H., Yan, L., Wang, X., Pei, R., Yan, T., Zhao, Y. & Guo, X. 2005. Cytotoxicity of carbon nanomaterials: single-wall nanotube, multi-wall nanotube, and fullerene. *Environmental Science & Technology,* 39**,** 1378-1383.

Jia, T., Serbina, N. V., Brandl, K., Zhong, M. X., Leiner, I. M., Charo, I. F. & Pamer, E. G. 2008. Additive roles for MCP-1 and MCP-3 in CCR2-mediated recruitment of inflammatory monocytes during Listeria monocytogenes infection. *The Journal of Immunology,* 180**,** 6846-6853.

Jiang, Y., Zhao, H., Lin, Y., Zhu, N., Ma, Y. & Mao, L. 2010. Colorimetric detection of glucose in rat brain using gold nanoparticles. *Angewandte Chemie International Edition,* 49**,** 4800-4804.

Jones, J. A., Starkey, J. R. & Kleinhofs, A. 1980. Toxicity and mutagenicity of sodium azide in mammalian cell cultures. *Mutation Research/Genetic Toxicology,* 77**,** 293-299.

Kamimura, M., Ueya, Y., Takamoto, E., Iso, K., Yoshida, M., Umezawa, M. & Soga, K. 2019. Fluorescent Polystyrene Latex Nanoparticles for NIR-II in vivo Imaging. *Journal of Photopolymer Science and Technology,* 32**,** 93-96.

Kaplanski, G., Marin, V., Montero-Julian, F., Mantovani, A. & Farnarier, C. 2003. IL-6: a regulator of the transition from neutrophil to monocyte recruitment during inflammation. *Trends in Immunology,* 24**,** 25-29.

Kidd, P. 2003. Th1/Th2 balance: the hypothesis, its limitations, and implications for health and disease. *Alternative Medicine Review,* 8**,** 223-246.

Kirchner, C., Liedl, T., Kudera, S., Pellegrino, T., Muñoz Javier, A., Gaub, H. E., Stölzle, S., Fertig, N. & Parak, W. J. 2005. Cytotoxicity of colloidal CdSe and CdSe/ZnS nanoparticles. *Nano Letters,* 5**,** 331-338.

Knott, A. B. & Bossy-Wetzel, E. 2009. Nitric oxide in health and disease of the nervous system. *Antioxidants & Redox Signaling,* 11**,** 541-553.

Kobayashi, M., Fitz, L., Ryan, M., Hewick, R. M., Clark, S. C., Chan, S., Loudon, R., Sherman, F., Perussia, B. & Trinchieri, G. 1989. Identification and purification of natural killer

cell stimulatory factor (NKSF), a cytokine with multiple biologic effects on human lymphocytes. *Journal of Experimental Medicine,* 170**,** 827-845.

Kotsokechagia, T., Zaki, N. M., Syres, K., Leonardis, P. D., Thomas, A., Cellesi, F. & Tirelli, N. 2012. PEGylation of nanosubstrates (titania) with multifunctional reagents: At the crossroads between nanoparticles and nanocomposites. *Langmuir,* 28**,** 11490-11501.

Kralj, S., Drofenik, M. & Makovec, D. 2011. Controlled surface functionalization of silica-coated magnetic nanoparticles with terminal amino and carboxyl groups. *Journal of Nanoparticle Research,* 13**,** 2829-2841.

Kumar, N. & Kumbhat, S. 2016. *Essentials In Nanoscience And Nanotechnology*, John Wiley & Sons, Inc.

Kumar, S., Aaron, J. & Sokolov, K. 2008. Directional conjugation of antibodies to nanoparticles for synthesis of multiplexed optical contrast agents with both delivery and targeting moieties. *Nature Protocols,* 3**,** 314.

Lambert, S. & Wagner, M. 2016. Characterisation of nanoplastics during the degradation of polystyrene. *Chemosphere,* 145**,** 265-268.

Lebreton, L., Slat, B., Ferrari, F., Sainte-Rose, B., Aitken, J., Marthouse, R., Hajbane, S., Cunsolo, S., Schwarz, A., Levivier, A., Noble, K., Debeljak, P., Maral, H., Schoeneich-Argent, R., Brambini, R. & Reisser, J. 2018. Evidence that the Great Pacific Garbage Patch is rapidly accumulating plastic. *Scientific Reports,* 8**,** 4666.

Lee, S. H., Bae, K. H., Kim, S. H., Lee, K. R. & Park, T. G. 2008. Amine-functionalized gold nanoparticles as non-cytotoxic and efficient intracellular siRNA delivery carriers. *International Journal of Pharmaceutics,* 364**,** 94-101.

Liu, Y., Feng, X., Shen, J., Zhu, J.-J. & Hou, W. 2008. Fabrication of a novel glucose biosensor based on a highly electroactive polystyrene/polyaniline/Au nanocomposite. *The Journal of Physical Chemistry B,* 112**,** 9237-9242.

Lock, E. H., Petrovykh, D. Y., Mack, P., Carney, T., White, R. G., Walton, S. G. & Fernsler, R. F. 2010. Surface composition, chemistry, and structure of polystyrene modified by electron-beam-generated plasma. *Langmuir,* 26**,** 8857-8868.

Loetscher, P., Seitz, M., Clark-Lewis, I., Baggiolini, M. & Moser, B. 1996. Activation of NK cells by CC chemokines. Chemotaxis, Ca2+ mobilization, and enzyme release. *The Journal of Immunology,* 156**,** 322-327.

Loos, C., Syrovets, T., Musyanovych, A., Mailänder, V., Landfester, K., Nienhaus, G. U. & Simmet, T. 2014a. Functionalized polystyrene nanoparticles as a platform for studying bio–nano interactions. *Beilstein Journal of Nanotechnology,* 5**,** 2403-2412.

Loos, C., Syrovets, T., Musyanovych, A., Mailänder, V., Landfester, K. & Simmet, T. 2014b. Amino-functionalized nanoparticles as inhibitors of mTOR and inducers of cell cycle arrest in leukemia cells. *Biomaterials,* 35**,** 1944-1953.

Lu, F., Wu, S. H., Hung, Y. & Mou, C. Y. 2009. Size effect on cell uptake in well-suspended, uniform mesoporous silica nanoparticles. *Small,* 5**,** 1408-1413.

Lundqvist, M., Stigler, J., Elia, G., Lynch, I., Cedervall, T. & Dawson, K. A. 2008. Nanoparticle size and surface properties determine the protein corona with possible implications for biological impacts. *Proceedings of the National Academy of Sciences,* 105**,** 14265-14270.

Lunov, O., Syrovets, T., Loos, C., Beil, J., Delacher, M., Tron, K., Nienhaus, G. U., Musyanovych, A., Mailänder, V., Landfester, K. & Simmet, T. 2011a. Differential Uptake of Functionalized Polystyrene Nanoparticles by Human Macrophages and a Monocytic Cell Line. *ACS Nano,* 5**,** 1657-1669.

Lunov, O., Syrovets, T., Loos, C., Nienhaus, G. U., Mailänder, V., Landfester, K., Rouis, M. & Simmet, T. 2011b. Amino-Functionalized Polystyrene Nanoparticles Activate the NLRP3 Inflammasome in Human Macrophages. *ACS Nano,* 5**,** 9648-9657.

Luster, M. I. & Rosenthal, G. J. 1993. Chemical agents and the immune response. *Environmental Health Perspectives,* 100**,** 219-226.

Lynch, I., Salvati, A. & Dawson, K. A. 2009. What does the cell see? *Nature Nanotechnology,* 4**,** 546-547.

Mak, T. & Saunders, M. 2006. Cytokines and Cytokine Receptors. *The Immune Response. Basic and Clinical Principals.* Elsevier Academic Press San Diego:.

Malugin, A. & Ghandehari, H. 2010. Cellular uptake and toxicity of gold nanoparticles in prostate cancer cells: a comparative study of rods and spheres. *Journal of Applied Toxicology: JAT,* 30**,** 212.

Marshall, J. S. 2004. Mast-cell responses to pathogens. *Nature Reviews Immunology,* 4**,** 787-799.

Maurer, M. & Von Stebut, E. 2004. Macrophage inflammatory protein-1. *The International Journal of Biochemistry & Cell Biology,* 36**,** 1882-1886.

Mckenzie, Z., Kendall, M., Mackay, R.-M., Whitwell, H., Elgy, C., Ding, P., Mahajan, S., Morgan, C., Griffiths, M. & Clark, H. 2015. Surfactant protein A (SP-A) inhibits agglomeration and macrophage uptake of toxic amine modified nanoparticles. *Nanotoxicology,* 9**,** 952-962.

Miller, J. F. 2002. The discovery of thymus function and of thymus-derived lymphocytes. *Immunological Reviews,* 185**,** 7-14.

Monopoli, M. P., Walczyk, D., Campbell, A., Elia, G., Lynch, I., Baldelli Bombelli, F. & Dawson, K. A. 2011. Physical− chemical aspects of protein corona: relevance to in vitro and in vivo biological impacts of nanoparticles. *Journal of the American Chemical Society,* 133**,** 2525-2534.

Mosmann, T. R. & Coffman, R. 1989. TH1 and TH2 cells: different patterns of lymphokine secretion lead to different functional properties. *Annual Review of Immunology,* 7**,** 145-173.

Mout, R., Moyano, D. F., Rana, S. & Rotello, V. M. 2012. Surface functionalization of nanoparticles for nanomedicine. *Chemical Society Reviews,* 41**,** 2539-2544.

Muhammad, Q., Jang, Y., Kang, S. H., Moon, J., Kim, W. J. & Park, H. 2020. Modulation of immune responses with nanoparticles and reduction of their immunotoxicity. *Biomaterials Science,* 8**,** 1490-1501.

Mukhopadhyay, S., Peiser, L. & Gordon, S. 2004. Activation of murine macrophages by Neisseria meningitidis and IFN-γ in vitro: distinct roles of class A scavenger and Toll-like pattern recognition receptors in selective modulation of surface phenotype. *Journal of Leukocyte Biology,* 76**,** 577-584.

Müller, K. H., Motskin, M., Philpott, A. J., Routh, A. F., Shanahan, C. M., Duer, M. J. & Skepper, J. N. 2014. The effect of particle agglomeration on the formation of a surface-connected compartment induced by hydroxyapatite nanoparticles in human monocyte-derived macrophages. *Biomaterials,* 35**,** 1074-1088.

Müller, N. 2019. The role of intercellular adhesion molecule-1 in the pathogenesis of psychiatric disorders. *Frontiers in Pharmacology,* 10**,** 1251.

Müller, N., Riedel, M., Ackenheil, M. & Schwarz, M. J. 1999. The role of immune function in schizophrenia: an overview. *European Archives of Psychiatry and Clinical Neuroscience,* 249**,** S62-S68.

Mulligan, M. & Ward, P. 1992. Immune complex-induced lung and dermal vascular injury. Differing requirements for tumor necrosis factor-alpha and IL-1. *The Journal of Immunology,* 149**,** 331-339.

Murphy, C. J., Gole, A. M., Stone, J. W., Sisco, P. N., Alkilany, A. M., Goldsmith, E. C. & Baxter, S. C. 2008. Gold nanoparticles in biology: beyond toxicity to cellular imaging. *Accounts of Chemical Research,* 41**,** 1721-1730.

Myhra, S. & Rivière, J. C. 2012. *Characterization of Nanostructures,* CRC Press.

Naahidi, S., Jafari, M., Edalat, F., Raymond, K., Khademhosseini, A. & Chen, P. 2013. Biocompatibility of engineered nanoparticles for drug delivery. *Journal of Controlled Release,* 166**,** 182-194.

Nagata, S., Hanayama, R. & Kawane, K. 2010. Autoimmunity and the clearance of dead cells. *Cell,* 140**,** 619-630.

Nauta, A. J., Roos, A. & Daha, M. R. 2004. A regulatory role for complement in innate immunity and autoimmunity. *International Archives of Allergy and Immunology,* 134**,** 310-323.

Nel, A., Xia, T., Mädler, L. & Li, N. 2006. Toxic potential of materials at the nanolevel. *Science,* 311**,** 622-627.

Nemmar, A., Hoylaerts, M. F., Hoet, P. H. M., Vermylen, J. & Nemery, B. 2003. Size effect of intratracheally instilled particles on pulmonary inflammation and vascular thrombosis. *Toxicology and Applied Pharmacology,* 186**,** 38-45.

Norman, J., Franz, M., Messina, J., Riker, A., Fabri, P. J., Rosemurgy, A. S. & Gower Jr, W. R. 1995. Interleukin-1 receptor antagonist decreases severity of experimental acute pancreatitis. *Surgery,* 117**,** 648-655.

Nygaard, U. C., Hansen, J. S., Samuelsen, M., Alberg, T., Marioara, C. D. & Løvik, M. 2009. Single-walled and multi-walled carbon nanotubes promote allergic immune responses in mice. *Toxicological Sciences,* 109**,** 113-123.

O'shea, J. J., Gadina, M. & Siegel, R. M. 2019. Cytokines and Cytokine Receptors. *In:* Rich, R. R., Fleisher, T. A., Shearer, W. T., Schroeder, H. W., Frew, A. J. & Weyand, C. M. (eds.) *Clinical Immunology* 5th ed. London: Elsevier.

O'brine, T. & Thompson, R. C. 2010. Degradation of plastic carrier bags in the marine environment. *Marine Pollution Bulletin,* 60**,** 2279-2283.

Oberdörster, G., Maynard, A., Donaldson, K., Castranova, V., Fitzpatrick, J., Ausman, K., Carter, J., Karn, B., Kreyling, W. & Lai, D. 2005. Principles for characterizing the potential human health effects from exposure to nanomaterials: elements of a screening strategy. *Particle and Fibre Toxicology,* 2**,** 8.

Oberdörster, G., Stone, V. & Donaldson, K. 2007. Toxicology of nanoparticles: a historical perspective. *Nanotoxicology,* 1**,** 2-25.

Oh, Y.-K. & Swanson, J. A. 1996. Different fates of phagocytosed particles after delivery into macrophage lysosomes. *The Journal of Cell Biology,* 132**,** 585-593.

Paciotti, G. F., Kingston, D. G. & Tamarkin, L. 2006. Colloidal gold nanoparticles: a novel nanoparticle platform for developing multifunctional tumor-targeted drug delivery vectors. *Drug Development Research,* 67**,** 47-54.

Parkin, J. & Cohen, B. 2001. An overview of the immune system. *The Lancet,* 357**,** 1777-1789.

Pavlidis, I. V., Vorhaben, T., Gournis, D., Papadopoulos, G. K., Bornscheuer, U. T. & Stamatis, H. 2012. Regulation of catalytic behaviour of hydrolases through interactions with functionalized carbon-based nanomaterials. *Journal of Nanoparticle Research,* 14**,** 842.

Peled, J. U., Kuang, F. L., Iglesias-Ussel, M. D., Roa, S., Kalis, S. L., Goodman, M. F. & Scharff, M. D. 2008. The biochemistry of somatic hypermutation. *Annual Review of Immunology,* 26**,** 481-511.

Plasticseurope, E. P. R. O. 2016. Plastics-the facts 2016. *An analysis of European plastics production***,** 1-38.

Plasticseurope, E. P. R. O. 2020. Plastics-the facts 2020. *An analysis of European plastics production, demand and waste data***,** 1-64.

Plaut, M., Pierce, J. H., Watson, C. J., Hanley-Hyde, J., Nordan, R. P. & Paul, W. E. 1989. Mast cell lines produce lymphokines in response to cross-linkage of FcεRI or to calcium ionophores. *Nature,* 339**,** 64-67.

Prietl, B., Meindl, C., Roblegg, E., Pieber, T., Lanzer, G. & Fröhlich, E. 2014. Nano-sized and micro-sized polystyrene particles affect phagocyte function. *Cell Biology and Toxicology,* 30**,** 1.

Pustulka, S. M., Ling, K., Pish, S. L. & Champion, J. A. 2020. Protein Nanoparticle Charge and Hydrophobicity Govern Protein Corona and Macrophage Uptake. *ACS Applied Materials & Interfaces,* 12**,** 48284-48295.

Qu, H., Ricklin, D. & Lambris, J. D. 2009. Recent developments in low molecular weight complement inhibitors. *Molecular Immunology,* 47**,** 185-195.

Rani, A., Kumar, A., Lal, A. & Pant, M. 2014. Cellular mechanisms of cadmium-induced toxicity: a review. *International Journal of Environmental Health Research,* 24**,** 378-399.

Real, E., Kaiser, A., Raposo, G., Amara, A., Nardin, A., Trautmann, A. & Donnadieu, E. 2004. Immature dendritic cells (DCs) use chemokines and intercellular adhesion molecule (ICAM)-1, but not DC-specific ICAM-3-grabbing nonintegrin, to stimulate CD4+ T cells in the absence of exogenous antigen. *The Journal of Immunology,* 173**,** 50-60.

Reeves, E. P., Lu, H., Jacobs, H. L., Messina, C. G., Bolsover, S., Gabella, G., Potma, E. O., Warley, A., Roes, J. & Segal, A. W. 2002. Killing activity of neutrophils is mediated through activation of proteases by K+ flux. *Nature,* 416**,** 291-297.

Rendón-Patiño, A., Niu, J., Doménech-Carbó, A., García, H. & Primo, A. 2019. Polystyrene as graphene film and 3D graphene sponge precursor. *Nanomaterials,* 9**,** 101.

Rezaei, R., Safaei, M., Mozaffari, H. R., Moradpoor, H., Karami, S., Golshah, A., Salimi, B. & Karami, H. 2019. The role of nanomaterials in the treatment of diseases and their effects on the immune system. *Open Access Macedonian Journal of Medical Sciences,* 7**,** 1884.

Rostek, A., Mahl, D. & Epple, M. 2011. Chemical composition of surface-functionalized gold nanoparticles. *Journal of Nanoparticle Research,* 13**,** 4809-4814.

Ruenraroengsak, P., Novak, P., Berhanu, D., Thorley, A. J., Valsami-Jones, E., Gorelik, J., Korchev, Y. E. & Tetley, T. D. 2012. Respiratory epithelial cytotoxicity and membrane damage (holes) caused by amine-modified nanoparticles. *Nanotoxicology,* 6**,** 94-108.

Ruenraroengsak, P. & Tetley, T. D. 2015. Differential bioreactivity of neutral, cationic and anionic polystyrene nanoparticles with cells from the human alveolar compartment: robust response of alveolar type 1 epithelial cells. *Particle and Fibre Toxicology,* 12**,** 19.

Ryan, J. J., Bateman, H. R., Stover, A., Gomez, G., Norton, S. K., Zhao, W., Schwartz, L. B., Lenk, R. & Kepley, C. L. 2007. Fullerene nanomaterials inhibit the allergic response. *The Journal of Immunology,* 179**,** 665-672.

Sanchez, C., Julián, B., Belleville, P. & Popall, M. 2005. Applications of hybrid organic–inorganic nanocomposites. *Journal of Materials Chemistry,* 15**,** 3559-3592.

Sanità, G., Carrese, B. & Lamberti, A. 2020. Nanoparticle surface functionalization: How to improve biocompatibility and cellular internalization. *Frontiers in Molecular Biosciences,* 7**,** 587012.

Sarma, J. V. & Ward, P. A. 2011. The complement system. *Cell and Tissue Research,* 343**,** 227-235.

Scheirs, J. & Priddy, D. 2003. *Modern styrenic polymers: polystyrenes and styrenic copolymers,* John Wiley & Sons.

Schnyder, J., Baggiolini, M., Gordon, S. & Thompson, J. 1980. Secretion of lysosomal enzymes by macrophages. *Mononuclear Phagocytes.* Springer.

Semete, B., Booysen, L. I. J., Kalombo, L., Venter, J. D., Katata, L., Ramalapa, B., Verschoor, J. A. & Swai, H. 2010. In vivo uptake and acute immune response to orally administered

chitosan and PEG coated PLGA nanoparticles. *Toxicology and Applied Pharmacology,* 249**,** 158-165.

Sethu, S., Govindappa, K., Alhaidari, M., Pirmohamed, M., Park, K. & Sathish, J. 2012. Immunogenicity to biologics: mechanisms, prediction and reduction. *Archivum Immunologiae Et Therapiae Experimentalis,* 60**,** 331-344.

Shang, L., Nienhaus, K. & Nienhaus, G. U. 2014. Engineered nanoparticles interacting with cells: size matters. *Journal of Nanobiotechnology,* 12**,** 5.

Sharma, A., Gorey, B. & Casey, A. 2019. In vitro comparative cytotoxicity study of aminated polystyrene, zinc oxide and silver nanoparticles on a cervical cancer cell line. *Drug and Chemical Toxicology,* 42**,** 9-23.

Shiloh, M. U., Macmicking, J. D., Nicholson, S., Brause, J. E., Potter, S., Marino, M., Fang, F., Dinauer, M. & Nathan, C. 1999. Phenotype of mice and macrophages deficient in both phagocyte oxidase and inducible nitric oxide synthase. *Immunity,* 10**,** 29-38.

Shukla, R., Bansal, V., Chaudhary, M., Basu, A., Bhonde, R. R. & Sastry, M. 2005. Biocompatibility of gold nanoparticles and their endocytotic fate inside the cellular compartment: a microscopic overview. *Langmuir,* 21**,** 10644-10654.

Silver, S., Phung, L. T. & Silver, G. 2006. Silver as biocides in burn and wound dressings and bacterial resistance to silver compounds. *Journal of Industrial Microbiology and Biotechnology,* 33**,** 627-634.

Singh, B. & Sharma, N. 2008. Mechanistic implications of plastic degradation. *Polymer Degradation and Stability,* 93**,** 561-584.

Singh, P., Pandit, S., Mokkapati, V., Garg, A., Ravikumar, V. & Mijakovic, I. 2018. Gold nanoparticles in diagnostics and therapeutics for human cancer. *International Journal of Molecular Sciences,* 19**,** 1979.

Sperling, R. A. & Parak, W. J. 2010. Surface modification, functionalization and bioconjugation of colloidal inorganic nanoparticles. *Philosophical Transactions of the Royal Society A: Mathematical, Physical and Engineering Sciences,* 368**,** 1333-1383.

Szolnoky, G., Bata-Csörgö, Z., Kenderessy, A. S., Kiss, M., Pivarcsi, A., Novák, Z., Nagy Newman, K., Michel, G., Ruzicka, T., Maródi, L., Dobozy, A. & Kemény, L. 2001. A Mannose-Binding Receptor is Expressed on Human Keratinocytes and Mediates Killing of Candida albicans. *Journal of Investigative Dermatology,* 117**,** 205-213.

Takeuchi, O. & Akira, S. 2010. Pattern Recognition Receptors and Inflammation. *Cell,* 140**,** 805-820.

Taub, D. D., Conlon, K., Lloyd, A. R., Oppenheim, J. J. & Kelvin, D. J. 1993. Preferential migration of activated CD4+ and CD8+ T cells in response to MIP-1 alpha and MIP-1 beta. *Science,* 260**,** 355-358.

Tesch, G. H., Lan, H. Y., Atkins, R. C. & Nikolic-Paterson, D. J. 1997. Role of interleukin-1 in mesangial cell proliferation and matrix deposition in experimental mesangioproliferative nephritis. *The American Journal of Pathology,* 151**,** 141.

Thomas, A. C. & Mattila, J. T. 2014. "Of mice and men": arginine metabolism in macrophages. *Frontiers In Immunology,* 5**,** 479.

Tonetti, M. S., Imboden, M. A., Gerber, L., Lang, N. P., Laissue, J. & Mueller, C. 1994. Localized expression of mRNA for phagocyte-specific chemotactic cytokines in human periodontal infections. *Infection and Immunity,* 62**,** 4005-4014.

Uguccioni, M., D'apuzzo, M., Loetscher, M., Dewald, B. & Baggiolini, M. 1995. Actions of the chemotactic cytokines MCP-1, MCP-2, MCP-3, RANTES, MIP-1α and MIP-1β on human monocytes. *European Journal of Immunology,* 25**,** 64-68.

Van Furth, R. & Cohn, Z. A. 1968. The origin and kinetics of mononuclear phagocytes. *The Journal of Experimental Medicine,* 128**,** 415-435.

Van Midwoud, P. M., Janse, A., Merema, M. T., Groothuis, G. M. M. & Verpoorte, E. 2012. Comparison of Biocompatibility and Adsorption Properties of Different Plastics for Advanced Microfluidic Cell and Tissue Culture Models. *Analytical Chemistry,* 84**,** 3938-3944.

Varadaradjalou, S., Féger, F., Thieblemont, N., Hamouda, N. B., Pleau, J. M., Dy, M. & Arock, M. 2003. Toll-like receptor 2 (TLR2) and TLR4 differentially activate human mast cells. *European Journal Of Immunology,* 33**,** 899-906.

Varela, J. A., Bexiga, M. G., Åberg, C., Simpson, J. C. & Dawson, K. A. 2012. Quantifying size-dependent interactions between fluorescently labeled polystyrene nanoparticles and mammalian cells. *Journal of Nanobiotechnology,* 10**,** 39.

Verma, A. & Stellacci, F. 2010. Effect of Surface Properties on Nanoparticle–Cell Interactions. *Small,* 6**,** 12-21.

Verreck, F. A., De Boer, T., Langenberg, D. M., Van Der Zanden, L. & Ottenhoff, T. H. 2006. Phenotypic and functional profiling of human proinflammatory type-1 and anti-inflammatory type-2 macrophages in response to microbial antigens and IFN-γ-and CD40L-mediated costimulation. *Journal of Leukocyte Biology,* 79**,** 285-293.

Vial, T. & Descotes, J. 2000. Drugs acting on the immune system. *Side Effects of Drugs Annual.* Elsevier.

Villanueva, A., Canete, M., Roca, A. G., Calero, M., Veintemillas-Verdaguer, S., Serna, C. J., Del Puerto Morales, M. & Miranda, R. 2009. The influence of surface functionalization on the enhanced internalization of magnetic nanoparticles in cancer cells. *Nanotechnology,* 20**,** 115103.

Wallis, R. 2007. Interactions between mannose-binding lectin and MASPs during complement activation by the lectin pathway. *Immunobiology,* 212**,** 289-299.

Wang, Y., Wang, J., Zhu, D., Wang, Y., Qing, G., Zhang, Y., Liu, X. & Liang, X.-J. 2021. Effect of physicochemical properties on in vivo fate of nanoparticle-based cancer immunotherapies. *Acta Pharmaceutica Sinica B,* 11**,** 886-902.

Weissenbach, J., Chernajovsky, Y., Zeevi, M., Shulman, L., Soreq, H., Nir, U., Wallach, D., Perricaudet, M., Tiollais, P. & Revel, M. 1980. Two interferon mRNAs in human fibroblasts: in vitro translation and Escherichia coli cloning studies. *Proceedings of the National Academy of Sciences,* 77**,** 7152-7156.

Whiteman, S. C., Bianco, A., Knight, R. A. & Spiteri, M. A. 2003. Human rhinovirus selectively modulates membranous and soluble forms of its intercellular adhesion Molecule–1 (ICAM-1) receptor to promote epithelial cell infectivity. *Journal of Biological Chemistry,* 278**,** 11954-11961.

Wilson, K. C., Center, D. M. & Cruikshank, W. W. 2004. The Effect of Interleukin-16 and its Precursor on T Lymphocyte Activation and Growth. *Growth Factors,* 22**,** 97-104.

Witkowska, A. M. & Borawska, M. H. 2004. Soluble intercellular adhesion molecule-1 (sICAM-1): an overview. *European Cytokine Network,* 15**,** 91-98.

Xia, T., Kovochich, M., Brant, J., Hotze, M., Sempf, J., Oberley, T., Sioutas, C., Yeh, J. I., Wiesner, M. R. & Nel, A. E. 2006. Comparison of the Abilities of Ambient and Manufactured Nanoparticles To Induce Cellular Toxicity According to an Oxidative Stress Paradigm. *Nano Letters,* 6**,** 1794-1807.

Xia, T., Kovochich, M., Liong, M., Zink, J. I. & Nel, A. E. 2008. Cationic Polystyrene Nanosphere Toxicity Depends on Cell-Specific Endocytic and Mitochondrial Injury Pathways. *ACS Nano,* 2**,** 85-96.

Xing, Z., Gauldie, J., Cox, G., Baumann, H., Jordana, M., Lei, X.-F. & Achong, M. K. 1998. IL-6 is an antiinflammatory cytokine required for controlling local or systemic acute inflammatory responses. *The Journal of Clinical Investigation,* 101**,** 311-320.

Yadav, T. P., Yadav, R. M. & Singh, D. P. 2012. Mechanical milling: a top down approach for the synthesis of nanomaterials and nanocomposites. *Nanoscience and Nanotechnology,* 2**,** 22-48.

Yan, Y., Gause, K., Kamphuis, M., Ang, C., O'brien-Simpson, N., Lenzo, J., Reynolds, E., Nice, E. & Caruso, F. 2013. Differential roles of the protein corona in the cellular uptake of nanoporous polymer particles by monocyte and macrophage cell lines. *ACS Nano,* 7**,** 10960-10970.

Yanagisawa, R., Takano, H., Inoue, K., Koike, E., Sadakane, K. & Ichinose, T. 2010. Size effects of polystyrene nanoparticles on atopic dermatitis-like skin lesions in NC/NGA mice. *International Journal of Immunopathology and Pharmacology,* 23**,** 131-141.

Yoffe, A. 2002. Low-dimensional systems: quantum size effects and electronic properties of semiconductor microcrystallites (zero-dimensional systems) and some quasi-two-dimensional systems. *Advances in Physics,* 51**,** 799-890.

Yu, S.-J., Yin, Y.-G. & Liu, J.-F. 2013. Silver nanoparticles in the environment. *Environmental Science: Processes & Impacts,* 15**,** 78-92.

Yuan, Y., Long, L., Liu, J., Lin, Y., Peng, C., Tang, Y., Zhou, X., Li, S., Zhang, C., Li, X. & Zhou, X. 2020. The double-edged sword effect of macrophage targeting delivery system in different macrophage subsets related diseases. *Journal of Nanobiotechnology,* 18**,** 168.

Zhan, S., Yang, Y., Shen, Z., Shan, J., Li, Y., Yang, S. & Zhu, D. 2014. Efficient removal of pathogenic bacteria and viruses by multifunctional amine-modified magnetic nanoparticles. *Journal of Hazardous Materials,* 274**,** 115-123.

Zhao, L., Seth, A., Wibowo, N., Zhao, C.-X., Mitter, N., Yu, C. & Middelberg, A. P. 2014. Nanoparticle vaccines. *Vaccine,* 32**,** 327-337.

Zielińska, A., Carreiró, F., Oliveira, A. M., Neves, A., Pires, B., Venkatesh, D. N., Durazzo, A., Lucarini, M., Eder, P., Silva, A. M., Santini, A. & Souto, E. B. 2020. Polymeric Nanoparticles: Production, Characterization, Toxicology and Ecotoxicology. *Molecules (Basel, Switzerland),* 25**,** 3731.

Zolnik, B. S., González-Fernández, Á., Sadrieh, N. & Dobrovolskaia, M. A. 2010. Minireview: nanoparticles and the immune system. *Endocrinology,* 151**,** 458-465.